

AN ABSTRACT OF THE THESIS OF

Yuzuru Ito for the degree of Doctor of Philosophy in Civil Engineering presented on June 29, 1993.

Title: Evaluation and Application of Ice Segregation Parameters for Frost Heave Prediction

Redacted for Privacy

Abstract approved: _____

Ted S. Vinson

The success of civil engineering construction in cold regions often depends on the assessment of the potential for frost heave. Over the past two decades two models have been presented to the engineering community to identify the frost heave potential, namely: (1) the segregation potential (SP), and (2) the discrete ice lens (DIL) models. These models are based on ice segregation parameters which can be obtained from simple laboratory freezing tests. However, the reliability of the ice segregation parameters obtained from the laboratory freezing tests is still in question.

In recognition of the need to improve the reliability of the measurement of ice segregation parameters in a frost heave test, a study was conducted to: (1) investigate several improvements in the step freezing test used to measure ice segregation parameters, (2) examine several approximations used to interpret the laboratory step freezing test results, (3) demonstrate the compatibility of the SP and DIL parameters, (4) propose a method to obtain reliable ice segregation parameters, and (5) demonstrate the applicability of the DIL model to address field frost heave problems.

The results of the study indicated: (1) the accuracy of measured ice segregation parameters may be improved if step freezing tests are conducted under shallower temperature gradients and the water intake velocity is accurately and continuously monitored, (2) inappropriate approximations may produce a significant error in the measurement of ice segregation parameters, (3) SP may be defined either by the ratios of the (i) heave velocity/1.09 to the overall temperature gradient of the frozen soil, or (ii) water intake velocity to the temperature gradient of the frozen fringe, (4) the SP and DIL ice segregation parameters are compatible, and (5) the reliability of both models is improved through the demonstration of the compatibility of the ice segregation parameters.

The application of the frost heave prediction models was studied based on ice segregation parameters determined with the improved laboratory procedure. A practical method to predict the influence of the groundwater level using the DIL ice segregation parameters was proposed. A probabilistic approach for the DIL frost heave model was developed.

**Evaluation and Application of Ice Segregation Parameters
for Frost Heave Prediction**

by

Yuzuru Ito

A THESIS

submitted to

Oregon State University

in partial fulfillment of
the requirements for the
degree of

Doctor of Philosophy

Completed June 29, 1993
Commencement June, 1994

APPROVED:

Redacted for Privacy

Professor of Civil Engineering in charge of Major

Redacted for Privacy

Head of Department of Civil Engineering

Redacted for Privacy

Dean of Graduate School

Date thesis is presented _____ June 29, 1993

Acknowledgement

Throughout the course of this research, as well as the rest of my education at Oregon State University, I have received and greatly appreciated the guidance, patience, and encouragement given by my major professor, Ted S. Vinson. I also wish to thank the other members of my graduate committee, Loren D. Kellogg, J. Richard Bell, James R. Lundy, and William G. McDougal, as well as the former graduate committee members Jonathan D. Istok and Marvin R. Pyles.

During this research program, a large amount of information and advice was gained from J. F. (Derick) Nixon, Douglas Stewart, Solomon C. S. Yim, and Jonathan D. Istok. Very precious technical advice was frequently received from Andy Brickman. Chuck Svensen and Loren Sunberg are thanked for their incredible craftsmanship in constructing the test equipment.

Exceptional thanks to my employer and financial supporter, Japan Highway Public Corporation (JH). Additional support, which I am very thankful, was provided by International Road Federation (Washington, D. C.), Japan Road Association, Express Highway Research Foundation of Japan, and Japan Highway Landscape Association. Also, Itaru Sera and Nobuo Mishima are thanked for permission of the extension of my program. Kunitoshi Toya and Seiya Yokota are appreciated for collecting and providing a number of experiment data for the research program. Distinctive appreciation also goes to Barbara Callner as my family friend and a proofreader of English throughout this thesis.

I thank my late grandparents Nisaku and Sute Ito for encouraging me to receive a higher education, and my parents Masao and Akiko Ito for their understanding and

financial support. Finally, I wish to acknowledge my wife Atsuko, and my sons Hajime and Wataru Ito. It was their love and support that made everything possible.

Contribution of Authors

This thesis is a compilation of four articles prepared for separate publication and inclusion herein. Chapters 2 through 5 were written to stand alone and some repetition may be noted. Citations in the text refer to references listed at the end of each chapter. These references are collected into a comprehensive bibliography at the end of the text. In Chapters 2 and 3, Dr. J. F. (Derick) Nixon is listed as a co-author because he offered advice on the conduct of the test program. In Chapter 2, Dr. Douglas Stewart is listed because he co-supervised the laboratory test program. In Chapter 5, Dr. Solomon C. S. Yim is listed because he guided the efforts to create the probabilistic computation method presented. Dr. Ted S. Vinson's most important contributions were as my consultant, overall project supervisor, coordinator, and editor.

Yuzuru Ito

June 1993

TABLE OF CONTENTS

1.0	Introduction	1
1.1	References	3
2.0	An Improved Step Freezing Test to Determine Segregation Potential	4
	Abstract	4
2.1	Introduction	5
2.2	Statement of Purpose	6
2.3	Segregation Potential Theory	6
2.4	Laboratory Evaluation of SP	16
2.5	Concerns Regarding the Evaluation of SP	18
2.6	Improvements to the Step Freezing Test to Determine SP	21
2.7	Improved Step Freezing Frost Heave Test System	22
2.8	Sample Preparation	25
2.9	Test Procedure	27
2.10	Analysis of Test Data	27
2.11	Test Results	29
2.12	Discussion	34
2.13	Summary and Conclusion	41
2.14	References	42
2.15	Notation	44
3.0	Examination of Approximations Which Support the Segregation Potential and Discrete Ice Lens Frost Heave Models	45
	Abstract	45
3.1	Introduction	46
3.2	Statement of Purpose	49
3.3	Idealization of a Freezing Soil	50
3.4	Examination of Simplifying Approximations Used to Interpret Freezing Tests	56
3.5	Research Program	62
3.6	Laboratory Test	63
3.7	Method to Analysis the Freezing Test Result	63
3.8	Test Results and Analysis	72
3.9	Summary and Conclusion	95
3.10	References	98
3.11	Notation	100

4.0	Method to Predict the Influence of Groundwater Level on Frost Heave	102
	Abstract	102
4.1	Introduction	103
4.2	Statement of Purpose	105
4.3	Relationship between Frost Heave and Groundwater Level	105
4.4	Prediction of Frost Heave from Laboratory Test and SFFT	107
4.5	Laboratory Test Procedure to Predict the Influence of Groundwater Level	110
4.6	Research Program	113
4.7	Description of the Test Facilities and Procedures	113
4.8	Test Results	129
4.9	Discussion	147
4.10	Summary and Conclusion	150
4.11	References	151
4.12	Notation	153
5.0	A Probabilistic Approach for Frost Heave Prediction -Discrete Ice Lens Model with Point Estimate Method for Parameter Evaluation-	154
	Abstract	154
5.1	Introduction	155
5.2	Statement of Purpose	156
5.3	Discrete Ice Lens Model	157
5.4	Extraction of the DIL Parameters	161
5.5	Limitation of the DIL model	162
5.6	Simplified Equations for Field Frost Heave Prediction	163
5.7	Probabilistic Frost Heave Prediction	164
5.8	Simulation of a Laboratory Test Result	169
5.9	Simulation of Field Frost Heave Observation at Asahikawa, Japan	175
5.10	Summary and Conclusion	181
5.11	References	182
5.12	Notation	184
6.0	Conclusion	185
	6.1 Summary	185
	6.2 Conclusion	185
	6.3 Future Study	187
	6.4 References	188
	Bibliography	189

LIST OF FIGURES

<u>Figure</u>		<u>Page</u>
2.1	Idealization of Formation of Segregated Ice in a Soil Mass (after Konrad and Morgenstern 1980)	8
2.2	Formation of Segregated Ice Under Two Different Temperature Gradients (after Konrad and Morgenstern 1980)	12
2.3	Flow Chart for Evaluation of SP	17
2.4	Approximate Relationship Between Heave Velocities, Cooling Rate of the Frozen Fringe, and Frozen Depth in a Step Freezing Test	23
2.5	Step Freezing Test System	24
2.6	Location of Thermistors in the Frost Heave Cell	26
2.7	Results From Test C-6 (Steep Temperature Gradient)	30
2.8	Results From Test C-11 (Shallow Temperature Gradient)	33
2.9	Results From Test C-14 (Shallowest Temperature Gradient)	35
2.10	Improvement of Temperature Fluctuation due to the Difference of Insulation	38
2.11	SP Evaluated from Heave Data	40
3.1	Frost Heave Model (modified from Gilpin 1980)	51
3.2	Ice Pressure Change across the Frozen Fringe during an Ice Lens Cycle (modified from Gilpin 1980)	54
3.3	Grain Size Distribution of Calgary Silt	65
3.4	Calculation of Temperature Gradient	70
3.5	Results from Test C-8	73
3.6	Unfrozen Water Content of the Frozen Soil	75
3.7	Relationships between A and B Constants	76
3.8	Thermal Conductivity versus Unfrozen Water Content	79

<u>Figure</u>	<u>Page</u>
3.9 Temperature Gradients of the Frozen Fringe	81
3.10 Relationships between the Various Temperature Gradients	83
3.11 Various Combinations of the Water Flow Velocities and Temperature Gradients	84
3.12 SP versus the Combined Pressure Term	86
3.13 Evaluation of DIL Parameters	89
3.14 Compatibility of the SP and DIL Parameters	92
3.15 Reproduced SP Parameters for Design Purpose	96
4.1 Frost Heave versus Groundwater Level for Kongodo Soil (after Kawaragawa et al. 1989)	108
4.2 Frost Heave versus Test Boundary Condition (after Ito et al. 1989)	109
4.3 Grain Size Distribution of Asahikawa Soil	115
4.4 Step Freezing Test System	116
4.5 Frost Susceptibility Test System	119
4.6 Semi-Full Scale Freezing Test System	124
4.7 Asahikawa Frost Heave Observation Site	127
4.8 Results from Test A-3	130
4.9 Unfrozen Water Content versus Overburden Pressure	134
4.10 Evaluation Ice Segregation Parameters	135
4.11 Frost Heave Test Result by the Conventional Frost Susceptibility Test System	138
4.12 Extraction of the DIL Parameters from the Conventional Frost Susceptibility Test Result	140
4.13 Frost Heave Test Result by the SFFT	141

<u>Figure</u>	<u>Page</u>
4.14 Frost Heave at 45 Days versus Groundwater Level	142
4.15 Field Frost Heave Observation (after Toya et al. 1992)	145
4.16 Ice Segregation Parameters: Predicted versus Observed	149
5.1 Frost Heave Model (modified from Gilpin 1980)	158
5.2 Beta Distribution (after Harr 1987)	167
5.3 Extraction of the DIL Parameters (modified from Ito et al. 1993)	170
5.4 Simulation of the Laboratory Test Result Using the Mean Parameters	171
5.5 Sensitivity Analysis Comparing Heave Velocity for Mean and Mean plus Twenty Percent DIL Parameters	173
5.6 Simulation of the Field Test at Asahikawa	179

LIST OF TABLES

<u>Table</u>	<u>Page</u>
3.1 Physical Properties of Calgary Silt	64
3.2 Test Boundary Conditions	66
3.3 Thermal Conductivity of a Freezing Soil (after ISGF 1991)	69
3.4 Various Temperature Gradients at the End of Transient Freezing	80
3.5 Estimates of the DIL Parameters	94
4.1 Physical Properties of Asahikawa Soil	114
4.2 Test Boundary Conditions Using the Proposed Test Method	117
4.3 Conventional Frost Susceptibility Criteria	121
4.4 Test Boundary Conditions Using the Conventional Frost Susceptibility Test System	122
4.5 Test Boundary Conditions Using the SFFT	125
4.6 Thermal Conductivity of a Freezing Soil (after ISGF 1991)	133
4.7 Ice Segregation Parameters from SFFT	144
4.8 Ice Segregation Parameters from the Field Observation	148
5.1 Mean Input Parameters	172
5.2 PEM Computation Example	176
5.3 Probabilistic Analysis of the Laboratory Test	177
5.4 Probabilistic Analysis of the Field Test	180

Evaluation and Application of Ice Segregation Parameters for Frost Heave Prediction

1.0 Introduction

In the construction of civil engineering structures in cold regions, frost heave problems must be resolved in the design stage. The greatest concerns relating to predictions of frost heave are the amount of heave at a specific time, heave velocity, and heave forces. A number of mathematical models have been proposed to predict frost heave. Among them, two models which have been presented over the past decade appear to be most practical for engineering purposes, namely, the segregation potential (SP) (Konrad and Morgenstern 1981), and the recently developed discrete ice lens (DIL) (Nixon 1991) models. The advantage of these prediction models over models previously presented is that the ice segregation parameters governing the models can easily be extracted from simple laboratory freezing tests.

Although several successful applications of the SP and DIL models have been reported in the literature, many practitioners have expressed concerns about their application to solve field problems. The greatest concern relates to the uncertainty in the laboratory measurements and interpretation of the ice segregation parameters (for either model) which are used to predict field frost heave. Three initiatives were undertaken in the research work presented herein to alleviate the concerns: (1) improve the laboratory test procedure, (2) examine the approximations used to extract ice segregation parameters, and (3) verify the compatibility of the SP and DIL parameters to improve the reliability to evaluate SP or DIL ice segregation parameters.

With the introduction of the DIL model, it became clear that the overburden pressure and suction, which have been treated separately, can be combined and treated as one term. This means that the effects of overburden pressure and suction are equivalent. It was hypothesized that one may substitute the laboratory freezing tests for the time consuming and expensive semi-full scale freezing test (SFFT) to predict the influence of groundwater level on frost heave. It was also believed that the applicability of the probabilistic method to frost heave prediction may be greater when the ice segregation parameters were evaluated in a reliable and consistent manner.

The evaluation of the laboratory methods and application of the SP and DIL ice segregation parameters in order to predict field frost heave for civil engineering construction are presented herein. Chapter 2 demonstrates the improvements to the simple freezing test to evaluate the ice segregation parameters. Chapter 3 examines the approximations used to extract ice segregation parameters from the freezing tests and proposes a method to increase the reliability of the parameter measurements. Chapter 4 demonstrates the use of the results of a freezing test to predict the influence of ground water level on frost heave. Chapter 5 presents an application of a probabilistic method to the DIL model.

1.1 References

1. Konrad, J. M., and Morgenstern, N. R., "The Segregation Potential of a Freezing Soil," *Canadian Geotechnical Journal*, Vol. 18, 1981, pp. 482-491.
2. Nixon, J. F., "Discrete Ice Lens Theory for Frost Heave in Soils," *Canadian Geotechnical Journal*, Vol. 28, 1991, pp. 843-859.

2.0 An Improved Step Freezing Test to Determine Segregation Potential

by

Yuzuru Ito, Ted S. Vinson, J. F. (Derick) Nixon, and Douglas Stewart

Abstract

The Segregation Potential (SP) concept has contributed greatly to an engineering approach to solve frost heave problems. The number of applications of SP to field problems has steadily increased since it was introduced to the profession over a decade ago. However, at the present time, there is still concern among practitioners regarding the consistency of SP and the reproducibility of its measurement in a laboratory freezing test. This unfortunate situation arises from the uncertainty in the evaluation of SP in a step freezing test. The two factors which influence the measurement of SP of greatest concern are: (1) the inaccuracy of existing methods used to measure the water intake velocity, and (2) the use of a steep temperature gradient during a freezing test.

To facilitate a consistent and reproducible measurement of SP, a laboratory research program was conducted in which three improvements to the conventional step freezing test were made. The improvements included: (1) the use of a more accurate water intake measurement, (2) a shallower temperature gradient, and (3) the addition of a cold bath to facilitate ice nucleation. The water intake during a freezing test was continuously monitored with an electric balance to obtain greater accuracy in the measurement of water intake velocity.

To demonstrate the effect of the improvements, the results from three step freezing tests with three different temperature gradients are presented. Based on the results of the laboratory tests, it was concluded that the improvements made allowed consistent and reproducible values of SP to be measured. With continuous measurement of water intake velocity SP can be determined with greater accuracy during the entire freezing test. A continuously recorded water intake velocity can also provide useful information to identify the end of transient freezing or the formation of the final ice lens. In addition, when a step freezing test was conducted with a shallower temperature gradient, it was observed that SP could be determined more accurately.

2.1 Introduction

The Segregation Potential (SP) concept introduced by Konrad and Morgenstern (1980, 1981, 1982, 1982b) has provided the opportunity to develop an engineering approach to address field frost heave problems. In theory, the determination of SP in the laboratory simply requires the measurement of the water intake velocity and the temperature gradient in the frozen fringe in a step freezing test in which the soil response is at the "near steady state" condition. Because of the relative simplicity of the theory which supports SP and the test method required to obtain the SP parameter, the application of this concept to many practical field situations has been increasing (e.g. Nixon 1982; Fukuda et al. 1988; Saarelainen 1992). Further, the SP concept provided a very powerful basis to develop soil frost heave susceptibility criteria based on the fines factor (Reike et al. 1983; Vinson et al. 1984).

To date, the procedure to obtain SP from a simple step freezing test has not been completely standardized. For example, the heave velocity (divided by 1.09) is often used in place of water intake velocity because an accurate method to continuously measure water intake is lacking. Further, in many cases SP changes rapidly near the end of transient freezing; the determination of the end of transient freezing greatly influences the evaluation of SP. A more sophisticated method employing a ramped freezing test is highly recommended to determine SP by Penner (1986) and Konrad (1988), but the test equipment to perform ramped freezing tests is not available to most practitioners. In addition, the many factors which influence SP have sometimes confused practitioners (Gassen and Segó 1993).

2.2 Statement of Purpose

The purpose of the research reported herein is to identify improvements to the step freezing frost heave test so that one can obtain consistent and reproducible values of SP. The scope of the work presented includes (1) a description of the test methods and laboratory program conducted to verify the improvements, and (2) a discussion of the significance of the improvements.

2.3 Segregation Potential Theory

The development of the concept of SP follows a recognition that (1) frost heave is the result of growing ice lenses in a soil mass subjected to subfreezing temperatures, and (2) water is drawn to the base of a growing ice lens owing to a suction gradient that

develops in response to the temperature gradient in the soil mass. The condition associated with frost heave may be visualized as shown in Figure 2.1. At the surface, there is a cold side temperature T_c . At some depth in the soil mass, the temperature is equal to the normal freezing point of the water T_i . Slightly above this depth there is a growing ice lens, with a base temperature of T_s . T_s has been termed the segregation freezing temperature and the depth corresponding to T_i , the frost front (Konrad and Morgenstern 1980). The zone between the base of the ice lens and the freezing front has been termed the frozen fringe (Miller 1972). The existence of the frozen fringe in a freezing system has been established experimentally (Loch and Kay 1978; Loch 1979).

In the frozen fringe liquid water exists in equilibrium with pore ice at a temperature below 0 °C, as absorbed films on the surface of soil particles. The amount of water that can flow to the base of an ice lens is a function of the thickness of the absorbed films, which in turn is a function of the soil particle characteristics and the temperature of the frozen fringe. Further, the amount of water that can flow to the base of the ice lens is a function of the suction gradient that exists across the frozen fringe, the suction gradient in the unfrozen soil below the frost front, and the hydraulic conductivity of the unfrozen soil. Indeed, frost heave may be viewed as a problem of impeded water flow to a growing ice lens (Konrad and Morgenstern 1980).

Under steady state conditions, water flows to the base of the growing ice lens, through the low hydraulic conductivity frozen fringe and underlying unfrozen soil. The volumetric heat and latent heat, released as water is transported to the base of the ice lens and eventually forms ice, equal the heat removed when the ice lens is stationary. The

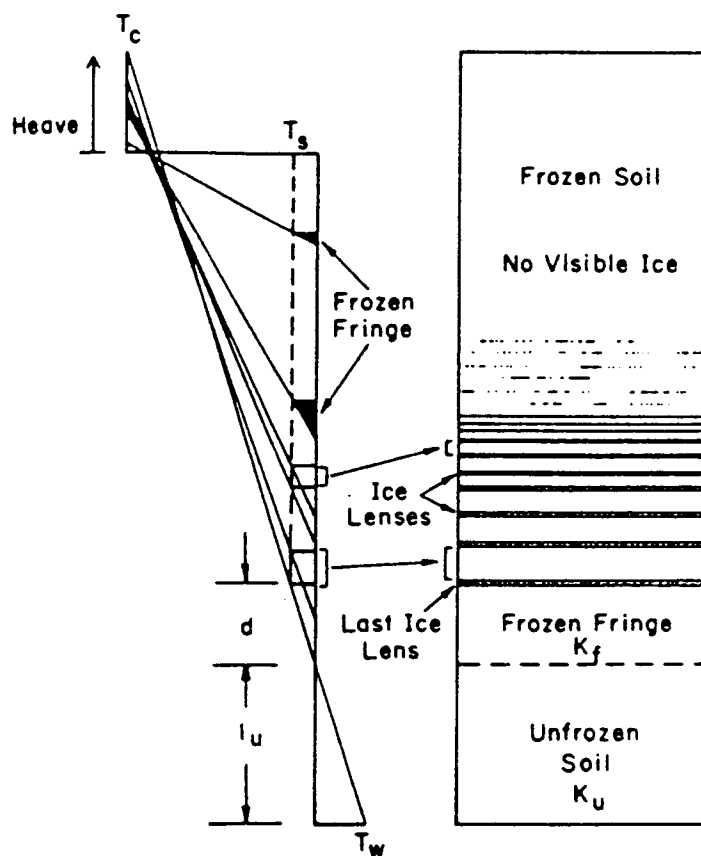


Figure 2.1 Idealization of Formation of Segregated Ice in a Soil Mass (after Konrad and Morgenstern 1980)

frost front advances when the heat removed is greater than the latent heat released. With the greater heat removed the temperature in the frozen fringe is lowered, the hydraulic conductivity of the frozen fringe is reduced, the flow of water is decreased, which in turn further reduces the latent heat released. This interrelated thermodynamic/water flow response results in finer ice lenses being formed near the surface of a soil column, where the temperature gradient is steep and rate of heat removal is greatest. Thicker ice lenses form at greater depths in the soil column, where the temperature gradient is shallow (Konrad and Morgenstern 1980). Also, with greater depths of frost front penetration, the thickness of the frozen fringe increases as a consequence of the shallower temperature gradient and T_s and T_i being nearly constants. The conceptual picture for the overall phenomena is shown in Figure 2.1.

As the frost front slows in its advance and a near steady-state thermodynamic/water flow condition is reached, the situation has been described mathematically by Konrad and Morgenstern (1980) and may be summarized as follows. It is generally accepted that the Clausius-Clapeyron equation may be used to relate pressure in the liquid film at the base of a growing ice lens, u_i , to temperature, that is

$$u_i = \left(\frac{L}{V_w} \right) \ln \left(\frac{T_{sk}}{T_{ok}} \right) = \left(\frac{L}{V_w} \right) \ln \left(1 + \frac{T_s}{T_{ok}} \right) = \left(\frac{L}{V_w * T_{ok}} \right) T_s \quad (2.1)$$

where, L = latent heat of fusion of water,
 V_w = specific volume of water,
 T_{ok} = freezing point of pure water ($^{\circ}$ K),

T_{sk} = segregation freezing temperature ($^{\circ}$ K), and

$$T_s = T_{sk} - T_{ok}$$

It is apparent that $L/(V_w * T_{ok})$ in Eq. 2.1 is a constant. Therefore, the suction that develops at the base of a growing ice lens under near steady state conditions (i.e. very slow frost penetration rate) is a function of a soil property only, namely, the segregation freezing temperature.

Now consider the two layer system consisting of the frozen fringe and unfrozen soil beneath the last ice lens. Assuming (1) there is no accumulation of water in the frozen fringe, (2) Darcy's law is valid for the flow regime that exists, and (3) the hydraulic conductivity in the frozen fringe and unfrozen soil are constant, then (by applying Darcy's law)

$$v = \frac{\Delta h_T}{\frac{d}{k_f} + \frac{l_u}{k_u}} \quad (2.2)$$

where, v = water flow velocity to the ice lens or water intake velocity from the unfrozen part of the soil column,

h_T = total head loss between base of ice lens and base of soil column,

l_u = thickness of unfrozen soil,

d = thickness of frozen fringe,

k_f = hydraulic conductivity of frozen fringe, and

k_u = hydraulic conductivity of unfrozen soil.

l_u and d may be evaluated for a given temperature gradient, warm side temperature T_w , and a soil with a specific value of T_s . The total head loss may be expressed in terms of the results obtained from the Clausius-Clapeyron equation, that is

$$\Delta h_T = \frac{u_i}{\gamma_w} + h_{ei} - \frac{u_b}{\gamma_w} - h_{eb} = \frac{1}{\gamma_w} \left(\frac{L}{V_w \cdot T_{ok}} \right) \cdot T_s + h_{ei} - \frac{u_b}{\gamma_w} - h_{eb} \quad (2.3)$$

where, h_{ei} = elevation head at the base of the last ice lens,
 h_{eb} = elevation head at the base of the soil column,
 u_b = porewater pressure at the base of the soil column, and
 γ_w = unit weight of water.

Taking the base of the soil column at the water level, $u_b=0$. Further, for a saturated soil column with the water level close to the last ice lens, $h_{ei}=h_{eb}$. Thus Eq. 2.3 reduces to

$$\Delta h_T = \left(\frac{L}{\gamma_w \cdot V_w \cdot T_{ok}} \right) \cdot T_s \quad (2.4)$$

By combining Eqs. 2.2 and 2.4, it is apparent that the velocity of water flow to the base of a growing ice lens, for a given temperature gradient, is a function of soil properties only, that is k_f , k_u , and T_s . Consequently, the heave velocity, 1.09 times the velocity of water flow, is also a function of soil properties only, for a given temperature gradient.

Next consider two columns of identical soil, freezing under different temperature gradients as shown in Figure 2.2. From Eq. 2.4. It may be noted that the total head loss

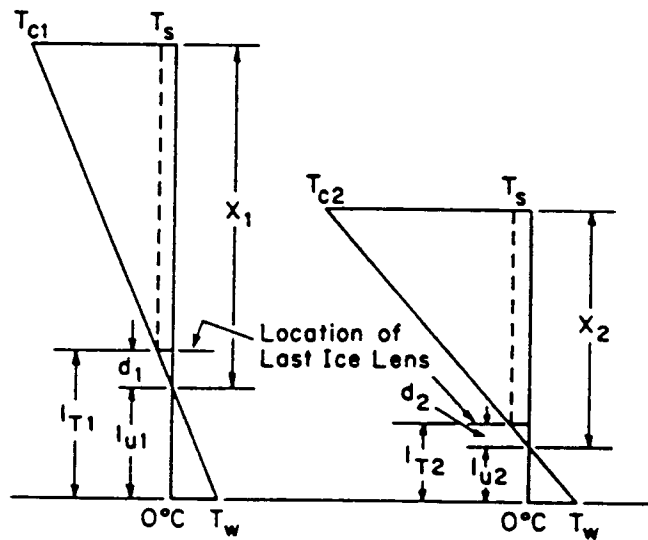


Figure 2.2 Formation of Segregated Ice Under Two Different Temperature Gradients (after Konrad and Morgenstern 1980)

from the base of the last ice lens and soil column (dh) is the same for both cases. Further, the average temperature in the frozen fringe is the same for both columns suggesting that the average unfrozen water content is the same. This implies that the average hydraulic conductivity (k_p) is the same in both cases.

As a consequence of these identities and assumptions, the flow velocities for the two cases may be written as

$$\frac{T_s}{d_1} = \frac{T_w}{l_{u1}}, \quad \frac{T_s}{d_2} = \frac{T_w}{l_{u2}} \quad (2.5)$$

By noting similar triangles under the two different conditions,

$$\frac{T_s}{T_w} = \frac{d_1}{l_{u1}} = \frac{d_2}{l_{u2}} \quad (2.6)$$

If the ratio of velocities is taken,

$$\frac{v_1}{v_2} = \frac{k_u \cdot d_2 + l_{u2} \cdot k_f}{k_u \cdot d_1 + l_{u1} \cdot k_f} \quad (2.7)$$

From Eq. 2.6

$$l_{u2} = \frac{d_2 \cdot l_{u1}}{d_1} \quad (2.8)$$

Substituting Eqs. 2.8 into 2.7 and factoring out d_1 and d_2 ,

$$\frac{v_1}{v_2} = \frac{d_2}{d_1} \cdot \frac{k_u + (l_{u1}/d_1) \cdot k_f}{k_u + (l_{u1}/d_1) \cdot k_f} = \frac{d_2}{d_1} \quad (2.9)$$

and

$$v_1 d_1 = v_2 d_2 \quad (2.10)$$

But

$$d_1 = \frac{T_s}{grad T_1}, \quad d_2 = \frac{T_s}{grad T_2} \quad (2.11)$$

where, $grad T$ = temperature gradient below the base of the ice lens.

Substituting Eqs. 2.11 into 2.10,

$$\frac{v_1}{grad T_1} = \frac{v_2}{grad T_2} = constant \quad (2.12)$$

Eq. 2.12 suggests that if the ratio of the water intake velocity and temperature gradient is a constant then the ratio may be established from the results of tests conducted at any temperature gradient. Further, if the ratio of flow velocity to temperature gradient is known for a particular soil then the flow velocity (and hence, heave velocity) may be established for another temperature gradient by simple multiplication.

Konrad and Morgenstern (1981) have termed the ratio of water intake velocity to temperature gradient at the frozen fringe the segregation potential (SP). They have shown

that the SP is

$$SP = \frac{v}{grad T_f} = \left(\frac{T_s \cdot L / (\gamma_w \cdot V_w \cdot T_{ok}) - u_0}{T_s} \right) \cdot k_f \quad (2.13)$$

where, u_0 = suction at the base of the frozen fringe.

The SP, when evaluated at near steady state conditions, and under the conditions previously noted (i.e., a saturated soil column with negligible overburden pressure), may be considered to be an index property of a soil that uniquely identifies the frost heave susceptibility considering the assumptions noted above. The greater the SP, the greater the heave in a soil mass in response to a given set of freezing conditions.

To relate the SP of a soil to field conditions, one must consider the influence of these variables: (1) the suction at the frost front (associated with the depth to the groundwater table), (2) the pressure applied to the warmest ice lens (associated with the weight of the soil column and surcharge loads above the lens), and (3) the rate of cooling of the frozen fringe (associated with frost penetration rates and average temperature gradients in the frozen zone). In a series of papers, Konrad and Morgenstern (1980, 1981, 1982, 1982b) have discussed the significance of these variables and extended the concept of SP to address frost heave prediction under field conditions. They have demonstrated that only a limited number of freezing tests are required to fully characterize the SP of a soil for most field problems.

2.4 Laboratory Evaluation of SP

Following the method proposed by Konrad (1987), a typical procedure to evaluate SP from a step freezing test is illustrated in Figure 2.3. A step freezing test is conducted and the amount of heave (Figure 2.3a) and temperature distribution (Figure 2.3b) are recorded. The total heave (H) is obtained directly from an LVDT reading and the segregational heave (h_s), which is the heave due to water migration through the unfrozen part of the soil, is calculated from the reading of water intake monitoring device (e.g. a buret) multiplied by 1.09 and divided by the sample's cross sectional area. The water intake velocity (v) (Figure 2.3c) can also be calculated from the water intake reading. The temperature distribution (Figure 2.3b) can be used to estimate the temperature gradient of the frozen fringe (Figure 2.3d) and the frozen depth (Figure 2.3e), which is the location of the 0 °C isotherm, by interpolation. Next the rate of cooling of the fringe (Figure 2.3h) is computed as

$$\frac{dT_f}{dt} = \text{grad} T_f \cdot \frac{dX}{dt} \quad (2.14)$$

where X is the frozen depth.

The time when the rate of cooling becomes zero is considered as the end of transient freezing. Within the period of transient freezing SP (Figure 2.3f) can be evaluated as the ratio of the water intake velocity (Figure 2.3c) to the temperature gradient of the fringe (Figure 2.3d):

Step Freezing Test

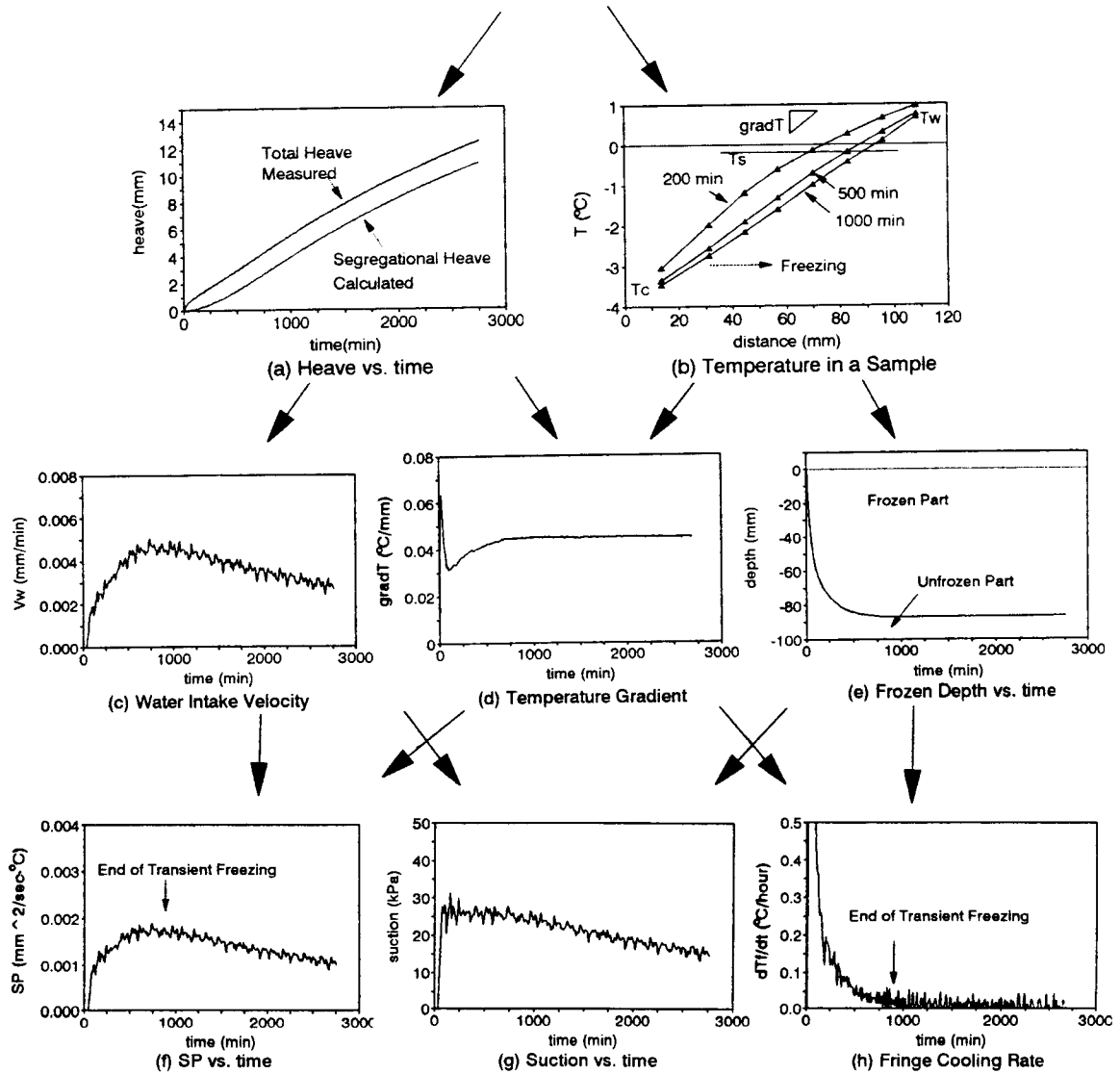


Figure 2.3 Flow Chart for Evaluation of SP

$$SP(t) = \frac{v(t)}{\text{grad } T_f(t)} \quad (2.15)$$

where, $SP(t)$ = segregation potential at time t ,
 $v(t)$ = water intake velocity, and
 $\text{grad } T_f(t)$ = overall temperature gradient of the frozen fringe.

This is the extended form of Eq. 2.13 for transient freezing. In the example shown in Figure 2.3 SP, at the end of transient freezing, is evaluated approximately as 0.0017 mm²/(s°C) when dT_f/dt is close to zero.

2.5 Concerns Regarding the Evaluation of SP

There are three major concerns regarding the method presently used to evaluate SP. The first concern is related to the water intake measurement. SP is defined by the ratio of water intake velocity to the temperature gradient of the frozen fringe. To date, a volume change device such as a buret, or a pressure transducer has been used to measure the water intake velocity. However, the accuracy of these devices is limited to 1/10 ml. This is equivalent to approximately 0.01 mm of heave for a 10 cm diameter sample. On the other hand, if the heave rate is used to establish SP, an LVDT may be used with a precision of 0.001 mm. It is apparent that SP based on water intake velocity will fluctuate to a much greater extent than SP based on heave velocity.

Using the following equations, it is possible to estimate the water intake velocity from the heave data if the amount of water, which changes phase below 0 °C, can be

reasonably estimated as such:

$$H(t) = h_s(t) + h_i(t) \quad (2.16)$$

$$v(t) = \frac{1}{1.09} \cdot \frac{dh_s(t)}{dt} = \frac{(H(t+\Delta t) - H(t-\Delta t)) - 0.09\epsilon n(X(t+\Delta t) - X(t-\Delta t))}{2.18\Delta t} \quad (2.17)$$

where,

- $H(t)$ = total heave measured at time t ,
- $h_s(t)$ = segregation heave at time t ,
- $h_i(t)$ = in-situ heave at time t ,
- $X(t)$ = frozen depth from the original surface,
- n = porosity, and
- ϵ = amount of water changing phase below 0 °C expressed as a decimal fraction.

The strict use of Eq. 2.17 requires knowledge of the amount of water which changes phase at the frost front. However, the second term in the numerator of Eq. 2.17 approaches zero when the frost front is advancing very slowly at the end of transient freezing. Consequently, the calculation of SP from a measurement of total heave is considered to be satisfactory. It is unfortunate, however, that there are no published reports which fully describe SP based on reliable water intake velocity measurements during the entire period of transient freezing. If reliable water intake velocity was obtained the validity of calculating SP from heave data could be assessed.

The second concern is the determination of the end of transient freezing or the time when a final ice lens starts to form. Since SP at this time is most often used for field predictions, the determination of this time is very important. The end of transient freezing is determined from the rate of cooling of the frozen fringe. Therefore, the reliability of SP depends on the determination of the end of transient freezing from the rate of cooling of the fringe, which is computed from the temperature distribution along the wall of the test cell. It is likely that some uncertainty may exist in the rate of cooling, since the temperatures along the inner walls of the frost heave cell are not exactly the temperature inside the specimen. In fact, the rate of cooling of the fringe usually fluctuates due to heat flow from outside the test cell. Although the thickness of the final ice lens can be used to back-calculate the end of transient freezing, the accuracy of this method is also questionable. This uncertainty is of greatest concern when SP changes rapidly in the freezing test.

The third concern is the boundary temperature condition of the test. In a step freezing test to obtain SP the temperature gradient is generally much steeper than the field temperature gradient. In a laboratory step freezing test the temperatures in a sample rapidly decrease during transient freezing and only become stable at the end of transient freezing. This thermal regime is completely different from the thermal regime when frost heave occurs in the field. It may not be possible to obtain a reliable SP to predict field frost heave from a laboratory test with a substantially different temperature gradient. It is reasonable to speculate that the use of a shallower temperature gradient would reduce the discrepancy between the laboratory and the field condition, and provide data from

which one could obtain a more reliable SP. Also it appears that there is no advantage to use a steeper temperature gradient in a step freezing test except that it makes ice-nucleation easier and reduces testing time.

2.6 Improvements to the Step Freezing Test to Determine SP

Three improvements were made to the procedure and equipment commonly used to evaluate SP to overcome the concerns identified. The first improvement was made in the measurement of water intake. The method used to establish water intake velocity in the present study utilizes an electric balance to obtain a continuous record of weight change in place of a volume change device. The electric balance insures a precision of 1/100 ml of water intake which is equivalent to 0.001 mm of heave for a 10 cm diameter sample. This allows a direct and precise computation of SP from water intake velocity and temperature gradient. Further, if a Mariot device (e.g. McCabe and Kettle 1985) is used in conjunction with an electric balance, it is possible to conduct a test with constant water pressure at the unfrozen end of the specimen.

The temperature measurements in the cell wall only provide information on the boundary condition during a freezing test. The expectation that knowledge of a thermal boundary condition could be used to conclusively identify the end of transient freezing is perhaps unrealistic. The water intake and heave velocities represent an overall condition of the freezing soil. Using a reliable water intake velocity the end of transient freezing can be evaluated by considering the relationship to the heave velocity. For a saturated soil at the end of transient freezing the following relationship should exist:

$$v(t) = \frac{1}{1.09} \frac{dh_s(t)}{dt} = \frac{1}{1.09} \frac{dH(t)}{dt} \quad \text{or} \quad \frac{dh_i(t)}{dt} = 0 \quad (2.18)$$

Eq. 2.18 indicates that the water intake velocity equals the heave velocity divided by 1.09 when the frost front stops advancing and the in situ heave velocity (h_i) approaches zero (re. Figure 2.4).

The second improvement was the use of a shallower temperature gradient for the step freezing test. The third improvement was the addition of a cold bath to facilitate ice-nucleation under a shallower temperature gradient.

2.7 Improved Step Freezing Frost Heave Test System

The test system used in the research program is shown in Figure 2.5. This system consists of the following items:

- Split frost heave cell;
- Two boundary temperature control baths;
- Ice-nucleation bath;
- Electric balance and Mariot device;
- LVDT;
- Surcharge loading device; and
- Data acquisition system.

The frost heave cell was originally fabricated by Reike (1982) and was modified for use in the test program. Temperatures were monitored by nine thermistors along the

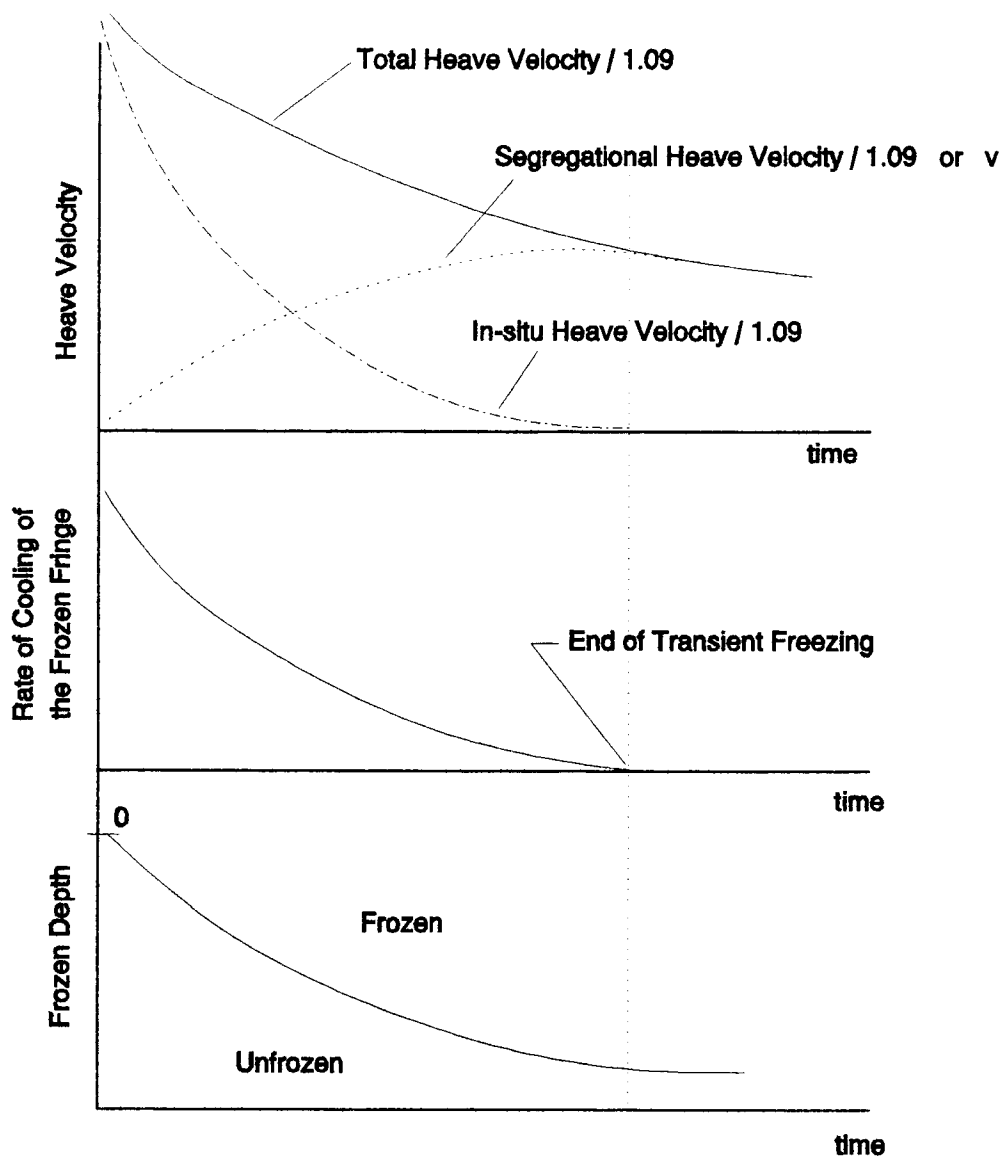


Figure 2.4 Approximate Relationship Between Heave Velocities, Cooling Rate of the Frozen Fringe, and Frozen Depth in a Step Freezing Test

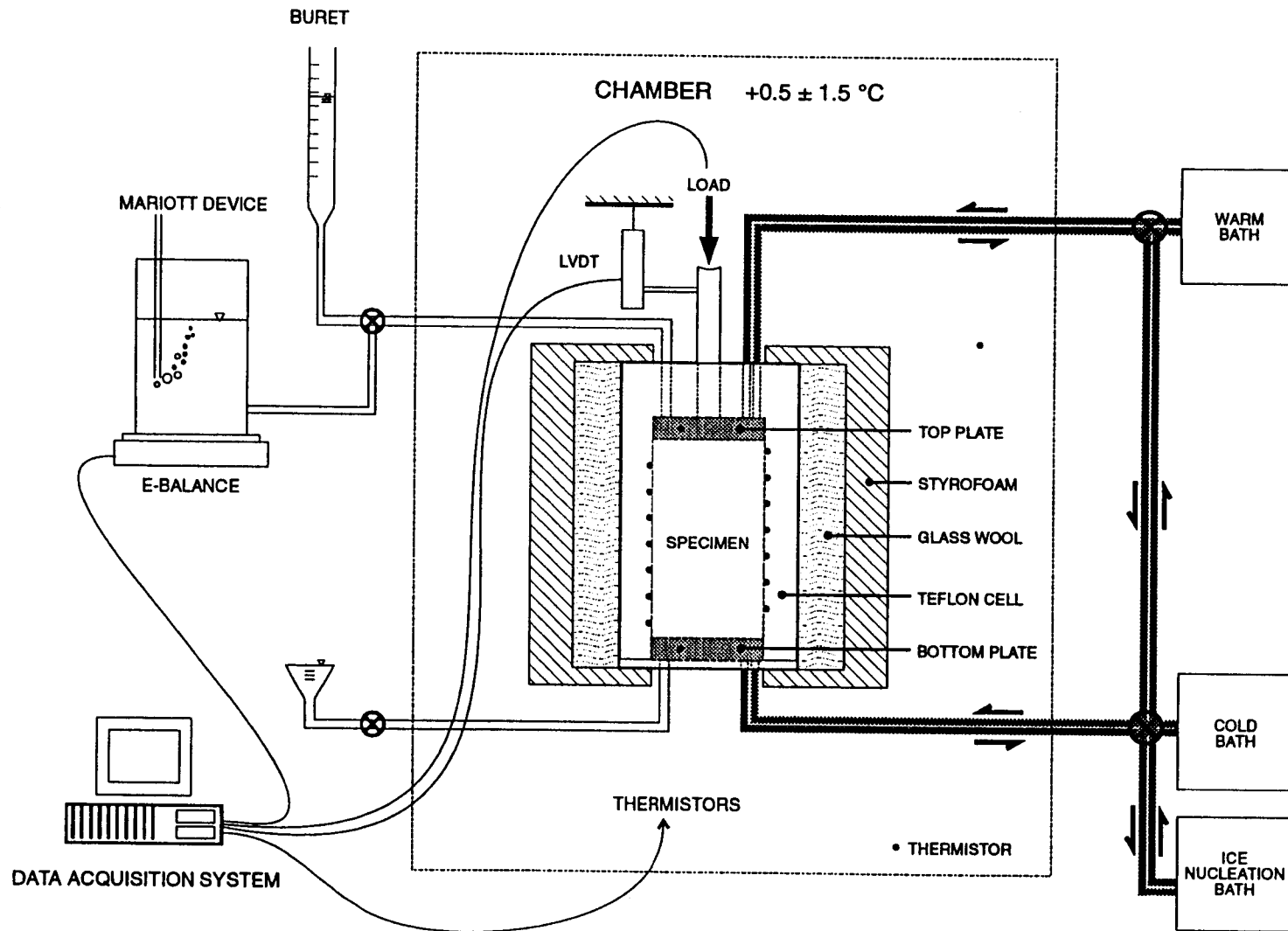


Figure 2.5 Step Freezing Test System

length of each half of the cell. The thermistors were placed at 7 to 13 mm intervals as shown in Figure 2.6. In addition to the 18 thermistors in the cell, two thermistors were placed in the chamber and one was placed on the top and bottom boundary plates. All the thermistors were calibrated in the ice bath (i.e. a bath in which a mixture of ice and water exist to maintain 0 °C). An LVDT was used to measure frost heave. An electric balance monitored water intake as the weight change in the Mariot device, which is used to maintain a constant water head. This system made it possible to obtain a reading with 1/100 ml of accuracy while maintaining a constant water level for the duration of a test.

2.8 Sample Preparation

Naturally occurring Calgary silt was used for all of the frost heave tests. The soils were initially prepared as a slurry (i.e. a mixture of soil and distilled water) at a water content of about 1.5 to 2 times the liquid limit. The slurry was allowed to soak overnight in a container. Finally, a vacuum was applied to the container for one day. The container was vibrated with a rubber hammer several times during this period until no more air bubbles appeared.

Consolidation of the slurry to 300 kPa was performed in four stages in a consolidometer. After consolidation, the 10 cm diameter specimen was extruded from the consolidometer and trimmed to a height of 8 to 12 cm.

The test specimen was placed on the bottom of the freezing cell and the sides were coated with silicon grease. A thin rubber membrane was placed over the specimen and the surface of the membrane was again coated with silicon grease. The application

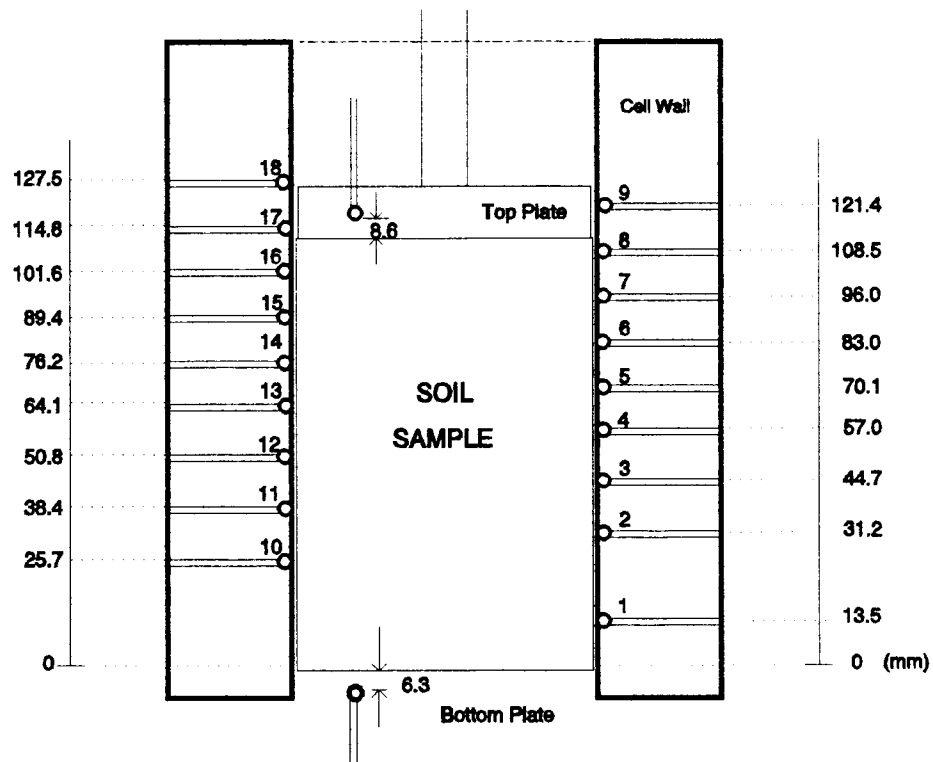


Figure 2.6 Location of Thermistors in the Frost Heave Cell

of silicon grease insured the side friction during freezing would be minimal. Finally, the two halves of the frost heave cell were clamped together to enclose the specimen.

2.9 Test Procedure

Three test results which demonstrate the improvements made are reported herein. The tests were conducted under three different temperature gradients at a constant overburden pressure of 45 kPa. A step freezing method was used and the samples were frozen from the bottom end to the top.

Following the application of the overburden pressure the specimen temperature was allowed to equilibrate at approximately +0.5 to +1.5 °C by circulating anti-freeze at a constant temperature from the warm bath through the top and bottom plates. Next, anti-freeze at -10 °C was circulated through the bottom plate to initiate ice nucleation. After observing a slight change in the electric balance and the load cell readings (usually 3 to 5 minutes after introduction of the -10 °C anti-freeze) the circulation through the bottom plate was changed to the cold bath at the prescribed temperature to achieve the desired step temperature boundary condition. The LVDT, electric balance, load cell, and thermistors were monitored at 10 or 15 min. intervals during the test.

2.10 Analysis of Test Data

Water Intake Rate

The water intake velocity at time t can be directly computed from the water intake reading:

$$v(t) = \frac{W_w(t - \Delta t) - W_w(t)}{\gamma_w A \Delta t} \quad (2.19)$$

where, $W_w(t)$ = weight of the water tank at time t ,
 A = cross sectional area of the specimen, and
 Δt = time interval.

On the other hand, the water flow to the base of the ice lens is computed from the LVDT reading:

$$V_f(t) = \frac{H(t) - H(t - \Delta t)}{1.09 \Delta t} \quad (2.20)$$

The segregational heave or heave due to water intake from the unfrozen part of the soil is computed directly from the water intake reading:

$$h_s(t) = \frac{1.09 (W_w(0) - W_w(t))}{\gamma_w A} \quad (2.21)$$

where, $W_w(0)$ = the weight of the water tank at time $t = 0$.

Using the total heave measured with the LVDT and the segregational heave, the in-situ heave is calculated as:

$$h_i(t) = H(t) - h_s(t) \quad (2.22)$$

The fraction of water which changes phase below 0 °C can be computed from

$$\varepsilon(t) = \frac{h_i(t)}{0.09nX(t)} \quad (2.23)$$

Segregation Potential

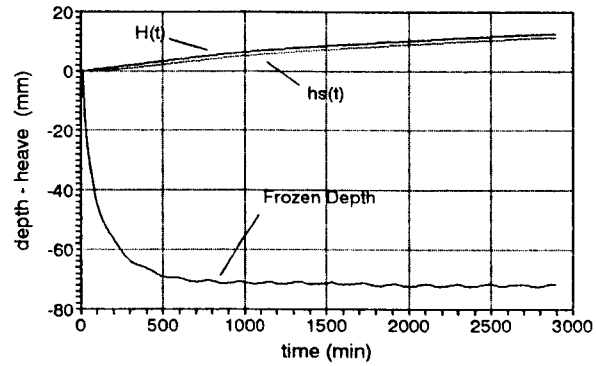
The SP was determined from Eq. 2.15 as the ratio of the exact water intake velocity $v(t)$ from Eq. 2.19 and the temperature gradient of the frozen fringe or $grad T_f(t)$. Assuming $T_s = -0.3$ °C, $grad T_f(t)$ was computed following the procedure presented by Konrad (1987).

2.11 Test Results

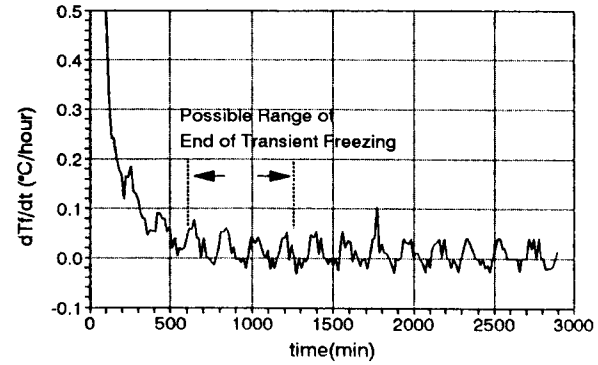
Three tests were conducted under three different temperature gradients at a constant 45 kPa overburden pressure. The unfrozen length of the specimen at steady state is expected to be very short for the three tests and, therefore, SP should be about the same for the three tests.

Test with a steeper temperature gradient

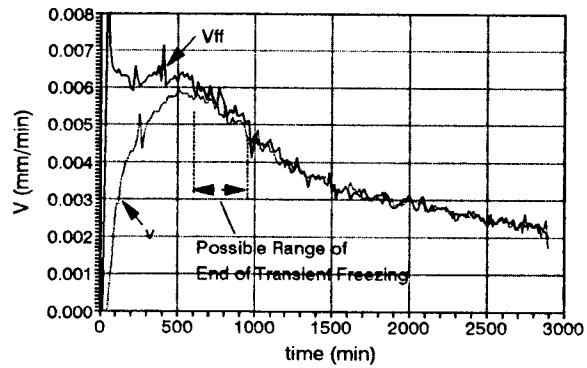
Figure 2.7 presents the results for test C-6 in which an 8 cm sample was frozen under the boundary temperature condition of -3.7 and +1.6 °C. Test data were recorded at 15 min intervals. In order to illustrate the advantage of the electric balance to monitor water intake, SP, at the end of the transient state, was estimated by two different procedures.



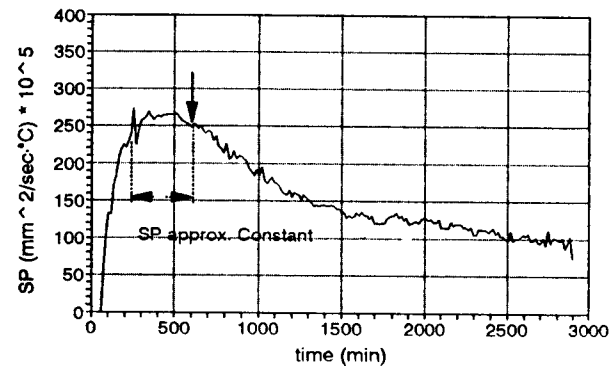
(a) Heave and Frozen Depth



(b) Rate of Cooling



(c) Vff and Vw



(d) SP

Figure 2.7 Results From Test C-6 (Steep Temperature Gradient)

First, according to the rate of cooling of the fringe defined by the cell wall temperature measurements (Figure 2.7b), transient freezing ended between approximately 600 and 1250 min. Observing the wide range of time for the end of transient freezing, SP could be evaluated as 0.0016 to 0.0025 mm²/(s°C) from Figure 2.7d. Given this wide range the use of the parameter SP for a practical field frost heave prediction would appear to be questionable.

The second procedure utilized the relationship between water intake and heave velocities (Figure 2.7c). The heave velocity divided by 1.09 (V_{ff}) equals the water intake velocity (v) when the frost front stops advancing. After this time there is no further in situ freezing (h_i). This time may be considered as the end of transient freezing when the final ice lens starts to form. Following this procedure, Figure 2.7c suggests that the end of transient freezing could conservatively be estimated as 600 to 950 min. Therefore, SP could be evaluated as 0.0019 to 0.0025 mm²/(s°C) from Figure 2.7d. The best estimate is that V_{ff} and v are equal at approximately 600 min. Since it is considered that the frost front may progress a little, and a small part of water remaining unfrozen in the frozen fringe will freeze after the formation of the final ice lens, it is reasonable to assume that the final ice lens may begin to form at approximately 600 min. Consequently, SP was interpreted as 0.0025 mm²/(s°C) at 600 min. It was obvious that SP estimated by the water intake velocity was much more definitive than SP estimated by the rate of cooling.

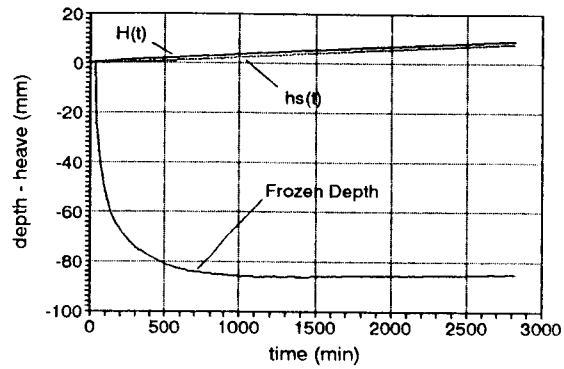
Further, it was observed that while both the frozen depth (Figure 2.7a) and rate of cooling were disturbed by the cyclic fluctuation in temperature readings due to the heat flow from outside the cell, both V_{ff} and v showed no such disturbance. This means

there was substantially no effect in the freezing test result caused from the thermal disturbance due to improper insulation.

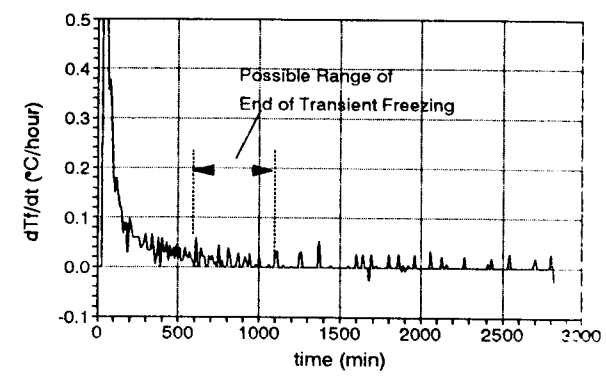
Tests with shallower temperature gradients

Figure 2.8 presents the results for test C-11 in which a 10 cm sample was frozen under the boundary temperature condition of -2.4 and $+0.8$ °C. This is about one half the gradient used in test C-6 (Figure 2.7). Test data were recorded at 10 min intervals. In this test the insulation of the freezing cell was greatly improved. As a result, there was less fluctuation in the temperature based information such as the rate of cooling (Figure 2.8b). But the end of transient freezing is still difficult to identify from Figure 2.8b. The cooling rate indicates that the end of transient freezing was between 600 and 1100 min and SP was estimated as 0.0024 to 0.0025 $\text{mm}^2/(\text{s}^\circ\text{C})$. However, according to Figure 2.8c, V_{ff} equals v at 850 min and SP was evaluated as 0.0025 $\text{mm}^2/(\text{s}^\circ\text{C})$. An advantage of the accurate water intake measurement was again demonstrated.

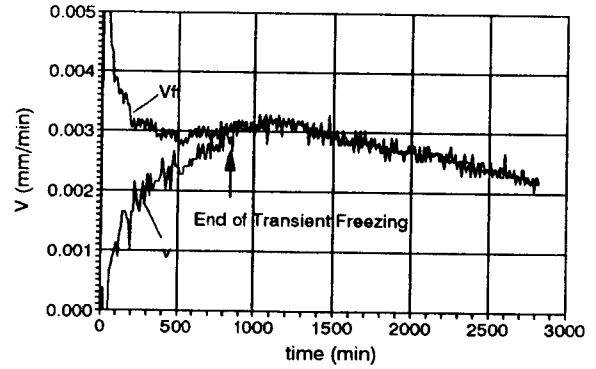
Another significant advantage associated with the shallow temperature gradient may be observed by comparing Figures 2.7d and 2.8d. The SP was approximately constant over a relatively wide range of time (SP changed only about 5 % at between 600 and 1100 min, Figure 2.8d) under a shallow temperature gradient. On the other hand, SP decreased substantially (approximately 40 % between 600 and 1100 min, Figure 2.7c) under a steep temperature gradient. The difference can be explained by the fact that in a test with a shallower temperature gradient freezing progresses slower and SP also changes slower. Therefore, it was obvious that for the Calgary silt used for this research,



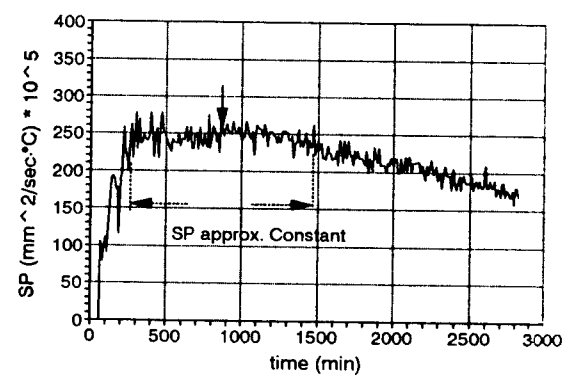
(a) Heave and Frozen Depth



(b) Rate of Cooling



(c) Vff and Vw



(d) SP

Figure 2.8 Results From Test C-11 (Shallow Temperature Gradient)

the test with a shallower temperature gradient facilitated the determination of SP compared to the test with a steeper temperature gradient.

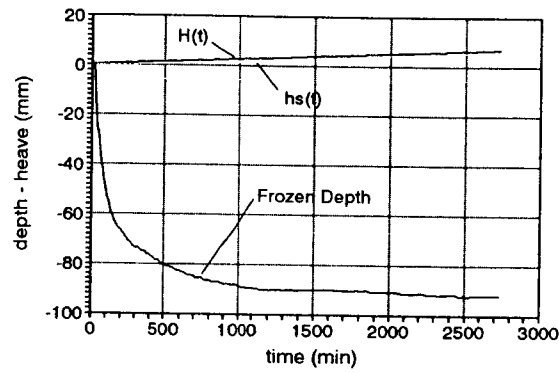
Figure 2.9 presents the results from test C-14 in which an 11 cm sample was frozen under the temperature boundary condition of -1.3 and $+0.4$ °C. This is approximately one half the gradient used in test C-11 (Figure 2.8). Figure 2.9b suggests that the end of transient freezing was between 350 to 1250 min, while Figure 2.9c indicates that V_{ff} and v are approximately equal between 750 and 1250 min. The SP was about $0.0034 \text{ mm}^2/(\text{s}^\circ\text{C})$ for either of the possible ranges of the end of transient freezing (Figures 2.9b and 1.9c). Significantly, the time period over which SP was constant was substantially longer than reported in the previous tests C-6 and C-11.

2.12 Discussion

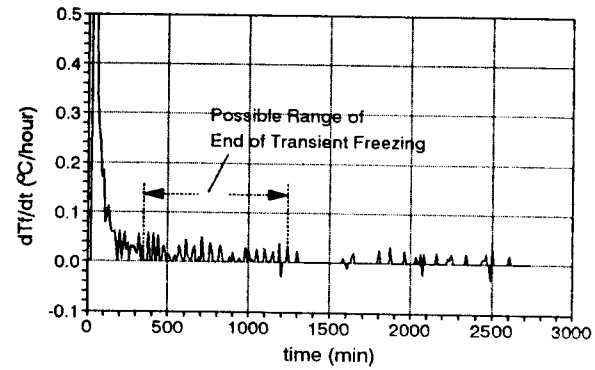
Water intake measurement

The advantage of using an electric balance for monitoring water intake was demonstrated. This method improved the accuracy of water intake data to the accuracy of the heave data. The three test results (Figures 2.7c, 2.8c, 2.9c) showed that the fluctuations of heave velocity divided by 1.09 (V_{ff}) and water intake velocity (v) were of the same order of magnitude. It would be difficult to compare V_{ff} and v if v was based on a measurement from either a buret or a pressure transducer which would result in a determination an order of magnitude lower in accuracy.

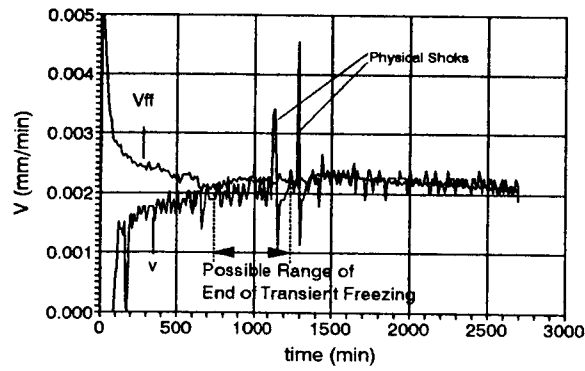
As a result of this improvement, it was possible to evaluate SP directly from water intake velocity. With accurate water intake data, there is no need to estimate the



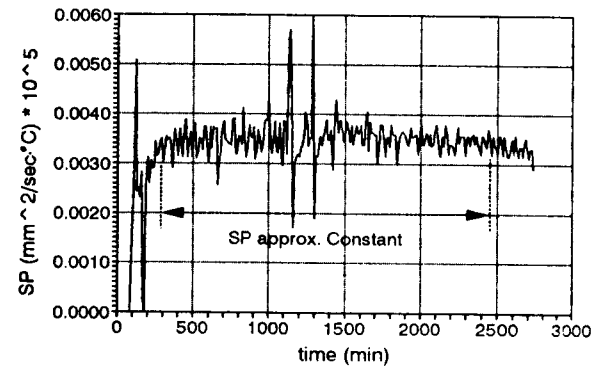
(a) Heave and Frozen Depth



(b) Rate of Cooling



(c) Vff and Vw



(d) SP

Figure 2.9 Results From Test C-14 (Shallowest Temperature Gradient)

fraction of water remaining unfrozen in the frozen part of soil in order to compute v from the heave data. Conversely, the fraction of the unfrozen water can be easily calculated from the relationship of V_{ff} and v using Eq. 2.23. As a result of computing the unfrozen water with Eq. 2.23, the proportion of unfrozen water under 0 °C were respectively 40% (C-6), 50% (C-11), and 62% (C-14), indicating it was, in fact, not constant at all. Therefore, it was predicted that the use of the assumed parameter ε in Eq. 2.17 would produce an inaccurate value of SP.

It was also demonstrated that the relationship between V_{ff} and v can be used to evaluate the end of transient freezing to obtain SP for most field predictions. The temperature based information, such as the cooling rate of the fringe and frozen depth, were easily influenced by the overall thermal environment when improper insulation was used. Thus it appears that the use of temperature based information to evaluate the end of transient freezing is questionable. On the other hand, based on the test results presented, it was observed that thermal disturbances did not influence the frost heave and water intake response. Therefore, it is concluded that the use of the relationship between V_{ff} and v to determine the end of transient freezing represents a significant advantage over the use of temperature data.

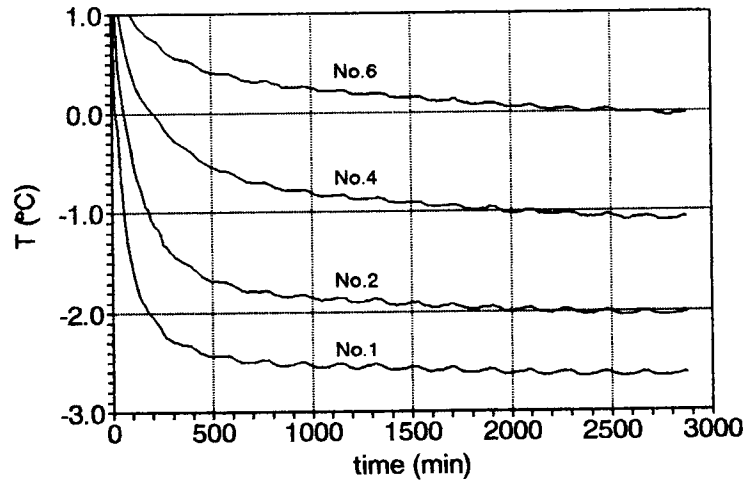
Temperature based information

The three tests results presented suggest it is necessary to examine the dependency on temperature information to determine SP. It must be emphasized that although the thermistors in the cell wall were in contact with the freezing sample through a very thin

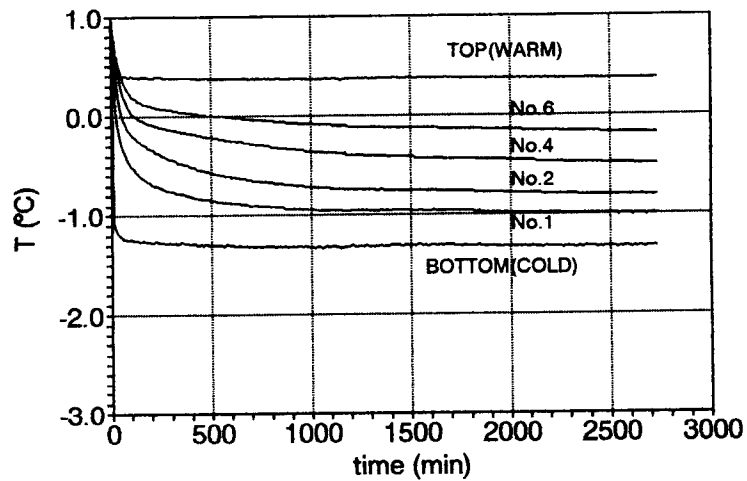
membrane, they actually monitored the cell wall and soil temperature in their immediate vicinity and not the temperature in the interior of the specimen. The quality of the cell insulation has a substantial influence on the accuracy of the temperature readings along the cell wall. In addition, it is recognized that there is a certain limit in accuracy of temperature readings monitored with this type of test system. There is always uncertainty in the recorded temperature which would inevitably influence the value of SP.

The frost heave cell for test C-6 was covered with insulation, consisting of a styrofoam box and glass wool covering the outside of the test cell. The chamber temperature outside the insulated box was controlled to ± 1.5 °C. To improve the insulation in the box, in tests C-11 and C-14 a thin styrofoam sheet was placed over the glass wool to prevent possible air movement inside the box. As illustrated in Figure 2.10, this simple improvement greatly reduced the temperature fluctuations.

Temperature fluctuations were easily observed in several freezing tests. As shown in Figure 2.7b, the temperature fluctuation directly influenced the computed rate of cooling and hence, the evaluation of the end of transient freezing. The end of transient freezing was difficult to interpret under these conditions and results in either a greater or smaller value of SP. SP obtained under these conditions may not be a reliable predictor of field frost heave.



(1) Test C-6



(2) Test C-14

Figure 2.10 Improvement of Temperature Fluctuation due to the Difference of Insulation

Segregation Potential

The SP defined by the exact water intake velocity and temperature gradient at the frozen fringe were plotted in Figures 2.7d, 2.8d and 2.9d. The three figures show that the shallower the temperature gradient the wider the range over which SP was approximately constant. As can be seen in the three figures, SP was constant when the rates of cooling were less than about $0.04\text{ }^{\circ}\text{C}/\text{hour}$. The range in which SP was constant started from 250 to 300 min and finished at 600 (Figure 2.7d), 1300 (Figure 2.8d) and 2400 min (Figure 2.9d), respectively. It can also be concluded that the shallower the temperature boundary condition the less important the determination of the end of transient freezing is when evaluating SP. Therefore, a step freezing test to obtain a consistent and reliable value of SP should be conducted with a shallower temperature gradient. To facilitate ice nucleation another cold bath should be added to the two existing baths.

If SP was estimated from the heave data, the range of response over which SP was constant would be difficult to determine without an accurate water intake velocity measurement. Figure 2.11 demonstrates that even the best estimate of SP using $\varepsilon = 50\%$ does not correspond to SP obtained with v . Therefore, the step freezing test to obtain a reliable SP should be conducted under a shallower temperature gradient with an ice nucleation bath and with continuous monitoring of water intake.

Another concern is the difference in SP values for tests C-6/11 and C-14; SP was $0.0025\text{ mm}^2/(\text{s}^{\circ}\text{C})$ in tests C-6 and C-11 while SP was $0.0034\text{ mm}^2/(\text{s}^{\circ}\text{C})$ in test C-14. The difference is difficult to explain based on the difference in suction and inherent

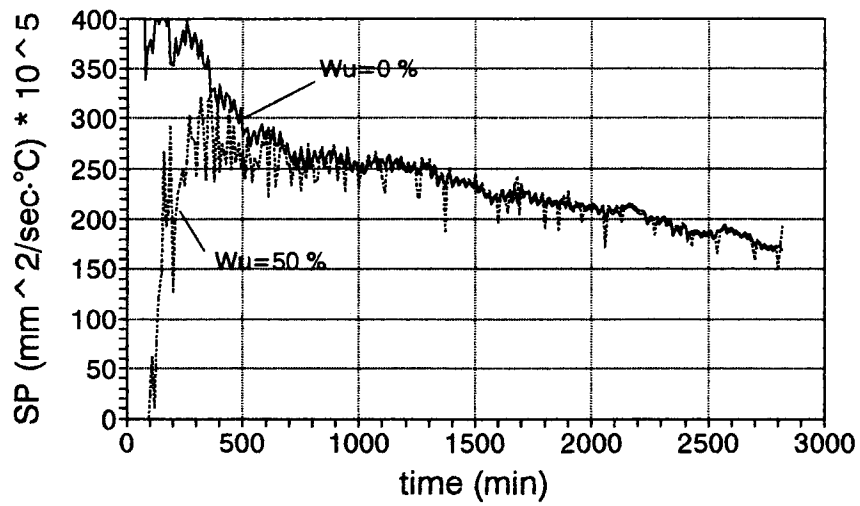


Figure 2.11 SP Evaluated from Heave Data

uncertainty in calculating the temperature gradient of the frozen fringe. A realistic approach to explain the difference of SP from the laboratory test is presented by Ito et al. (1993).

2.13 Summary and Conclusion

Improvements were made to a step freezing test to facilitate the consistent and reproducible evaluation of SP. The improvements include the use of an electric balance to measure water intake velocity, the use of a shallow temperature boundary condition, and an additional cold bath for ice nucleation.

Test results were presented which demonstrated the relationship between V_{ff} and v . These results could be used to estimate the end of transient freezing (or the formation of the final ice lens) if accurate water intake data was available. It was also shown that SP calculated as the ratio of the water intake velocity from the improved water intake measurement and temperature gradient at the frozen fringe was constant over a greater time period for a test conducted with a shallow temperature gradient.

Overall, it may be concluded that the step freezing test to evaluate SP should be conducted with a shallow temperature gradient, an ice nucleation cold bath, and a continuous water intake monitoring system. As a result of these improvements, it was demonstrated that consistent and reproducible measurements of SP are possible.

2.14 References

1. Fukuda, M., Ogawa, S., and Kamei, T., "Prediction of Field Frost Heave Using the Segregation Potential Theory," *Japan Society of Civil Engineers Reports*, No.400, 1988, pp. 253-259.
2. Gassen, Wim van., and Sego, D. C., "Problems with the Segregation Potential Theory," *Cold Region Science and Technology*, 17, 1989, pp. 95-97.
3. Ito, Y., Vinson, T. S., and Nixon, J. F., "Examination of the Approximation Used to Interpret Freezing Tests and Verification of the Compatibility of the Segregation Potential and Discrete Ice Lens Frost Heave Models," manuscript, 1993.
4. Konrad, J. M., and Morgenstern, N. R., "A Mechanistic Theory of Ice Lens Formation in Fine-Grained Soils," *Canadian Geotechnical Journal*, Vol.17, 1980, pp. 473-486.
5. Konrad, J. M., and Morgenstern, N. R., "The Segregation Potential of a Freezing Soil," *Canadian Geotechnical Journal*, Vol.18, 1981, pp. 482-491.
6. Konrad, J. M., and Morgenstern, N. R., "Prediction of Frost Heave in the Laboratory During Transient Freezing," *Canadian Geotechnical Journal*, Vol.19, 1982, pp. 250-259.
7. Konrad, J. M., and Morgenstern, N. R., "Effects of Applied Pressure on Freezing Soils," *Canadian Geotechnical Journal*, Vol.19, 1982b, pp. 494-505.
8. Konrad, J. M., "Procedure for Determining the Segregation Potential of Freezing Soils," *Geotechnical Testing Journal*, Vol.10, No.2, 1987.
9. Konrad, J. M., "Influence of Freezing Mode on Frost Heave Characteristics," *Cold Region Science and Technology*, 15, 1988, pp. 161-175.
10. McCabe, E. Y., and Kettle, R. J., "Thermal Aspects of Frost Action," In *Proc., Fourth International Symposium on Ground Freezing*, Sapporo, 1985, pp. 47-54.
11. Miller, R. D., "Freezing and Heaving of Saturated and Unsaturated Soils," *Highway Research Record 393*, TRB, National Research Council, Washington, D. C., 1972, pp. 1-11.
12. Loch, J. P., and Kay, B. D., "Water Redistribution in Partially Frozen Saturated Silt Under Several Temperature Gradients and Overburden Loads," *Journal of the Soil Science Society of America*, Vol.42, No.3, 1978.

13. Loch, J. P., "Influence of the Heat Extraction Rate on the Ice Segregation Rate of Soils." *Frost i Jord*, No.20, 1979.
14. Nixon, J. F., "Field Frost Heave Prediction Using the Segregation Potential Concept," *Canadian Geotechnical Journal*, Vol.19, 1982, pp. 526-529.
15. Penner, E., "Aspects of Ice Lens Growth in Soils," *Cold Region Science and Technology*, 13, 1986, pp. 91-100.
16. Reike, R. D., "The Role of the Specific Surface Area and Related Index Properties in the Frost Heave Susceptibility of Soils," M.S.thesis, Oregon State University, Corvallis, 1982.
17. Reike, R. D., Vinson, T. S., and Mageau, D. W., "The Role of the Specific Surface Area and Related Index Properties in the Frost Heave Susceptibility of Soils," In *Proc., Fourth International Conference on Permafrost*, National Research Council, Washington, D. C., 1983.
18. Saarelainen, S., "Modelling Frost Heaving and Frost Penetration in Soils at Some Observation Sites in Finland," *Technical Research Center of Finland (VTT) Publications 95*, 1992.
19. Vinson, T. S., Ahmad, F., and Rieke, R. D., "Factors Important to the Development of Frost Heave Susceptibility Criteria for Coarse-Grained Soils," *Transportation Research Record 1089*, 1984, pp. 124-131.

2.15 Notation

The following symbols are used in this chapter:

A	=	cross sectional area;
d	=	thickness of frozen fringe;
$gradT$	=	temperature gradient below the base of the ice lens;
$gradT_f$	=	temperature gradient at the frozen fringe;
H	=	total heave;
h_T	=	total head loss between base of ice lens and base of soil column;
h_{eb}	=	elevation head at the base of the soil column;
h_{ei}	=	elevation head at the base of the last ice lens;
h_i	=	in-situ heave;
h_s	=	segregational heave;
k_f	=	hydraulic conductivity of frozen fringe;
k_u	=	hydraulic conductivity of unfrozen soil;
L	=	latent heat of fusion of water;
l_u	=	thickness of unfrozen soil;
n	=	porosity;
SP	=	segregation potential;
T_c	=	cold side temperature;
T_{ok}	=	freezing point of pure water ($^{\circ}\text{K}$);
T_{sk}	=	segregation freezing temperature ($^{\circ}\text{K}$);
T_s	=	$T_{sk} - T_{ok}$;
T_w	=	warm side temperature;
(t)	=	at time t ;
u_0	=	suction at the base of the frozen fringe;
u_b	=	porewater pressure at the base of the soil column;
u_i	=	pressure in the liquid film at the base of a growing ice lens;
V_{ff}	=	water flow velocity to the ice lens;
V_w	=	specific volume of water;
v	=	water intake velocity from the unfrozen part of the soil column;
W_w	=	weight of water tank;
X	=	frozen depth;
Δt	=	time interval;
ε	=	amount of water changing phase below 0°C expressed as a decimal fraction; and
γ_w	=	unit weight of water.

3.0 Examination of Approximations Which Support the Segregation Potential and Discrete Ice Lens Frost Heave Models

by

Yuzuru Ito, T.S.Vinson, and J.F.(Derick) Nixon

Abstract

An engineering approach to frost heave relies on the extraction of ice segregation parameters from laboratory step freezing tests. In both the Segregation Potential (SP) and Discrete Ice Lens (DIL) frost heave models, the temperature gradient, water flow velocity in the frozen fringe, and/or the thermal conductivity of the freezing soil, are used to evaluate ice segregation parameters which characterize a freezing soil. However, there is concern over the validity of the frost heave models due, in part, to the data scatter observed in the ice segregation parameters which were evaluated.

One reason for the data scatter may be from the simplifying approximations made to evaluate laboratory test results, the temperature gradients, and water flow velocities. However, the engineering models are already based on some approximations of the conditions that describe a freezing soil. Further approximations in interpreting freezing tests may result in wrongly evaluated ice segregation parameters and, hence, data scatter in the evaluated ice segregation parameters.

The other reason for the data scatter may be due to the validity of the frost heave models itself. In practice, although data scatter may be observed in the evaluated ice segregation parameters, it is usually understood to be the result of reading errors in measurement. No effort has yet been made to understand the scatter in the data set.

It was considered that concerns about the validity of the models may partly be due to the oversimplifications used to evaluate ice segregation parameters. Therefore, an examination of the approximations used to interpret a freezing test was appropriate.

The simplifying approximations made to evaluate the ice segregation parameters were examined. Also, the scatter observed in the evaluated ice segregation parameters was interpreted in terms of the relationship to unfrozen water content in a freezing soil. Finally, the method to obtain reliable ice segregation parameters were demonstrated based on the compatibility of the SP and DIL parameters.

A series of freezing tests were conducted with Calgary silt. Based on the results of the analysis, it was suggested: (1) SP should be defined either by the ratio of water intake velocity and temperature gradient in the frozen fringe (v/G_{ff}), or by the heave velocity divided by 1.09 and the overall temperature gradient of the frozen part of the sample (V_{ff}/G_f'); (2) the scatter observed in the ice segregation parameters appeared to be related to the unfrozen water content of a freezing soil; and (3) the SP and DIL parameters are entirely compatible. As a result, it was anticipated that the reliability of the SP and DIL ice segregation parameters would be increased.

3.1 Introduction

An engineering approach to frost heave relies on the extraction of ice segregation parameters from laboratory step freezing tests. In the Segregation Potential (SP) model (Konrad and Morgenstern 1981), the ice segregation parameter SP was originally defined as

$$SP = \frac{v}{G_{ff}} \quad (3.1)$$

where, v = water intake velocity, and
 G_{ff} = temperature gradient at the frozen fringe.

The v and G_{ff} can be obtained from a simple step freezing test with constant boundary temperatures. In the Discrete Ice Lens (DIL) model (Nixon 1991), the ice segregation parameters was represented by the hydraulic conductivity of a frozen soil at a temperature T ($^{\circ}\text{C}$) as follows:

$$k = \frac{k_0}{\left(\frac{T}{-1^{\circ}\text{C}}\right)^{\alpha}} \quad (3.2)$$

where, k_0 = hydraulic conductivity at -1°C in cm/sec, and
 α = slope of the relationship between k and $(T/-1^{\circ}\text{C})$ on a log-log plot.

The ice segregation parameters k_0 and α can also be determined from a set of step freezing tests.

In order to estimate the SP or DIL ice segregation parameters from laboratory freezing tests, a number of simplifying approximations was made. For example, in the SP model, G_{ff} is replaced by the temperature gradient of the active system (i.e., the unfrozen soil plus the frozen fringe), which was approximately equal to the temperature

gradient of the unfrozen part of the soil (G_u) (Konrad and Morgenstern 1980). In practice, it was also possible to approximate G_{ff} as the overall temperature gradient of the frozen part of a soil (G_f') (Konrad and Morgenstern 1982b). The heave velocity divided by 1.09 (V_{ff}) has been used to replace v . Strictly speaking, this replacement is valid only at the end of transient freezing when v becomes equal to V_{ff} . When the approximations are taken collectively, SP can be defined as the combination of v and V_{ff} , and G_{ff} , G_f' and G_u . It is obvious that the use of different combinations of terms will result in different estimates of SP.

The DIL model appears to predict many of the phenomena which are observed during freezing tests, such as, the early expulsion of water, the location of the ice lenses, etc. The ice segregation parameters in the DIL model, which govern the hydraulic conductivity of a frozen soil, do not depend on factors such as the overburden pressure, suction, and the rate of cooling of the frozen fringe. The parameters governing the hydraulic conductivity of a freezing soil can be estimated from a simple freezing test. However, the procedure to obtain the DIL parameters α and k_o require an approximation of the relationship between the water flow and temperature gradient in the vicinity of the ice lens. In addition, the independence of the DIL parameters on pressure, etc. has not yet been fully confirmed.

It is important to understand the limits of the approximations on which the evaluation of ice segregation parameters in both the SP and DIL models are based. The scatter observed in the evaluation of the ice segregation parameters is undoubtedly related, in part, to the inappropriateness of the approximations which were made to

interpret the laboratory measurements. The scatter may also be related to the test procedures. For example, the ice segregation parameters for both models are most often obtained at the end of transient freezing (the formation of a final ice lens). Unfortunately, the identification of the time associated with this condition is often very subjective (Ito et al. 1989). As a result, the ice segregation parameters greatly depend on the time of their evaluation, especially when v and V_{ff} change rapidly.

It is surprising that favorable comparisons of actual to computed frost heave response have been reported in the literature given the uncertainty which follow the determination of the ice segregation parameters in the laboratory. In order to overcome the uncertainty, a statistical interpretation of the ice segregation parameters was proposed (Kujara 1991). However, a statistical interpretation is only effective when the test data are analyzed with an appropriate procedure. The application of a statistical approach is very difficult if the ice segregation parameters have a great standard error. Combined with the uncertainty of the geologic and ground thermal regime, etc. at a field site, the predicted frost heave must have considerable uncertainty. Prior to the advancement of a probabilistic approach to frost heave, the factors causing the scatter observed in the measurement of ice segregation parameters in the laboratory must be examined.

3.2 Statement of Purpose

The purpose of the research work presented herein is to critically examine the simplifying approximations made to estimate the ice segregation parameters SP , α and k_o . The scope of the work includes (1) a critical examination of the definitions and

approximations used to extract ice segregation parameters, (2) an investigation of the scatter observed in measured ice segregation parameters, and (3) a demonstration of the method to obtain reliable ice segregation parameters.

3.3 Idealization of a Freezing Soil

The model proposed by Gilpin (1980) and Nixon (1991) illustrates an idealized freezing soil and allows one to correlate both the SP and DIL models. In a freezing soil when the frost front is slowly advancing, the temperature distribution may be approximated as in Figure 3.1. Assuming a linear temperature gradient in a freezing soil, the heat balance across the frozen fringe may be written:

At the ice lens,

$$K_f G_f - K_{ff} G_{ff} = LV_{ff} \quad (3.3)$$

and at the frost front,

$$K_{ff} G_{ff} - K_u G_u = n_f L \frac{dz}{dt} \quad (3.4)$$

where, K_f, K_{ff}, K_u = thermal conductivities of frozen soil, frozen fringe and unfrozen soil,

G_f, G_{ff}, G_u = temperature gradients of frozen soil, frozen fringe and unfrozen soil,

L = latent heat of fusion of water,

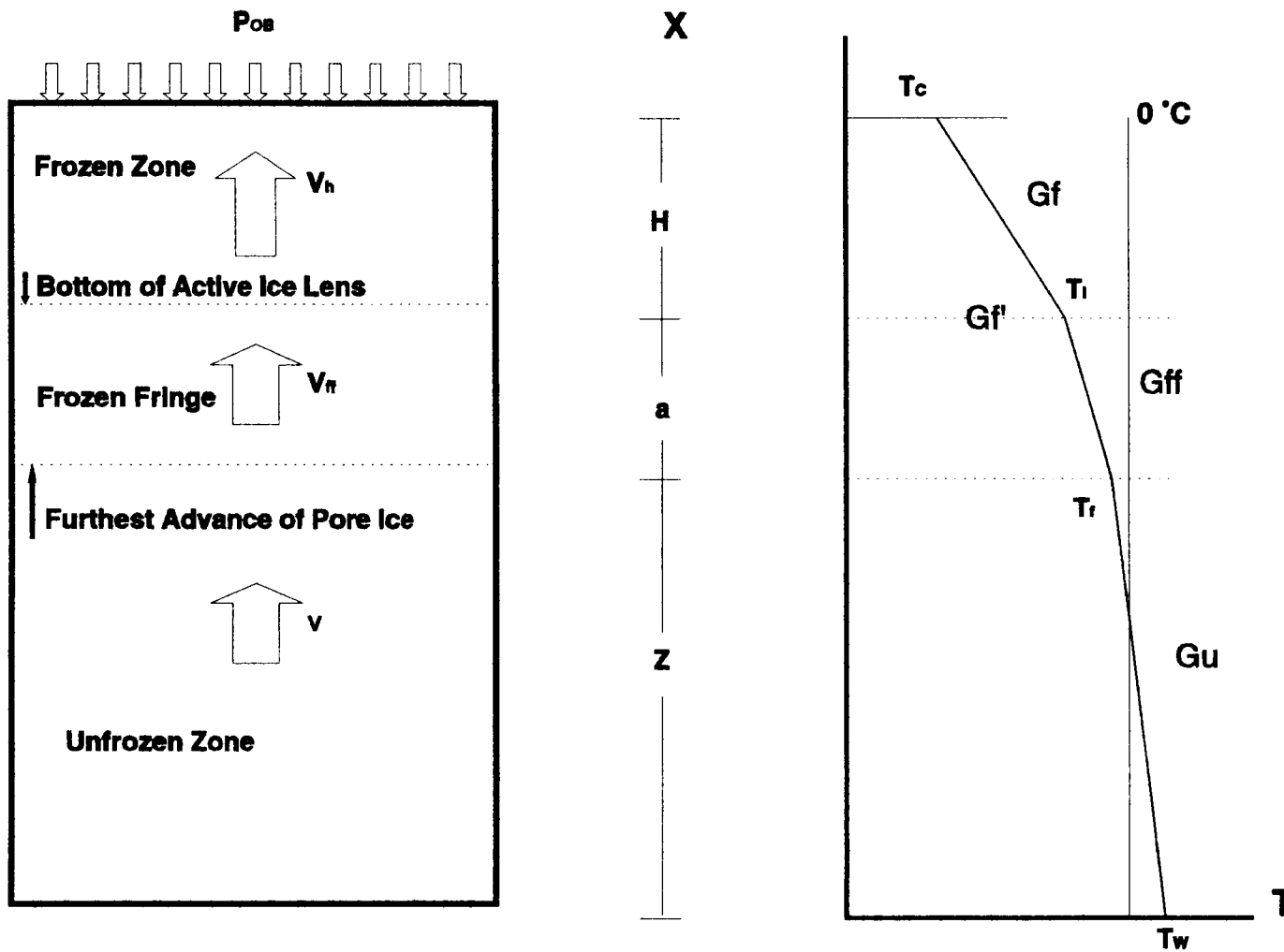


Figure 3.1 Frost Heave Model (modified from Gilpin 1980)

- V_{ff} = water flow velocity to the ice lens base, and
 n_f = fraction of total soil volume changing phase at the frost front.

V_{ff} is expressed as:

$$V_{ff} = k_0(-T)^{-\alpha} \frac{d}{dx} (1.09P_i + \beta T) \quad (3.5)$$

- where, k_0 = hydraulic conductivity of the frozen soil at -1°C ,
 α = slope of the relationship between k and $-T$,
 T = temperature,
 P_i = ice pressure, and
 β = thermodynamic constant.

By setting $dP_i/dx = dT/dx \cdot dP_i/dT$ and replacing dT/dx with G_{ff} , Eq. 3.5 becomes

$$\frac{V_{ff}}{k_0 G_{ff}} (-T)^{-\alpha} - \beta = 1.09 \frac{dP_i}{dT} \quad (3.6)$$

Integration of Eq. 3.6 over the frozen fringe is expressed as

$$\int_{T_l}^{T_f} \left[\frac{V_{ff}}{k_0 G_{ff}} (-T)^{-\alpha} - \beta \right] dT = 1.09 \int_{x=0}^{x=a} dP_i \quad (3.7)$$

- where, T_f = temperature at the warm end of the frozen fringe, and
 T_l = temperature at the base of the ice lens.

At the base of the ice lens or at temperature T_i , P_i is equal to the overburden pressure P_o ; at the frozen fringe - unfrozen soil interface or at T_f , P_i is equal to $(P_u - \beta T_f)/1.09$, where P_u is the suction at the interface. Integrating Eq. 3.7,

$$-\frac{1}{\alpha+1} \frac{V_{ff}}{k_0 G_{ff}} (-T_i)^{\alpha+1} - \beta T_i = 1.09 P_o - P_u \quad (3.8)$$

The pressure profile change when a new ice lens starts to form is illustrated in Figure 3.2. A new ice lens starts to form in the frozen fringe at the location where P_i exceeds P_o plus an additional pressure P_{sep} to initiate separation of the soil skeleton, that is

$$P_i > P_o + P_{sep} \quad (3.9)$$

At the time the ice lens has just jumped to the new location and started to form, one can substitute $dP_i/dx = 0$ in Eq. 3.5. As a result,

$$\frac{V_{ff}}{G_{ff}} = k_0 (-T_i)^{-\alpha} \beta \quad (3.10)$$

Eq. 3.10 suggests that SP is a function of both the segregation freezing temperature and the overall hydraulic conductivity of the frozen fringe (Konrad and Morgenstern 1981). Substituting Eq. 3.10 into Eq. 3.8, the temperature at the base of the ice lens is expressed as

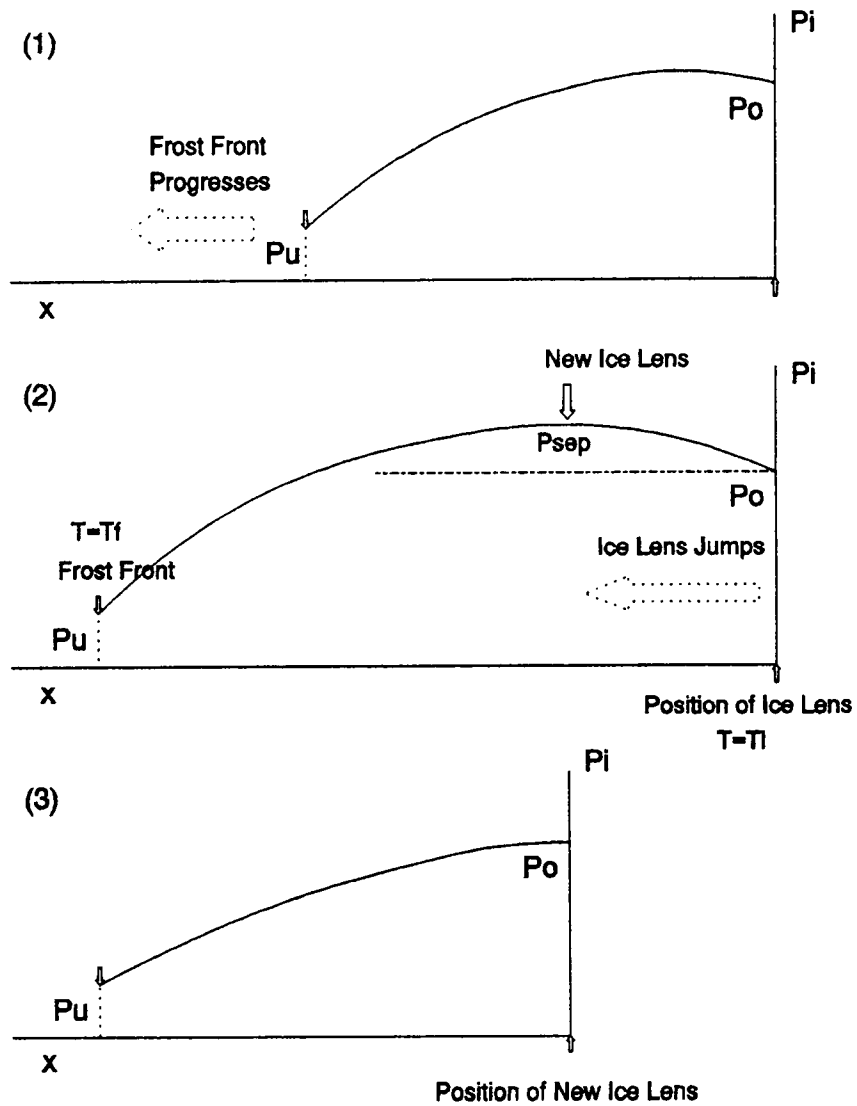


Figure 3.2 Ice Pressure Change across the Frozen Fringe during an Ice Lens Cycle (modified from Gilpin 1980)

$$T_i = -\frac{1}{\beta} \frac{\alpha+1}{\alpha} (1.09P_o - P_u) \quad (3.11)$$

Substituting Eq. 3.11 into Eq. 3.10 eliminates T_i and SP can be expressed as a function of the pressures and DIL parameters:

$$SP = \frac{V_{ff}}{G_{ff}} = k_0 \frac{\beta^{1+\alpha}}{\left(\frac{\alpha+1}{\alpha} (1.09P_o - P_u)\right)^\alpha} \quad (3.12)$$

The significance of Eq. 3.12 is that the overburden pressure P_o and suction P_u can now be treated as one term. Two of the three factors which govern SP, namely, overburden pressure and suction, are effectively reduced to one in Eq. 3.12.

Combining Eq. 3.12 with the heat balance equation across the frozen fringe (Eq. 3.1), the following equation is obtained:

$$\frac{K_f}{K_{ff}} \left(\frac{G_f}{V_{ff}} - \frac{L}{K_f} \right) = \frac{\left(\frac{\alpha+1}{\alpha} (1.09P_o - P_u)\right)^\alpha}{k_0 \beta^{1+\alpha}} = \frac{1}{SP} \quad (3.13)$$

Nixon (1991) simplified Eq. 3.13 to extract the ice segregation parameters α and k_0 .

It is clearly demonstrated from Eqs. 3.12 and 3.13 that the SP and DIL parameters are compatible. Comparing Eq. 3.12 with Eq. 3.13, it is understood that DIL parameters can be obtained either from SP (Eq. 3.12) or Eq. 3.13. If G_{ff} can be obtained

with great accuracy, Eq. 3.12 is recommended. However, it is usually difficult to measure G_{ff} with great accuracy. Therefore, it is proposed that DIL parameters be evaluated from Eq. 3.13 which requires G_f instead of G_{ff} .

The heat balance equation (Eq. 3.4) provides another relationship between the temperature gradients. The right hand side of Eq. 3.4 approaches zero when the final ice lens starts to form. The resulting relationship between G_{ff} and G_u produces

$$SP = \frac{V_{ff} K_{ff}}{G_u K_u} \quad (3.14)$$

Eq. 3.14 means that G_f can replace G_{ff} only if K_{ff} is approximately equal to K_f .

3.4 Examination of Simplifying Approximations Used to Interpret Freezing Tests

Approximation of G_{ff} to evaluate SP

As previously noted in Eq. 3.1, SP was originally defined as the ratio of the water intake velocity (v) to the temperature gradient in the frozen fringe (G_{ff}). However, in the first report which supported the uniqueness of SP (Konrad and Morgenstern 1980), the temperature gradient across the active system, which was close to G_u , was used in place of G_{ff} . Following the initial success in verifying the SP concept from a series of the freezing tests, Konrad and Morgenstern (1980, 1981, 1982, 1982b) further developed the model. The frost heave test cell used to obtain the data for the reports had only four to six thermistors along the cell sides (Konrad 1980). Since the thermistor intervals were

much greater than the thickness of a frozen fringe, it can easily be recognized that G_{ff} reported by Konrad and Morgenstern was influenced by the temperature distribution in the frozen and unfrozen part of the soil surrounding the frozen fringe. While the contribution of the first series of papers was great, they might give the impression that any temperature gradients in the vicinity of the frozen fringe could be used to represent G_{ff} .

Nixon (1982) interpreted G_{ff} as the temperature gradient adjacent to the growing ice lens and later as G_f (1987). Other researchers made different assumptions: Fukuda et al. (1988) used the temperature gradient at 0 °C to interpret his field data; Ito et al. (1989) used G_u ; Svec (1989) used the temperature gradients defined by the sample end temperatures to report his frost heave tests in terms of SP. Konrad (1987) again argued that G_{ff} is close to G_u at the formation of the final ice lens if the thermal properties of the frozen fringe and unfrozen parts are identical. The numerous approximations have been made simply because it is more difficult to measure G_{ff} than G_f and G_u .

The variations in SP caused by the use of different temperature gradients may be as great as 30 % (based on the authors' experience). This variation, when combined with errors associated with inappropriate test conditions (e.g., such as the fluctuation of the temperature readings along the cell walls caused by improper insulation of the test cell) will result in useless values of SP for field frost heave prediction. Therefore, it is very important to examine the simplifying approximations made in the estimation of SP based on the different assumptions for G_{ff} .

Definition of SP

Several combinations of flow velocities and temperature gradients have been used to define SP. Although the original form was defined as Eq. 3.1, Nixon (1987) proposed an alternative definition of SP stating that it is the water flow in the frozen fringe not the flow into the fringe which must be related to G_{ff} :

$$SP = \frac{V_{ff}}{G_{ff}} \quad (3.15)$$

This definition differs from Eq. 3.1 except at the end of transient freezing when the water intake velocity (v) and the flow velocity in the frozen fringe (V_{ff}), or heave velocity divided by 1.09 are equal. In fact, the two flow velocities, v and V_{ff} , are distinct and measurable at both sides of the frozen fringe. It is understood from Eq. 3.1 that G_{ff} reflects the water flow into the fringe, while in Eq. 3.15 it reflects the water flow at the cold side of the fringe. Therefore, it follows that the two velocities relate to the temperature gradient at each location. In the strictest sense, SP may be defined at the warm and cold sides of the frozen fringe:

At the frozen fringe - unfrozen soil interface,

$$SP_{T_f} = \frac{v}{G_{ff-T_f}} \quad (3.16)$$

where, G_{ff-T_f} = temperature gradient of the frozen fringe close to the frost front.

At the frozen soil behind the ice lens - frozen fringe interface,

$$SP_{T_i} = \frac{dH/dt}{1.09 G_{ff-T_i}} = \frac{V_{ff}}{G_{ff-T_i}} \quad (3.17)$$

where, G_{ff-T_i} = temperature gradient of the frozen fringe close to the ice lens.

The SP defined by Eq. 3.1, in which the water intake velocity was of concern, is a simplification of Eq. 3.16; the alternative definition (Eq. 3.15), in which the flow velocity at the base of the ice lens is significant, is a simplification of Eq. 3.17. Therefore, it is understood that the original definition (Eq. 3.1) and the alternative definition (Eq. 3.15) are expressing the responses of the continuous temperature and water flow changes in the frozen fringe at each side of the region.

Recalling the discussion previously presented, there are two flow velocities (v , V_{ff}) and three temperature gradients (G_f , G_{ff} , G_u) that can be considered when evaluating SP. As a result, there are six possible combinations of the flow velocity and temperature gradient which may be considered when evaluating SP. However, only the two forms of SP given in Eqs. 3.16 and 3.17 (or Eqs. 3.1 and 3.15) represent the true ice segregation parameters for the soil.

DIL parameters α and k_0

Similar approximations were made to extract DIL parameters (Nixon 1991). In Eq. 3.13, two approximations were used: (1) the thermal conductivities of the frozen soil

behind the ice lens and the frozen fringe are equal ($K_f = K_{ff}$), and (2) G_f is approximately equal to G_{ff} . As a result, the DIL parameters were initially evaluated from the following relationship:

$$\frac{G_{ff}}{V_{ff}} - \frac{L}{K_f} = \frac{\left(\frac{\alpha + 1}{\alpha} (1.09P_o - P_u) \right)^\alpha}{k_o \beta^{1+\alpha}} \quad (3.18)$$

Using Eq. 3.18, Nixon (1991) successfully demonstrated the method to extract the DIL parameters.

Reliability and Compatibility of the Ice Segregation Parameters

As stated in the previous section, precise measurement of the temperature gradient of the frozen fringe is not possible with the conventional temperature monitoring method. With the conventional system the temperature in the cell wall very close to the freezing specimen is measured, but it is not the temperature inside the specimen. A method to monitor the temperature inside the sample was presented by Akagawa (1990), but this method is so complicated that it is not practical. Therefore the evaluation of temperature gradient of the frozen fringe with Eq. 3.1 appears to have an inherent limitation in accuracy. Eq. 3.13, which uses the more accurately measured temperature gradient of the frozen soil, appears to have an advantage over Eq. 3.1. However, it may be difficult to make a reasonable assumption for K_f/K_{ff} . Further, even if the tests and analysis were conducted properly with an accurate procedure, there may be a scatter in the parameters

evaluated which cannot be explained by the inappropriateness of the approximations discussed above. Three explanations are possible to understand the scatter: (1) it is caused by the local temperature disturbances, (2) it is due to the error in readings of both the temperature and water intake velocity around their mean values, and (3) the parameters are all real responses of the freezing soil. In practice, the first and second explanations are advocated and the measured ice segregation parameters are averaged to obtain the design parameter. If there is evidence to support the third explanation, no justification to simply average all the data points would be necessary.

Two possibilities to support the third explanation may be advanced by considering Eqs. 3.12 and 3.13. First, the information related to the unfrozen water content might be used. According to the DIL model, the parameters α and k_0 , which define the unfrozen water content, are independent of the pressure. However, if the unfrozen water were influenced by pressure, α and k_0 might not be independent of pressure. Therefore it is possible that the scatter in the ice segregation parameters α and k_0 is due to the change in unfrozen water content. The estimation of unfrozen water in the frozen part of the sample freezing soil is relatively simple and is based on: (1) knowledge of the total water content, (2) in situ heave (h_i), and (3) frozen depth of the sample.

Second, it is obvious from Eqs. 3.12 and 3.13 that the DIL parameters α and k_0 can be evaluated if a set of reliable SP is available. Conversely, SP can be evaluated if a pair of reliable DIL parameters are available. Therefore, SP and DIL parameters should be compatible if they are evaluated correctly. In other words, the scatter of SP

data points obtained from Eqs. 3.1 or 3.15 can be confirmed if the same scatter is observed in the data points estimated from Eq. 3.13. It is considered that ice segregation parameters may be more reliable when evaluated from both Eqs. 3.12 and 3.13.

3.5 Research Program

To examine the concerns discussed in the previous section regarding the simplifying approximations made to obtain ice segregation parameters, a set of frost heave test result with different temperature gradients and overburden pressures was analyzed for the following purpose:

- (1) To interpret the observed scatter in the ice segregation parameters; the relation with the unfrozen water content was examined by analyzing the parameters governing the amount of unfrozen water; the unfrozen water content was also used to provide information to estimate K_f and K_{ff} .
- (2) To verify the several approximations currently used to evaluate ice segregation parameters (SP, α and k_o); six different combinations of flow velocities (v , V_{ff}) and temperature gradients (G_f' , G_{ff} , G_u) were compared.
- (3) To examine the scatter observed in the best estimated SP, α and k_o parameters by considering their relationship to the unfrozen water content.
- (4) To demonstrate the relationship and compatibility of SP and DIL parameters and propose a reliable method to evaluate SP and DIL ice segregation parameters.

3.6 Laboratory Test

Fifteen freezing tests were conducted with Calgary silt (Table 3.1, Figure 3.3) under various temperature gradients and overburden pressures (Table 3.2). The samples were prepared by consolidating a slurry of Calgary silt under 300 kPa. Step freezing tests were performed in which, following a - 10 °C thermal shock to nucleate ice formation, both the top and bottom plate temperatures were maintained constant during the tests. For a number of tests, the hydraulic conductivity of the soil was measured with the falling head method prior to freezing. The details of the test procedure and the test equipment are described by Ito et al. (1993). The ice segregation parameters (SP, α , k_0) were analyzed in terms of the combined pressure $1.09P_o - P_u$.

3.7 Method to Analysis the Freezing Test Result

Frost heave and water intake

The total heave (H) was measured directly with an LVDT and V_{ff} was calculated from H . The water intake velocity (v) was continuously monitored with a weight change device and a higher degree of accuracy was maintained throughout the freezing test. The segregational heave h_s is 1.09 times the total water flow into the soil per unit area of the specimen. In situ freezing (h_i) is computed by subtracting h_s from H .

Unfrozen water parameters

Nixon (1991) presented an equation to estimate the amount of water frozen in the frozen fringe assuming a linear temperature distribution in the frozen part of the soil.

Table 3.1 Physical Properties of Calgary Silt

Specific Gravity	2.65
Grain Size, %	
Gravel (5.0mm <)	0
Sand (0.075-5.0mm)	16
Silt (0.002-0.075mm)	58
Clay (<0.002mm)	26
Consistency, %	
Liquid Limit	23.7
Plastic Limit	15.4

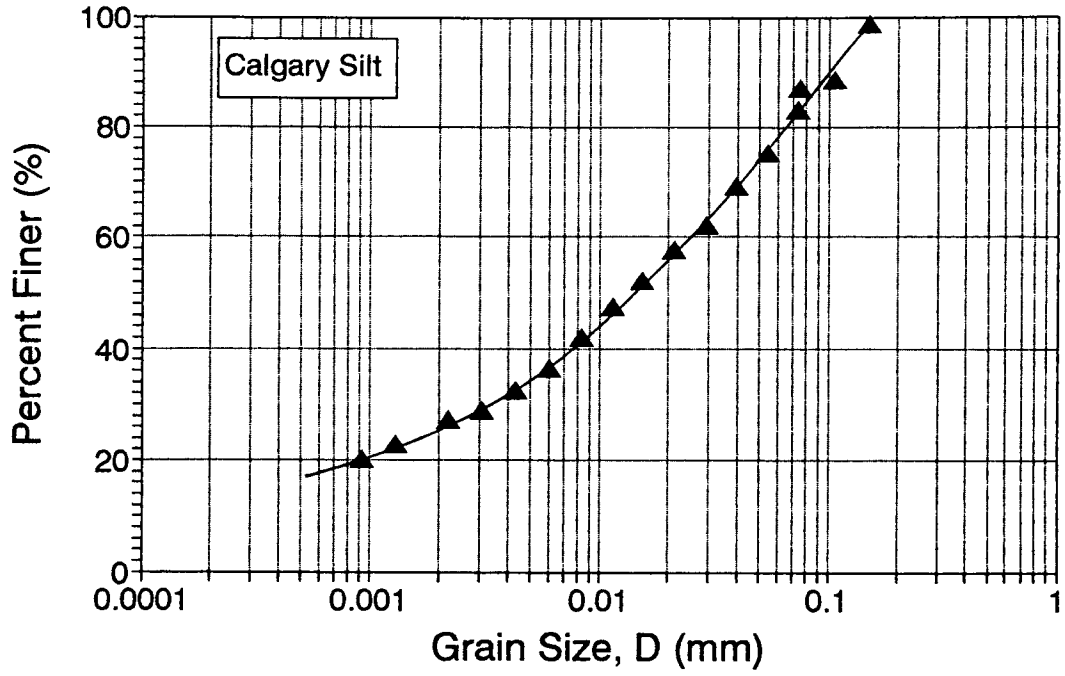


Figure 3.3 Grain Size Distribution of Calgary Silt

Table 3.2 Test Boundary Conditions

Test No.	Tw (°C)	Tc (°C)	Overburden Pressure (kPa)	Specimen Height (mm)
1	+1.6	-3.7	30	80
2	+1.6	-3.7	60	80
3	+1.6	-3.7	90	80
4	+1.6	-3.7	15	80
5	+1.6	-3.7	120	80
6	+1.6	-3.7	45	80
7	+1.6	-3.7	75	80
8	+0.4	-1.3	10	99
9	+0.7	-2.35	90	95
10	+0.65	-2.35	195	95
11	+0.7	-2.35	45	100
12	+0.4	-1.65	100	119
13	+0.5	-1.65	160	110
14	+0.4	-1.3	45	110
15	+1.6	-4.6	45	103

This equation can be extended to the total frozen part of soil assuming, the ice distribute uniformly in the frozen soil. The amount of water in the frozen part of soil is given by

$$H_f = n \int_0^d (1 - W_u) dx \quad (3.19)$$

where, n = porosity,
 d = thickness of the frozen part of the soil, and
 W_u = proportion of water remaining unfrozen in the frozen soil.

Using the equation presented by Anderson et al. (1972), W_u can be expressed as a function of temperature T as

$$W_u = \frac{w_u}{w_{tot}} = \frac{A(-T)^B}{w_{tot}} \quad (3.20)$$

where, w_u = unfrozen water content,
 w_{tot} = total water content, and
 A, B = constants.

Thus, Eq. 3.19 becomes

$$H_f = nd \left(1 + \frac{A}{w_{tot}(T_f - T_c)(B+1)} ((-T_f)^{B+1} - (-T_c)^{B+1}) \right) = \frac{h_i}{0.09} \quad (3.21)$$

where, T_c = cold side temperature.

Assuming A and B are independent of the boundary conditions, they can be estimated from a series of the freezing tests.

Thermal conductivity

Knowledge of the amount of unfrozen water in the frozen soil can also be used to estimate the thermal conductivity. Based on Johansen's method (Frivik 1980), the thermal conductivity of the frozen soil can be expressed as a linear function of the unfrozen water (ISGF 1991),

$$K_{f(u)} = k_f + (k_u - k_f)W_u \quad (3.22)$$

where, $K_{f(u)}$ = thermal conductivities of the frozen soil and the frozen fringe,
 $k_{u(f)}$ = thermal conductivities of the frozen (no unfrozen water) and unfrozen soils.

The method to compute k_f and k_u is presented in Table 3.3.

Temperature distribution

Two methods were used to estimate the temperature gradient across the frozen fringe (Figure 3.4). The method explained by Konrad (1987) is most often used. In the present study, another method was compared with the conventional method. This method utilized the least square fitting of the temperature distribution measured by the thermistors along the cell wall:

Table 3.3 Thermal Conductivity of a Freezing Soil (after ISGF 1991)

$$k_u = k^\circ + (k_u^1 - k^\circ) \cdot K_e,$$

$$\text{or } k_f = k^\circ + (k_f^1 - k^\circ) \cdot K_e$$

where,

k°	$= 0.034 \cdot n^{-2.1}$	dry conductivity
k_u^1	$= 0.57^n \cdot k_s^{(1-n)}$	unfrozen saturated
k_f^1	$= 2.3^n \cdot k_s^{(1-n)}$	frozen conductivity
K_e	$= S_r$	frozen
	$= 0.68 \cdot \log S_r + 1$	clay content < 2%, unfrozen
	$= 0.94 \cdot \log S_r + 1$	clay content > 2%, unfrozen
K	$= k_f + (k_u - k_f) \cdot w_u / w_{\text{tot}}$	consideration of the unfrozen water content
q		quartz content
S_r		degree of saturation
w_{tot}		total water content (% by dry weight)
w_u		unfrozen water content (% by dry weight)
n		porosity
K_e		Kersten number
k_s		particle conductivity
K, k		thermal conductivity (W/mK)

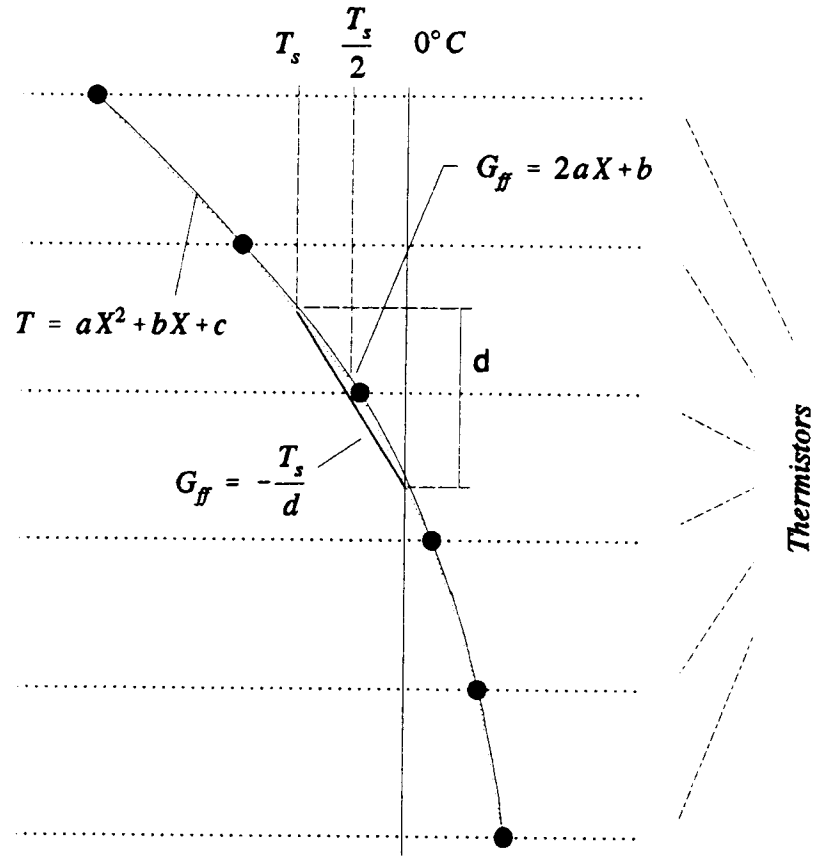


Figure 3.4 Calculation of Temperature Gradient

$$T = aX^2 + bX + c \quad (3.23)$$

where, T = temperatures,
 X = locations, and
 a, b, c = constants.

and at the location X where $T = T_s/2$, the temperature gradient of the frozen fringe is computed as

$$G_{ff} = \frac{dT}{dX} = 2aX + b \quad (3.24)$$

The temperatures used in the computation are based on the thermistors located in the frozen soil on both sides of the cell. Next the same computation was performed with one additional temperature point which is in the unfrozen part adjacent to 0 °C. The same calculation was carried out by changing T and Y in Eq. 3.24. In all, the four results were averaged to obtain the best estimated G_{ff} in each time step.

In the present study, the temperature of both specimen ends was monitored several mm behind the specimen ends. Thus, the temperature gradient in the frozen zone behind the ice lens (G_f) was best estimated by the equation:

$$G_f = \frac{-(T_c - T_l)}{l_f + t_{top}} \quad (3.25)$$

where, l_f = thickness of the frozen soil behind the ice lens, and

t_{top} = thickness of the cold plate.

The overall temperature gradient of the frozen zone including the frozen fringe G_f' was estimated as

$$G_f' = \frac{T_f - T_c}{l_f + t_{top}} \quad (3.26)$$

In a similar way, the temperature gradient in the unfrozen zone G_u was estimated as

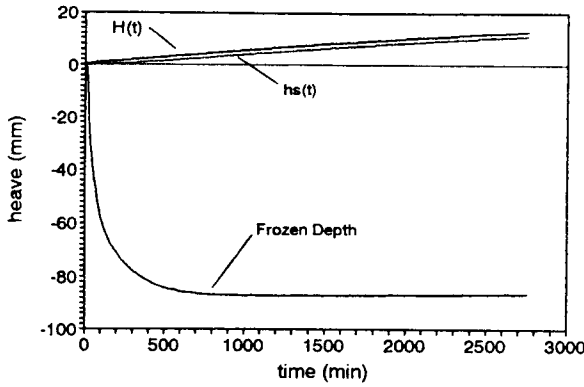
$$G_u = \frac{T_w - T_f}{l_u + t_{base}} \quad (3.27)$$

where, t_{base} = thickness of the bottom plate.

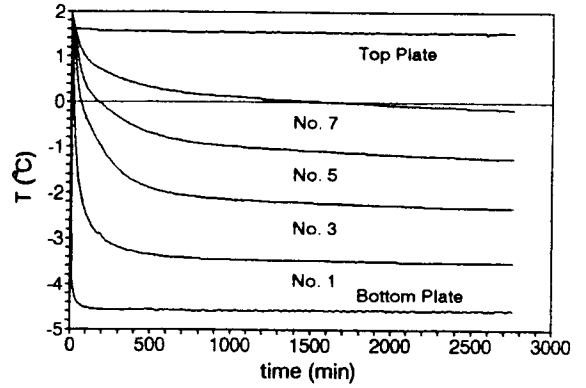
3.8 Test Results and Analysis

Example of the Test Results

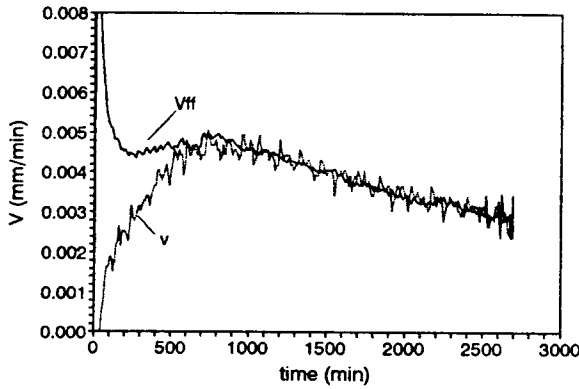
Figure 3.5 (test C-8) represents an example of the test results. The total heave (H) based on an LVDT reading, the segregational heave (h_s), which was computed from the water intake to the freezing soil, and the frozen depth are illustrated in Figure 3.5a. Figure 3.5a is used to compute the heave velocities (Figure 3.5c). Figure 3.5b shows several thermistor readings along the cell wall. Figure 3.5b was used to compute the temperature gradients (Figure 3.5d) in the freezing soil by Eqs. 3.26 through 3.29. The rate of cooling (Figure 3.5e) was also computed from Figure 3.5b. Figure 3.5f illustrates



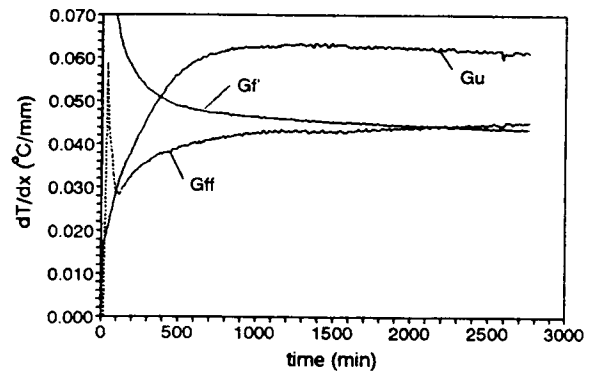
(a) Heave and Frozen Depth



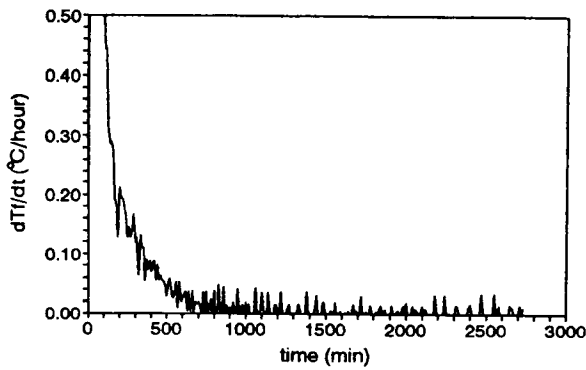
(b) Temperature Readings vs. time



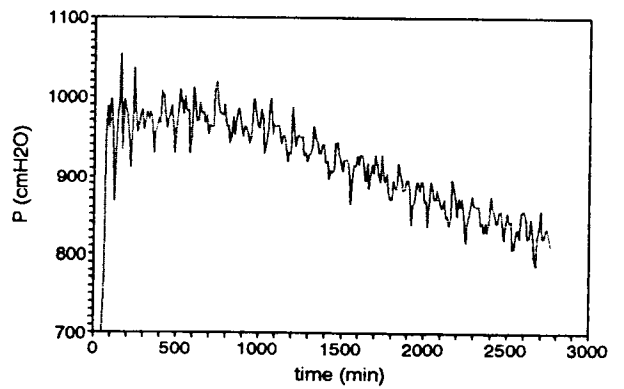
(c) Vff and v



(d) temperature gradients



(e) Rate of Cooling



(f) 1.09Po-Pu

Figure 3.5 Results from Test C-8

the pressure term $1.09P_o - P_u$ which was computed from overburden pressure, unfrozen length of the specimen or initial specimen length minus frozen depth (Figure 3.5a), and water intake velocity (Figure 3.5c).

In Test C-8 through C-15, the location of the base of the final ice lens was measured after the freezing test. Knowing the locations of the ice lens base, T_i was estimated from the temperature readings along the cell wall (Figure 3.5b). Although T_i was not consistent, an average value of $T_i = -0.3$ °C was used to compute SP for all freezing tests.

Unfrozen Water in the Frozen Zone

Figure 3.6 presents the overall unfrozen water content in the frozen part of a freezing soil. As can be seen, the unfrozen water content is in a range from 20 to 60 %. It was anticipated that the warmer the cold side temperature the greater the unfrozen water content in the frozen soil. The results presented verify this hypothesis. An interesting but reasonable observation is that the greater the overburden pressure the greater the unfrozen water content. This result indicates that the parameters governing hydraulic conductivity of a frozen soil are also influenced by the overburden pressure.

Figure 3.7 presents the relationship for the A and B parameters computed by Eq. 3.20. It was anticipated that there was only one set of A and B parameters since the unfrozen water in the frozen soil was assumed to be independent of the boundary condition. Figure 3.7a presents the A-B relationship when the overburden pressure changed under a constant temperature boundary condition $T_c = -3.71$ °C / $T_w = 1.6$ °C.

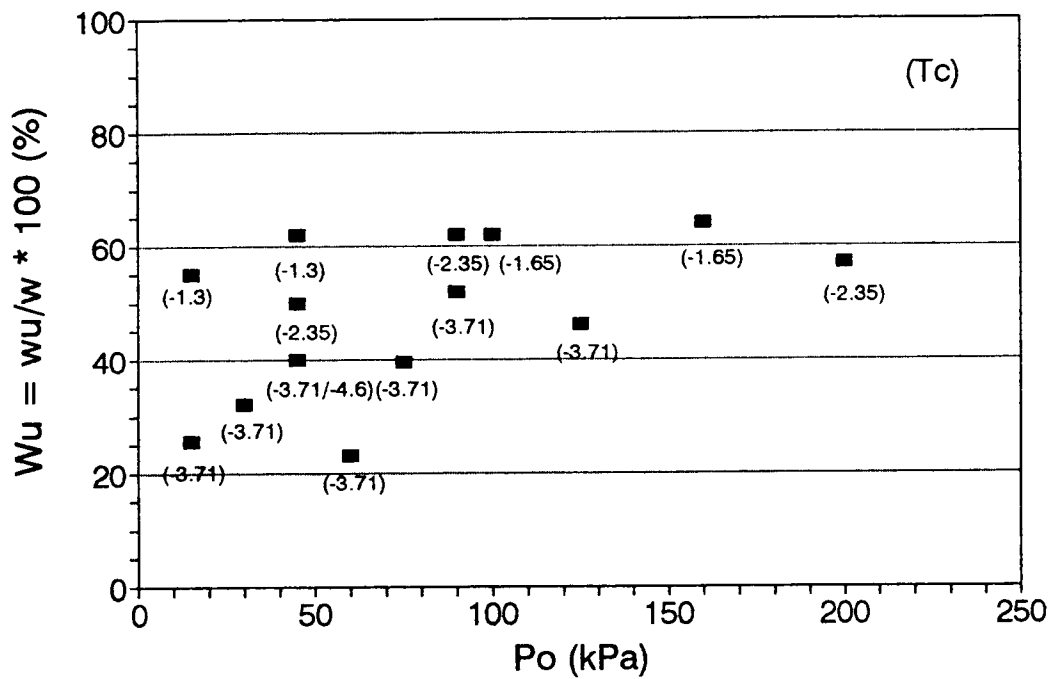
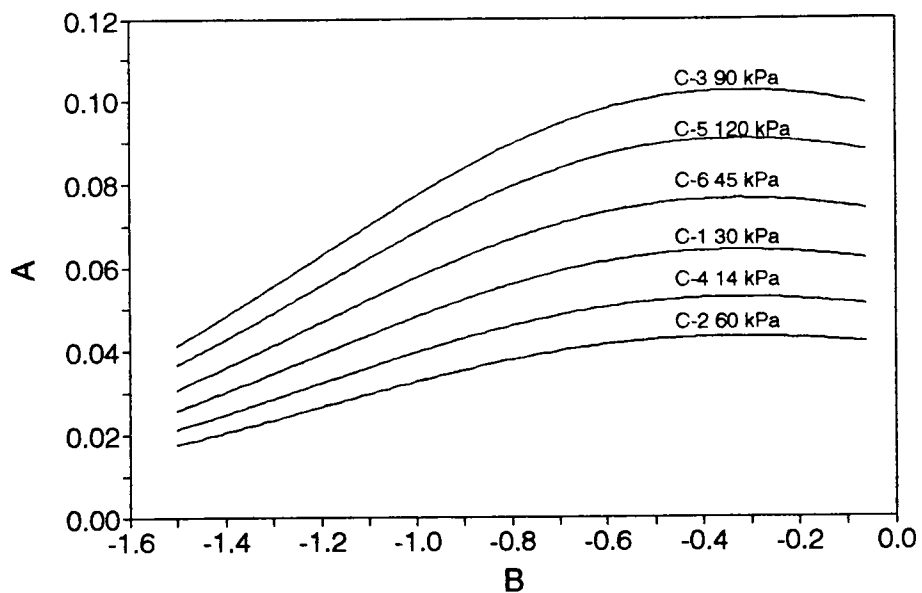
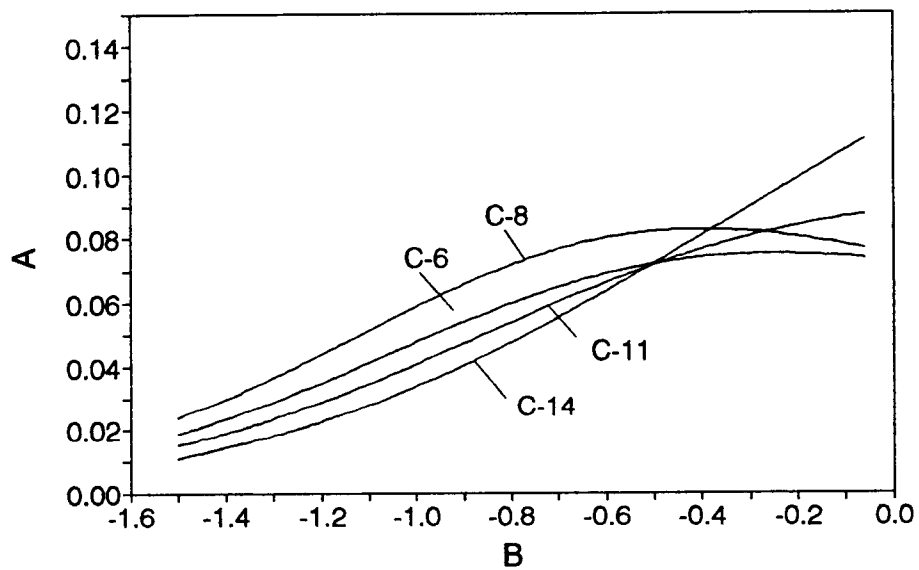


Figure 3.6 Unfrozen Water Content of the Frozen Soil



(a) A and B under $T_c = -3.7^\circ\text{C}$ / $T_w = +1.6^\circ\text{C}$



(b) A and B under 45 kPa

Figure 3.7 Relationships between A and B Constants

The six relationships shown parallel to each other indicate there was not a unique relationship between A and B. This means A and B are not independent of overburden pressure. In addition, the six lines appeared to shift toward the A direction. It may be stated that A may be a function of the overburden pressure. However, the order of the six lines are not necessarily related to the pressure. The relative position is considered to be an influence of slight differences in sample preparation.

Figure 3.7b shows the A and B relationship when the boundary temperatures changed while maintaining a constant 45 kPa overburden pressure. The result is not conclusive, however, it appears that there is an approximate intersection or a set of A and B in Figure 3.7a. Therefore, it may be inferred that A and B are independent of the temperature boundary condition.

The two figures indicate that A and B may change with different overburden pressures, but do not change with the temperature boundary conditions. Since A and B are related to α and k_o , it is suggested that α and k_o also have some relationship to overburden pressure. As A is anticipated to have a strong correlation with k_o , the overburden pressure should have a greater influence on k_o compared to α .

Thermal conductivity

Assuming $k_s = 2.5$ W/mK, $K_e = 1.0$ and $n = 0.33$ in Eq. 3.22 and Table 3.3, Eq. 3.22 becomes

$$K_{eff} = 2.43 - 0.9 * W_u \quad (W/mk) \quad (3.28)$$

The relationship of Eq. 3.28 is illustrated in Figure 3.8. Knowing the unfrozen water content, Eq. 3.28 or Figure 3.8 can be used to estimate the thermal conductivity of the frozen part of soil. As T_l was approximately -0.3 °C in the tests, W_u at the frozen fringe is estimated at 80 % and K_{ff} is assumed to be 1.71 (W/mK). Based on the unfrozen water content in the frozen part, K_f was then estimated for each soil.

Temperature Gradients

An example of the temperature gradient change with time was shown in Figure 3.5d. Although the temperature gradients in various parts of a freezing soil converged to a constant value, during the transient freezing phase they were markedly different. The results presented in Figure 3.5d indicate that the improper choice of temperature gradient to evaluate ice segregation parameters will not only cause an error in the parameters but will also produce meaningless values for field prediction.

Table 3.4 lists the various temperature gradients evaluated at the end of transient freezing. There was less than 10 % difference in the values of G_{ff} obtained by the conventional method and the method proposed in Eq. 3.24. Further, as shown in Figure 3.9, both methods to calculate G_{ff} exhibit similar trends throughout a freezing test. There is no evidence which strongly supports the use of one method over the other. This means the ice segregation parameters evaluated from this type of freezing test system may have up to a 10 % of error which originates from the estimated temperature.

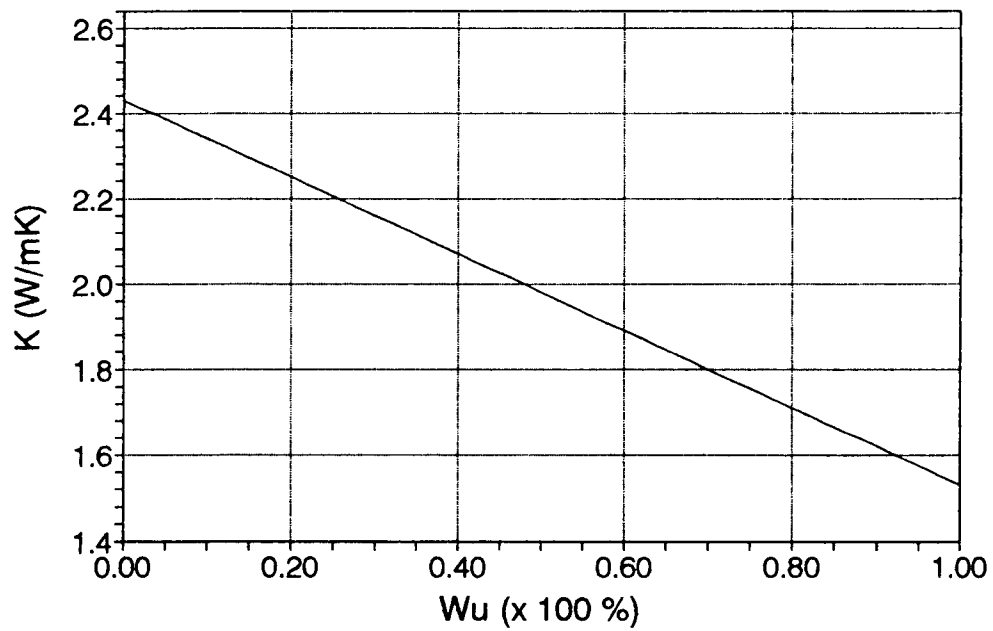


Figure 3.8 Thermal Conductivity versus Unfrozen Water Content

Table 3.4 Various Temperature Gradients at the End of Transient Freezing

Test No.	t	Gff(Conv.)	Gff(Eq.3.24)	Gf	Gf'	Gu	v	Vff	1.09Po-Pu
1	600	0.037	0.040	0.049	0.047	0.049	0.0066	0.0066	851
2	600	0.039	0.040	0.045	0.044	0.058	0.0062	0.0062	834
3	600	0.040	0.043	0.048	0.047	0.053	0.0048	0.0048	1295
4	600	0.036	0.038	0.046	0.045	0.055	0.0073	0.0073	532
5	600	0.039	0.042	0.048	0.047	0.053	0.0042	0.0042	1562
6	600	0.038	0.040	0.047	0.046	0.049	0.0058	0.0060	874
7	600	0.040	0.041	0.048	0.047	0.049	0.0045	0.0045	1138
8	1200	0.011	0.012	0.015	0.014	0.017	0.0029	0.0029	374
9	750	0.022	0.022	0.027	0.026	0.029	0.0026	0.0027	1398
10	800	0.024	0.023	0.027	0.026	0.029	0.0016	0.0017	2359
11	850	0.020	0.020	0.026	0.025	0.029	0.0029	0.0031	755
12	1000	0.011	0.012	0.017	0.016	0.014	0.0016	0.0017	1365
13	900	0.013	0.013	0.018	0.017	0.016	0.0011	0.0012	1973
14	1000	0.010	0.010	0.015	0.013	0.012	0.0021	0.0022	827
15	600	0.040	0.044	0.049	0.048	0.059	0.0045	0.0047	1011
	min	°C/mm	°C/mm	°C/mm	°C/mm	°C/mm	mm/min	mm/min	cmH ₂ O

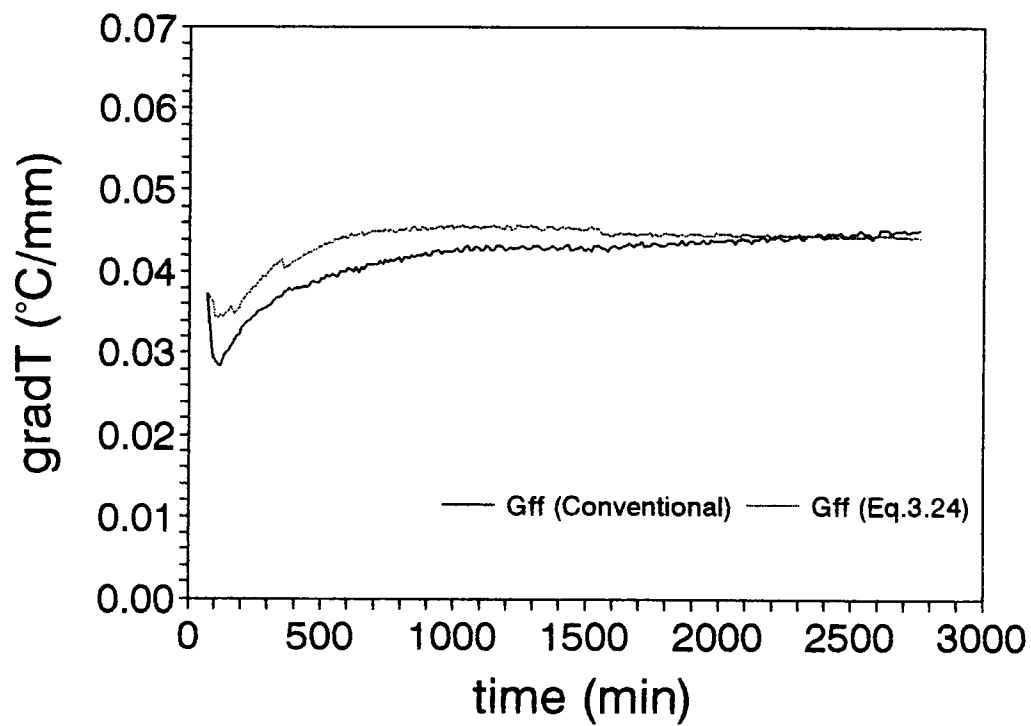


Figure 3.9 Temperature Gradients of the Frozen Fringe

Figure 3.10 shows the relationship between G_{ff} by the conventional method and other temperature gradients listed in Table 3.4. For Calgary silt substitution of G_{ff} by G_f , G_f' or G_u caused 20 to 40 % greater temperature gradients. In other words, for Calgary silt these simplifications would result in ice segregation parameters 15 to 30 % less than the true values. Consequently, G_{ff} should not simply be substituted by G_f , G_f' , or G_u to compute ice segregation parameters. If an approximate linear relationship between the temperature gradient is confirmed, however, G_{ff} may be estimated from G_f , G_f' , and G_u . Figure 3.10 also indicated that there was practically no difference between G_f and G_f' .

Segregation potential

Figures 3.11a, 3.11b, and 3.11c illustrate the SP defined by the ratio of V_{ff} versus G_f' , G_{ff} , and G_u . The shallower the overall temperature gradient of the test the greater the difference between G_f' and G_{ff} or G_u . When the test was conducted with the steeper temperature gradient (Figure 3.11a), V_{ff}/G_f' reached a peak at the end of transient freezing then dropped. But when a test was conducted with a shallower temperature gradient, V_{ff}/G_f' was nearly constant through an entire test period. On the other hand, in V_{ff}/G_{ff} and V_{ff}/G_u this contrast was not detected.

Figures 3.11d, 11e and 11f illustrate the SP defined by the ratio of v versus G_f' , G_{ff} and G_u . When the test was conducted with the steeper temperature gradient, v/G_f' , v/G_{ff} , and v/G_u reached a peak then dropped. But when the test was conducted with the shallower temperature gradient v/G_f' increased in the transient freezing period while v/G_{ff} and v/G_u stayed approximately constant; especially v/G_{ff} (Figure 3.11f).

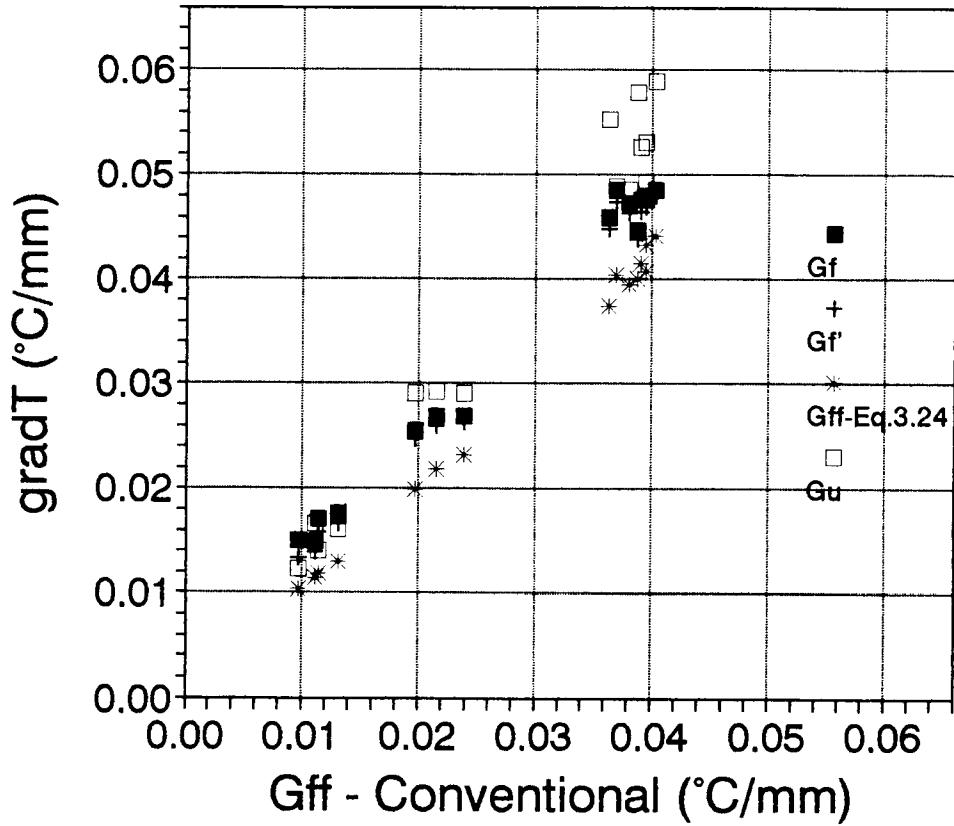


Figure 3.10 Relationships between the Various Temperature Gradients

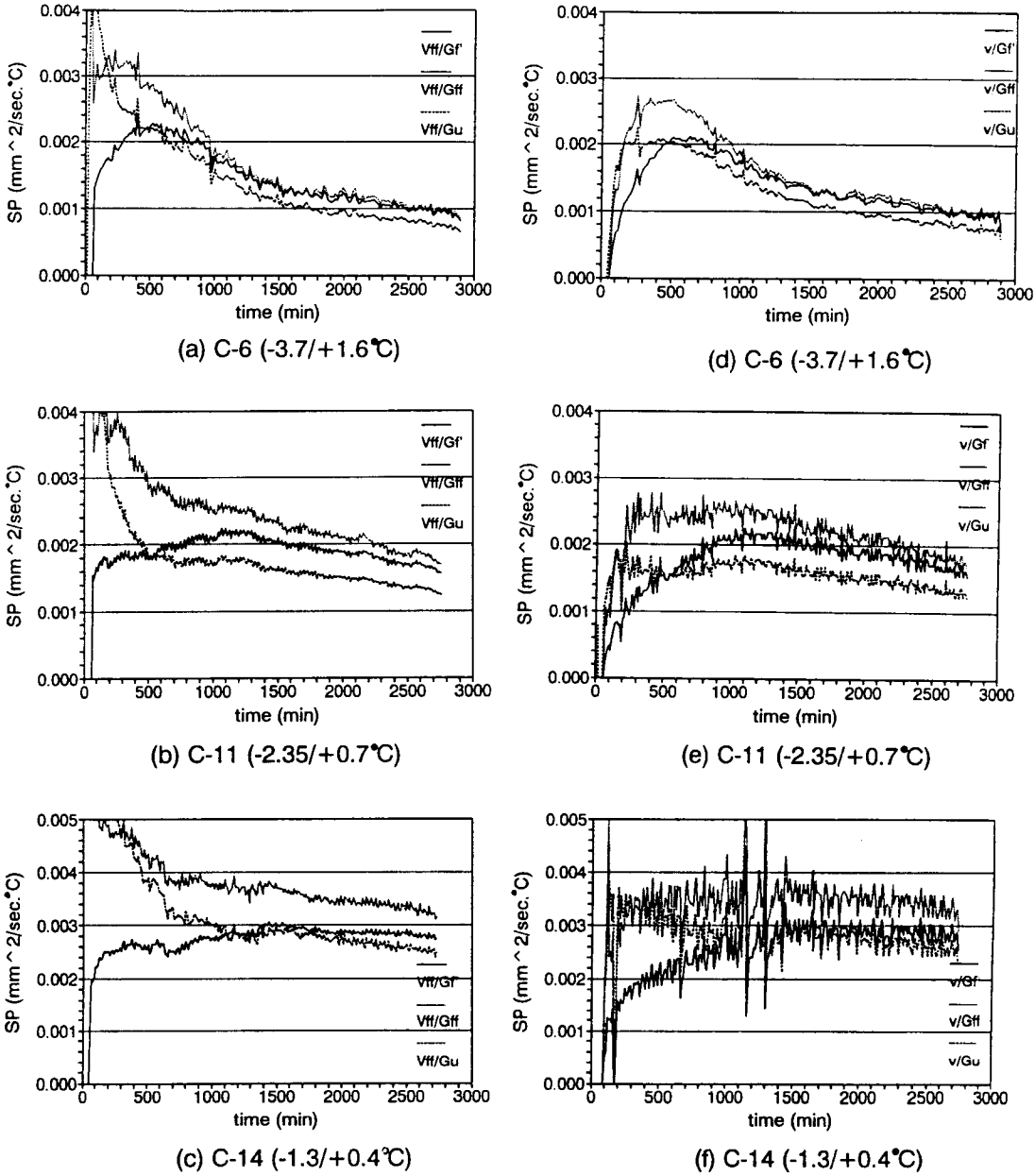


Figure 3.11 Various Combinations of the Water Flow Velocities and Temperature Gradients

Based on these observations, two important conclusions may be made. First, the magnitude and response of SP during a freezing test depends on the choice of simplified definitions which are used to evaluate SP; the differences in SP were especially great during the early stage of freezing. Second, similar behavior was observed in the pair V_{ff}/G_f' and v/G_{ff} , which represent the frost heave potential expressed at each end of the frozen fringe. Therefore, it was concluded that SP should be defined by V_{ff}/G_f' or v/G_{ff} (which represents SP at the both ends of a frozen fringe. It should be emphasized that the shallow temperature gradient shows the advance of the frost front and facilitates the determination of SP.

Figures 3.12a and 3.12b present the SP defined by v/G_{ff} and V_{ff}/G_f' at the end of transient freezing. As predicted from Figure 3.10, SP defined by V_{ff}/G_f' (Figure 3.12b) is less than SP defined by v/G_{ff} (Figure 3.12a). But, the relative location of the individual points is quite similar in both cases. In both Figures, a similar distribution was observed. In practice, the only interpretation of the scatter is a "best-fit" line to obtain SP for a field prediction. If there is only a set of α and k_o independent of $1.09P_o - P_u$, SP must be distributed around a single line in both Figures 3.12a and 3.12b. Comparing C-6 with C-8 and C-14, it can be assumed that SP was influenced by the freezing mode, since the steeper the temperature boundary condition the smaller the SP. It was also observed that the tests with shallower temperature gradients tended to result in greater SP (C-12, C-13, C-14).

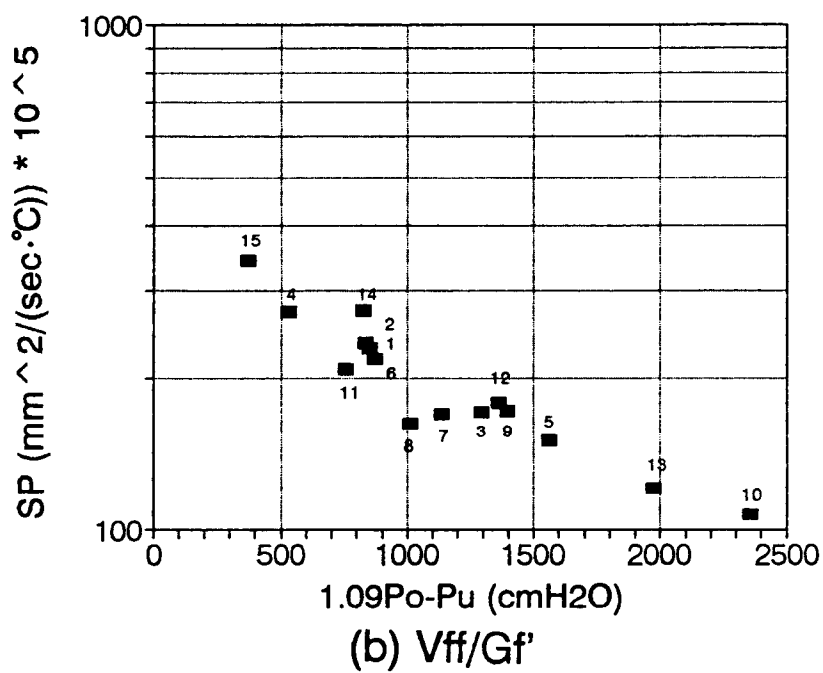
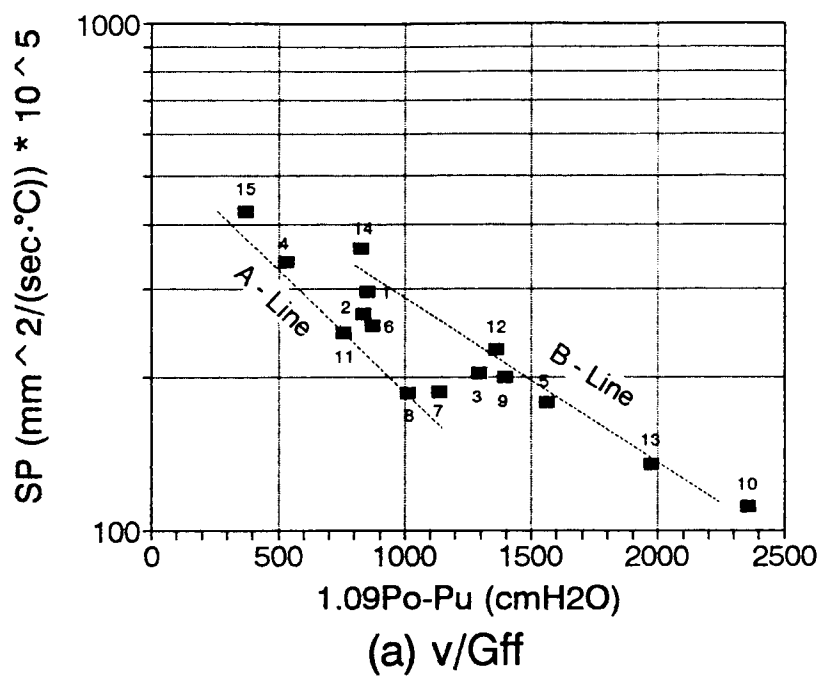


Figure 3.12 SP versus the Combined Pressure Term

Two reasons for the observation are proposed. First, in a test with a steeper temperature gradient, the frost front rapidly progresses and transient freezing ends quickly. In the frozen fringe, a number of ice lenses are independently growing separated by numerous cracks. Therefore, it is probable that part of the frozen fringe might already be deteriorated at the end of transient freezing, when the final ice lens was believed to start to form. Second, in a test with a shallower temperature boundary condition, the freezing process proceeds slowly. As a result, part of the water in a soil under the freezing temperature remains unfrozen (i.e. super-cooled) in the frozen fringe. Consequently, the hydraulic conductivity of the frozen fringe and SP may be greater.

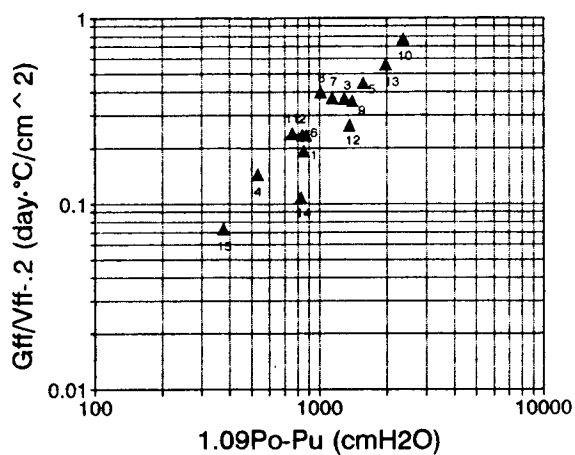
The scatter may also be interpreted in terms of pressure. According to the previous interpretation, C-11 and C-15 on the A - line, and C-3 and C-5 on the B - line in Figure 3.12a are contradicting. Figures 3.12a and 3.12b indicate that SP is expressed by the B-line in the lower pressure region, and SP gradually moves to the A - line when the pressure becomes greater. Recalling Figure 3.5, in which the higher the overburden pressure the greater the unfrozen water content, it is suggested that the frozen soil under greater pressure may have a greater unfrozen water content, and thus the hydraulic conductivity may be greater than predicted by the test under lower pressure. As a result, SP under greater pressure in Figures 3.12a and 3.12b is distributed over greater range than the SP under smaller pressure. Combined with the influence of the temperature boundary condition stated above, SP is expressed for the Calgary silt as the zone between the A and B-lines instead of a singular relationship. As there seems to be an upper limit in unfrozen water content in Figure 3.5, the B - line appears to be the upper limit of SP

in Figure 3.12. For field frost heave prediction under natural conditions, where the frost front progresses very slowly, the use of B-line is recommended.

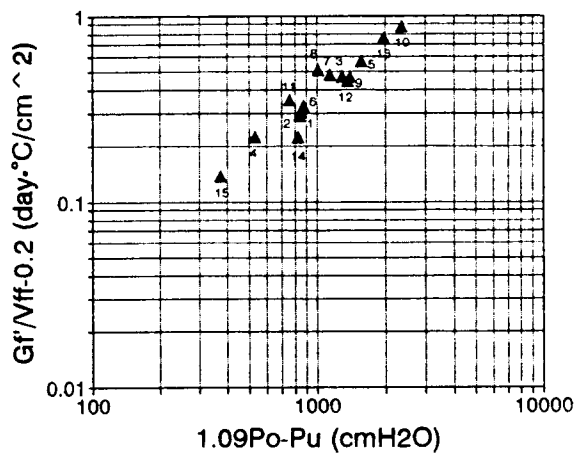
DIL Parameters α and k_0

Figure 3.13 presents the DIL parameters obtained using different simplifying approximations in Eq. 3.13. In Figures 3.13a to 3.13d, K_f/K_{ff} was assumed to be 1.0. Figure 3.13a presents the parameters in the simplest form initially used by Nixon (1991) to demonstrate the DIL model. G_{ff} was replaced by G_f' in Figure 3.13b and by G_f in Figure 3.13c. Among the three figures, it was observed that Figure 3.13a showed the greatest scatter indicating the inappropriateness of the approximation of G_f by G_{ff} . There is practically no difference between Figure 3.13b and 13c. In Figure 3.13d, K_f was estimated from Eq. 3.28, knowing the unfrozen water content (Figure 3.6). The difference between Figures 3.13c and 13d was also inconclusive. Finally, Eq. 3.13 was used to plot the data with the assumption $K_f/K_{ff} = 1.1$ as shown in Figure 3.13e.

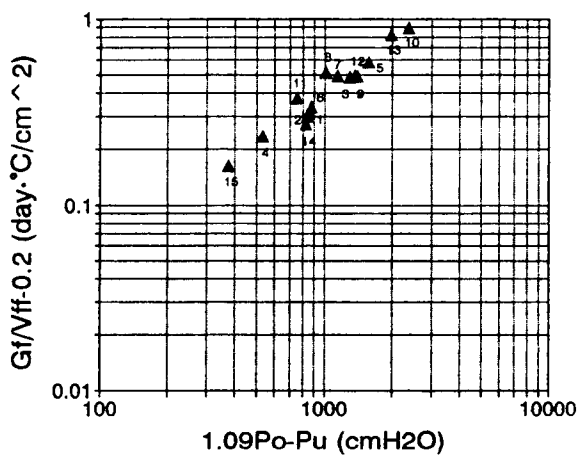
It was obvious from the relationship shown in Figures 3.13b to 3.13e that the data points could be represented by two distinct parallel lines (L and U). The points from the shallower temperature gradient tests tended to group around the L - line (greater SP), while the points from the steeper temperature gradients group around the U-line (smaller SP). This tendency is similar to the A and B lines observed in Figure 3.12a. It appears that both the SP and DIL approaches result in the same conclusion. Therefore, the points, such as C-4, C-5, C-14, or C-15, which are distributed away from the center line (e.g. Figure 3.13e), were not generated by an error in temperature sensor readings or local



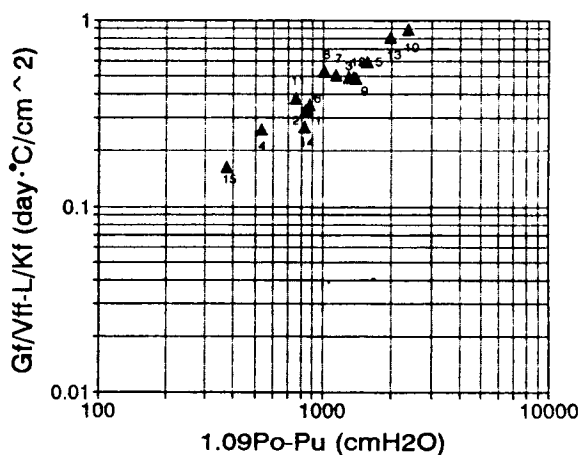
(a) $Gf/Vff-0.2$



(b) $Gf'/Vff-0.2$

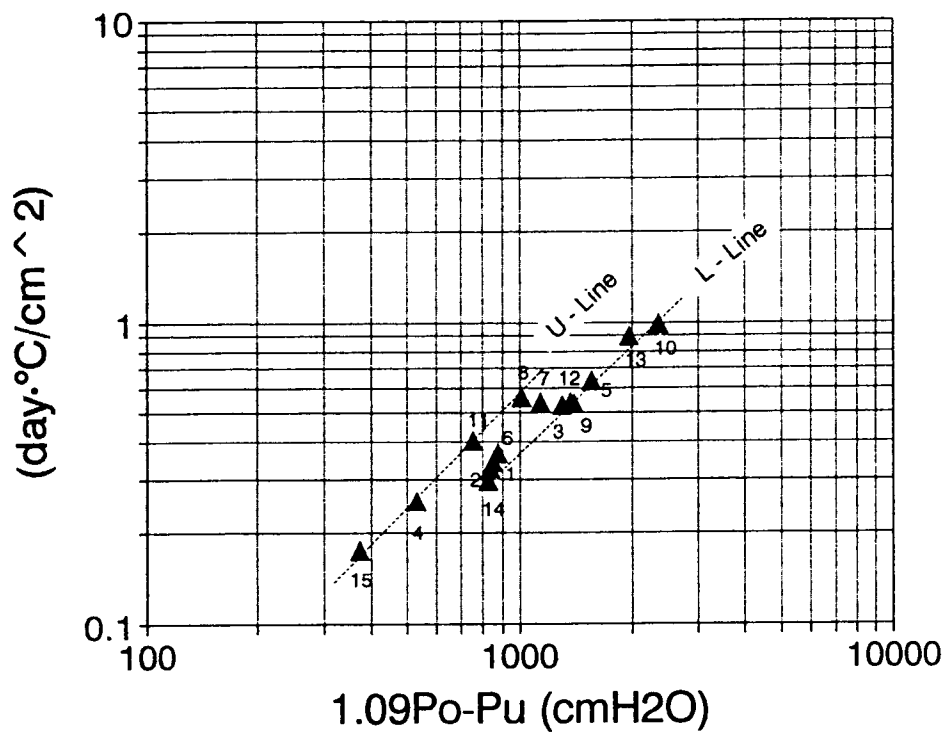


(c) $Gf/Vff-0.2$



(d) $Gf/Vff-L/Kf$

Figure 3.13 Evaluation of DIL Parameters



(e) $1.1 \cdot (Gf/Vff-L/Kf)$

Figure 3.13, Continued Evaluation of DIL Parameters

disturbance. The shift of the L line to the U line, when the pressure increased, means that k_0 increases when pressure increased. This is in contrast to Figure 3.5 in which the greater the overburden pressure the greater the unfrozen water content. This observation is also supported in Figure 3.6, in which the curves move toward the direction of the constant A with increasing loads, maintaining the constant B. The constant A is related to the DIL parameter k_0 and B is the slope of the unfrozen water content and is related to the DIL parameter α . Therefore, it is reasonable that the DIL parameter k_0 was observed to increase with increasing pressure.

Compatibility Between the SP and DIL Ice Segregation Parameters

The major difference in the extraction of the SP and DIL parameters is the use of different temperature gradients (i.e. SP uses G_{ff} while DIL uses G_p). However, as predicted by Eq. 3.13, the ice segregation parameters for each method should be compatible if they are properly evaluated. In other words, SP can be used to estimate the DIL parameters α and k_0 . This means if Figure 3.12a is converted to the form of Figure 3.13e, the converted figure and Figure 3.13 should be identical.

The converted result of Figure 3.12a is shown in Figure 3.14 together with the results presented in Figure 3.13e. It is significant that there is a good agreement between the two groups of the plots in Figure 3.14. The good agreement suggests that the scatter observed in the SP and DIL parameters was not related to the inappropriate measuring procedures or local temperature disturbance, but the real response of a freezing soil. The best agreement was observed under the tests with the greatest pressure; the greatest

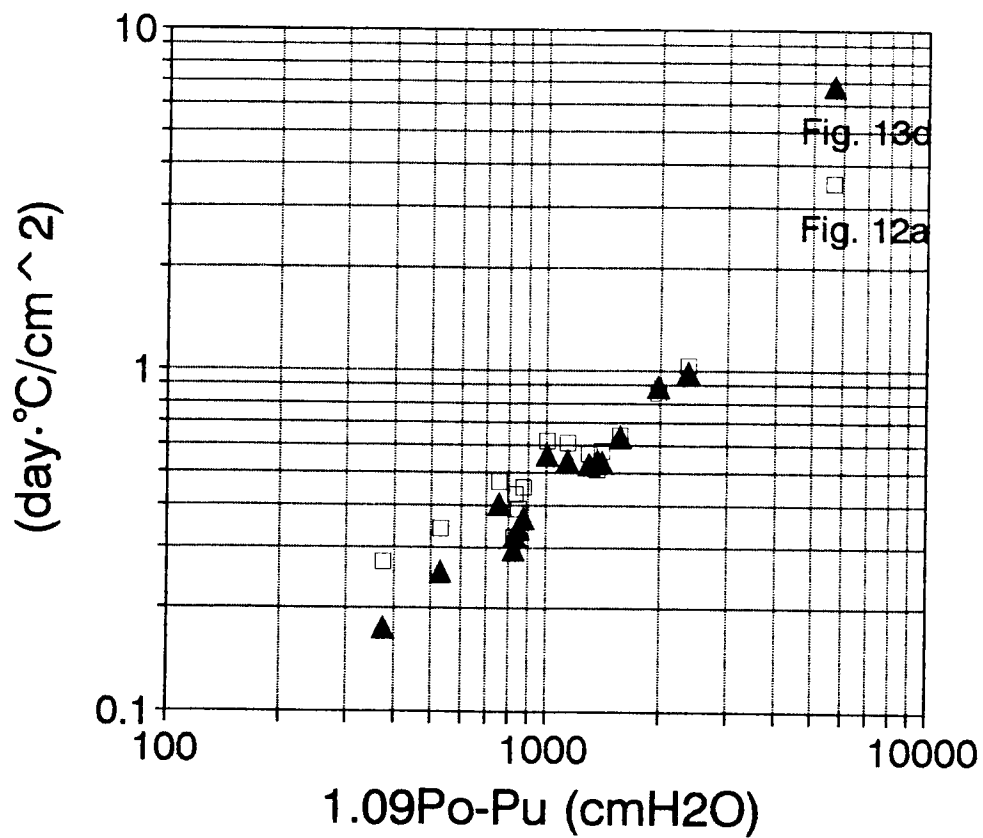


Figure 3.14 Compatibility of the SP and DIL Parameters

discrepancy was observed under the low pressure region. The discrepancy may be the result of either the error in measurement of G_{ff} , or the inappropriate assumption of K_f/K_{ff} . This result also indicates the limitation in the evaluation of ice segregation parameters from a laboratory freezing test.

In comparison with Figures 3.13e and 3.14, Figure 3.13d which assumes $K_f/K_{ff} = 1.0$, shows a similar in shape but all the data points are shifted downwards. This indicates that in the estimation of α and k_o by the DIL approach, the estimation of K_f/K_{ff} plays an important role. Therefore, the direct measurement of thermal conductivity at the temperature of concern is recommended to improve the accuracy of the DIL approach. This is much simpler than a direct measurement of hydraulic conductivity of the freezing soil. On the other hand, in the SP approach, there is an inherent difficulty in measuring the temperature gradient of the frozen fringe, G_{ff} .

It was demonstrated that the ice segregation parameters SP, α and k_o can be estimated either from the boundary information (G_f , DIL approach), or from the information in the frozen fringe (G_{ff} , SP approach). To improve the reliability of measurement of ice segregation parameters it is recommended to check the parameters of concern from the other approach. If both interpretations of freezing tests are correct, the result should be identical. The test results shown in this paper (Figure 3.14) appear to be reliable enough for practical purpose.

Two options are possible to present the DIL ice segregation parameters: (1) assuming one set of α and k_o , (2) assuming two or three set of α and k_o . Table 3.5 lists the α and k_o computed from Figure 3.14. The relationship between the log(SP) and

Table 3.5 Estimates of DIL Parameters

No.	α	$k_0(\text{cm/sec})$	Data
U1	1.20	1.70×10^{-10}	4,8,11,15 (Fig.13e)
U2	0.83	3.63×10^{-10}	4,8,11,15 (Fig.12a)
L	1.15	2.74×10^{-10}	3,5,9,10,12,13,14
Average	0.78	5.32×10^{-10}	All 1 - 15

pressure computed from the α and k_0 in Table 3.5 were plotted in Figure 3.15 using the format of Figure 3.12a. The two U lines and an L line clearly reproduced the range of data points observed in Figure 3.12a. The average line was drawn using the α and k_0 obtained from all thirty (15 x 2) data points. The average line may represent the result used most often by the practitioners. The difference of these lines indicate the possible uncertainty in the evaluation of ice segregation parameters. For example, if the average line is used as the design SP, approximately an error of $\pm 20\%$ in the evaluated SP may be inevitable. The best estimate may be the U lines if used under 1000 cmH₂O, and the L line if used over 1000 cmH₂O.

3.9 Summary and Conclusion

Several simplifying approximations to evaluate ice segregation parameters were examined using freezing test results for Calgary silt. The scatter in the evaluated parameters was interpreted in relation to the unfrozen water content. Finally, the compatibility of the SP and DIL parameters was demonstrated and a method to obtain reliable ice segregation parameters was proposed. As a result of the research, the following conclusions are appropriate:

- (1) The meaningful definition of SP may be either V_{ff}/G_f' or v/G_{ff} ; other combinations of flow velocities and temperature gradients should be used with caution.

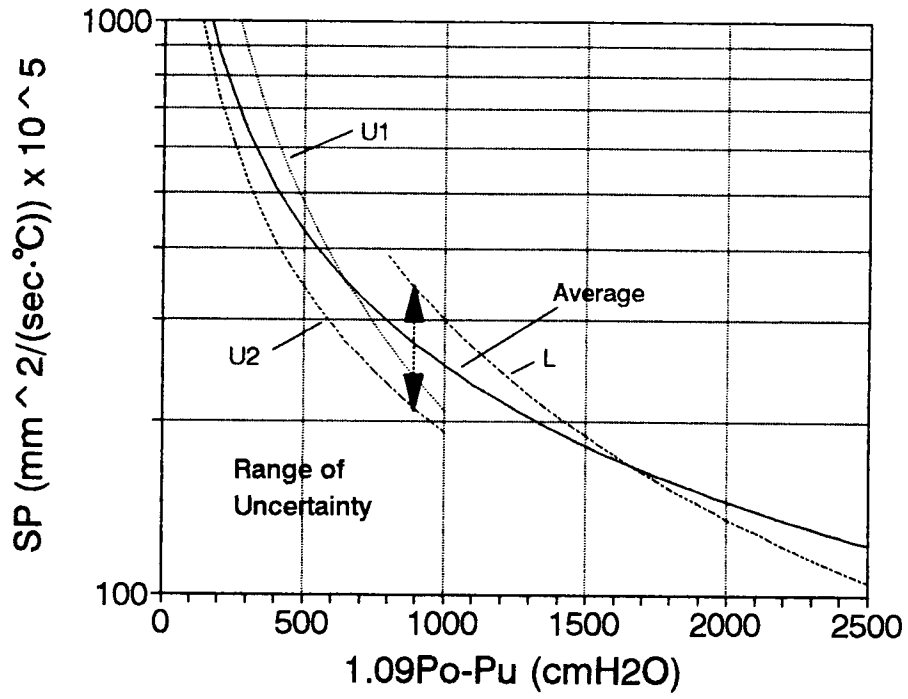


Figure 3.15 Reproduced SP Parameters for Design Purpose

- (2) The DIL parameters α and k_o must be defined by Eq. 3.13. The estimated parameters are sensitive to the assumption K_f/K_{ff} . For the Calgary silt used in the research program, $K_f/K_{ff} = 1.1$ appeared to be reasonable.
- (3) The scatter observed in the ice segregation parameters SP, α and k_o could be explained by considering the unfrozen water content. The parameters A and B which govern the unfrozen water content seemed to change with increasing pressure and the test temperature boundary condition. Therefore, it is reasonable that the SP and DIL parameters were observed not on a single straight line but between two distinct lines.
- (4) To obtain ice segregation parameters for field prediction, it is recommended that the frost heave tests be conducted with shallower temperature gradients or under the greater overburden pressures. This test condition may result in greater amount of unfrozen water in a freezing soil and produce greater values of SP.
- (5) The compatibility of the SP and DIL approaches was experimentally verified. If a test result was properly analyzed, the SP and DIL ice segregation parameters should be compatible. To obtain reliable ice segregation parameters, therefore, it is proposed to use both the SP and DIL approaches.

3.10 References

1. Akagawa, S., "X-Ray Photography Method for Experimental Studies of the Frozen Fringe Characteristics of Freezing Soil," *CRREL Report*, 90-5, 1990.
2. Anderson, D. M., and Tice, A. R., "Predicting Unfrozen Water Contents in Frozen Soils From Surface Area Measurements," *Highway Research Record No. 393*, 1972, pp. 12-18.
3. Frivik, P. E., "State of the Art Report. Ground Freezing: Thermal Properties, Modeling of Processes and Thermal Design," In *Proc., Second International Symposium on Ground Freezing*, 1980, pp. 115-133.
4. Fukuda, M., Ogawa, S., and Kamei, T., "Prediction of Field Frost Heave Using the Segregation Potential Theory." *Japan Society of Civil Engineers Reports*, No. 400, 1988, pp. 253-259. (in Japanese)
5. Gilpin, R. R., "A Model for the Prediction of Ice Lensing and Frost Heave in Soils," *Water Resources Research*, Vol. 16, No. 5, 1980, pp. 918-930.
6. Gilpin, R. R., "A Frost Heave Interface Condition for Use in Numerical Modelling," In *Proc., Fourth Canadian Permafrost Conference*, Calgary, Alberta, 1982, pp. 459-465.
7. ISGF Working Group 2, "Guidelines for Mechanical and Technical Design of Frozen Soil Structure (Draft)," In Reports from *Sixth International Symposium on Ground Freezing*, China, 1991, pp. 1-21.
8. Ito, Y., Kawaragawa, Z., and Ryokai, K., "Study on Frost Heave of Highway (Part. 3) - Interpretation of Frost Heave Test," In *Proc., Japan Society of Soil Mechanics and Foundation Engineering Annual Conference*, 1989. (in Japanese)
9. Ito, Y., Vinson, T. S., Nixon, J. F., and Stewart, D., "An Improved Step Freezing Test to Determine Segregation Potential," manuscript, 1993.
10. Konrad, J. M., "Frost Heave Mechanics," Ph. D. thesis, Department of Civil Engineering, University of Alberta, Edmonton, Alberta, 1980.
11. Konrad, J. M., and Morgenstern, N. R., "A Mechanic Theory of Ice Lens Formation in Fine-Grained Soils," *Canadian Geotechnical Journal*, Vol. 17, 1980, pp. 473-486.
12. Konrad, J. M., and Morgenstern, N. R., "The Segregation Potential of a Freezing Soil," *Canadian Geotechnical Journal*, Vol. 18, 1981, pp. 482-491.

13. Konrad, J. M., and Morgenstern, N. R., "Prediction of Frost Heave in the Laboratory during Transient Freezing," *Canadian Geotechnical Journal*, Vol. 19, 1982a, pp. 250-259.
14. Konrad, J. M., and Morgenstern, N. R., "Effects of Applied Pressure on Freezing Soils," *Canadian Geotechnical Journal*, Vol. 19, 1982b, pp. 494-505.
15. Konrad, J. M., "Procedure for Determining the Segregation Potential of Freezing Soils," *Geotechnical Testing Journal*, Vol. 10, No. 2, 1987.
16. Kujara, K., "Factors Affecting Frost Susceptibility and Heaving Pressure in Soils," Ph. D. thesis, Department of Civil Engineering, University of Oulu, Oulu, Finland, 1991.
17. Nixon, J. F., "Field Frost Heave Prediction Using the Segregation Potential Concept," *Canadian Geotechnical Journal*, Vol. 19, 1982, pp. 526-529.
18. Nixon, J. F., "Ground Freezing And Frost Heave - A Review," *Northern Engineer*, Vol. 19, 1987, pp. 8-19.
19. Nixon, J. F., "Discrete Ice Lens Theory for Frost Heave in Soils," *Canadian Geotechnical Journal*, Vol. 28, 1991, pp. 843-859.
20. Svec, O. J., "A New Concept of Frost-Heave Characteristics of Soils," *Cold Region Science and Technology*, 16, 1989, pp. 271-279.
21. Vinson, T. S., Ahmad, F., and Reike, R., "Factors Important to the Development of Frost Heave Susceptibility Criteria for Coarse-Grained Soils," *Transportation Research Record 1089*, 1984, pp. 124-131.

3.11 Notation

The following symbols are used in this paper:

A, B	=	constants;
a, b, c	=	constants;
d	=	thickness of the frozen part of the soil;
G_f	=	temperature gradient of the frozen soil behind the ice lens;
\bar{G}_f	=	overall temperature gradient of the frozen soil;
G_{ff}	=	temperature gradient of the frozen fringe;
G_u	=	temperature gradient of the unfrozen soil;
G_{ff-Tf}	=	temperature gradient at the warmest side of the frozen fringe;
G_{ff-Tc}	=	temperature gradient at the coldest side of the frozen fringe;
H	=	total heave;
h_i	=	in-situ heave;
h_s	=	segregational heave;
K_f	=	thermal conductivity of the frozen soil;
K_{ff}	=	thermal conductivity of the frozen fringe;
K_u	=	thermal conductivity of the unfrozen soil;
k_0	=	hydraulic conductivity of the frozen soil at -1 °C;
L	=	latent heat of fusion of water;
l_f	=	thickness of the frozen soil behind the ice lens;
n	=	porosity;
n_f	=	fraction of total soil volume changing phase at the frost front;
P_i	=	ice pressure;
P_o	=	overburden pressure;
P_u	=	suction at the frozen fringe - unfrozen soil interface;
P_{sep}	=	separation pressure;
SP	=	segregation potential;
T	=	temperature in °C;
T_c	=	temperature at the cold side of the specimen;
T_f	=	temperature at the frozen fringe - unfrozen soil interface or at the frost front;
T_l	=	temperature at the base of the ice lens;
T_w	=	temperature at the warm side of the specimen;
t_{base}	=	thickness of the base plate;
t_{top}	=	thickness of the cold plate;
V_{ff}	=	water flow velocity to the ice lens;
v	=	water intake velocity from the unfrozen soil;
W_u	=	proportion of water remaining unfrozen in the frozen soil;
w_u	=	unfrozen water content;
w_{tot}	=	total water content;
X	=	location;

α = slope of the relationship between hydraulic conductivity and temperature;
and
 β = thermodynamic constant.

4.0 Method to Predict the Influence of Groundwater Level on Frost Heave

by

Yuzuru Ito and Ted S. Vinson

Abstract

Frost heave is a serious problem for highway construction in northern Japan. Frost heave may result in increased highway maintenance costs when the frost susceptibility of the embankment soil is not properly evaluated prior to construction. Highway construction in Japan differs from that in other nations in that large embankments are common. The frost susceptibility of the embankment soil must, therefore, be evaluated considering the height of the embankment which is generally equivalent to the distance from the groundwater level.

The semi-full scale freezing test (SFFT) facility was built at the Japan Highway Public Corporation (JH) Research Institute to evaluate the influence of the groundwater level on frost heave. A number of soils from highway construction sites in northern Japan have been evaluated at the SFFT facility. However, because of the expense and time required to conduct a test, use of the SFFT facility is limited to only a few types of soils used in JH's construction projects in a given year. Therefore, it is highly desirable to develop a simpler test procedure than that by SFFT.

A simple laboratory procedure was proposed to evaluate the influence of the distance to the groundwater table on ice segregation parameters. According to the discrete ice lens frost heave model, the influence of the groundwater level on ice

segregation parameters is considered to be equivalent to that of the overburden pressure. Consequently, a frost heave test may be conducted with different overburden pressures instead of different groundwater levels. This substitution allows a simple laboratory test to replace the SFFT.

The validity of the proposed laboratory test was demonstrated by comparing the ice segregation parameters extracted from laboratory tests with parameters extracted from the SFFT and field observations. The results suggest that the proposed method gives a reasonable estimate of the ice segregation parameters and, hence, can be used for design purposes.

4.1 Introduction

In northern Japan, 2000 km of expressways are scheduled for construction by Japan Highway Public Corporation (JH) over the next two decades. Unlike middle or southern Japan, the northern region suffers from heavy snowfall and freezing during winter. In this region, snow accumulates from two to three meters every winter and the temperature drops to -30 to -40 °C several times during the winter. The harsh environment has delayed the development of the region. The expansion of the expressways, which would enable uninterrupted transportation in the winter time to the northern region, is expected to be a key to the stimulation of industry in the region.

The northern region, like other parts of the Japanese islands, consists of volcanic mountains, small valleys and plains. Expressway construction is complicated and requires excavation, bridges, tunnels, and compacted embankment fills. Of the total length of

expressways, nearly 50 % are planned with embankment structures. Freezing problems of roadways in the northern region require additional construction costs if an embankment soil is determined to be frost susceptible.

A laboratory frost susceptible test is generally used to identify the frost susceptibility of the embankment soil. Conventional frost heave susceptibility criteria are based on experience with roads built directly on natural ground. Although the criteria are satisfactory for most road construction, the criteria are not considered to be appropriate for expressway construction, where half of the roadways are built on high embankments (usually, higher than 7 meter). The experience of expressway construction in northern Japan, however, suggests there is substantially less frost heave in higher embankments. Laboratory research results using longer specimens indicate that frost heave decreases with increasing specimen height (equivalent to distance to the groundwater table).

The semi-full scale freezing test (SFFT) facility was constructed to study the relationship between frost heave and groundwater level at the JH Research Institute (JHRI). Initial test results with an artificially blended frost susceptible soil indicated the frost heave and heave velocity decreased with increasing distance from the ground water table. Further, it also became obvious that the conventional laboratory frost susceptibility test and the criteria used to evaluate the soil's frost heave susceptibility cannot be used to predict the frost heave response of high embankments.

4.2 Statement of Purpose

The purpose of the research work reported herein is to develop a laboratory test procedure to effectively predict the influence of the distance to the groundwater table on ice segregation parameters. The results of the research work will be used to assess the frost heave response of an embankment with respect to the location of groundwater table (or the height of embankment). The proposed method to predict the ice segregation parameters is based on the Segregation Potential (SP) (Konrad and Morgenstern 1981) and the discrete ice lens (DIL) (Nixon 1991) models. To demonstrate the validity of the method, the predicted parameters from the proposed method were compared with the results from conventional frost heave susceptibility tests, SFFT and field observations.

4.3 Relationship between Frost Heave and Groundwater Level

Previous Research

Frost heave can result from the freezing of water present in the voids of a soil mass. Excessive heave occurs when water is pulled up through the soil to build up layers of segregated ice (Taber 1929, 1930). Three conditions must be present simultaneously for excessive heave and the associated formation of segregated ice to occur:

- freezing temperatures must penetrate the soil
- the soil must be frost susceptible, and
- there must be an available source of water.

The first condition can be easily checked with the climate records of the region. The second condition may be judged by a frost susceptibility test. The third condition is

considered to be related to the groundwater level. Because most expressways in Japan are constructed directly on existing ground or on low embankments, where the groundwater level is usually very close to the roadway surface, the third criterion is always considered to be satisfied. Existing frost heave susceptibility tests and associated criteria developed by various organizations throughout the world are mostly based on the assumption that the third condition is satisfied.

In the construction of high embankments in which the distance to the groundwater table is great the assumption that the third condition is satisfied may be questioned. To investigate appropriateness of the assumption, a field study was conducted by JHRI. The result of the study indicated that frost heave problem occurred ten times less frequently in the embankments compared with the cut section (Sezai et al. 1985). Further, the embankments where frost heave problems were observed were less than three to four meters in height. This result supports the importance of groundwater level on frost heave. In addition, the results from laboratory experiments conducted with specimens one meter in length indicated that the deeper groundwater level limited both the amount of heave and heave velocity (McGaw 1972). The specific relationship between the water intake into the freezing soil and the location of groundwater table depends on the soil type (Weiyue and Xiaozu 1988). Efforts to develop techniques to prevent water migration from the groundwater level to a freezing soil were reported by Bell et al. (1982), Henry (1990) and Tsuchiya et al. (1992).

Research at JHRI

Based on the field observation noted above, the SFFT facility was constructed to study the influence of groundwater level on frost heave and to predict frost heave in embankments. An initial series of tests was conducted with Kongodo soil (blended soil) changing the groundwater at several levels. Figure 4.1 presents the result of SFFTs with groundwater levels from 50 to 300 cm. It was observed that the lower the ground water level the smaller the frost heave (Kawaragawa et al. 1989). Kongodo soil was also tested with JH's conventional frost susceptibility test method prior to the SFFT. The frost susceptibility test results demonstrated that Kongodo soil was highly frost susceptible and several thick ice lenses were reported after a six day freezing test. Figure 4.2 presents test results for different soil samples using different boundary conditions (Ito et al. 1989). The results suggest that the relationship between the frost heave response and groundwater level was influenced by both the freezing condition and soil type. It was concluded that some embankment soils rejected under existing frost heave susceptibility tests and associated criteria could be used for soils in the upper part of the embankment where the influence of groundwater table is negligible.

4.4 Prediction of Frost Heave from Laboratory Test and SFFT

According to JH's design specification (1983), 70 % of the expected maximum frozen depth in embankments must be constructed with non-frost susceptible materials, usually expensive crushed aggregate. If the natural soil is determined to be frost susceptible, the earthwork plan must be reconsidered and which will result in increased

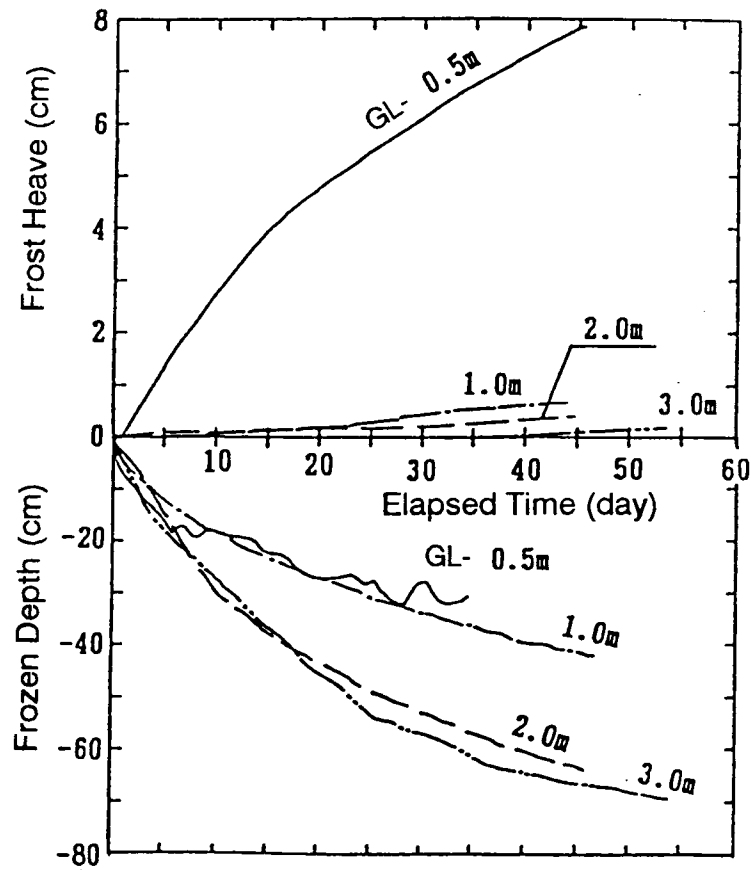


Figure 4.1 Frost Heave versus Groundwater Level for Kongodo Soil (after Kawaragawa et al. 1989)

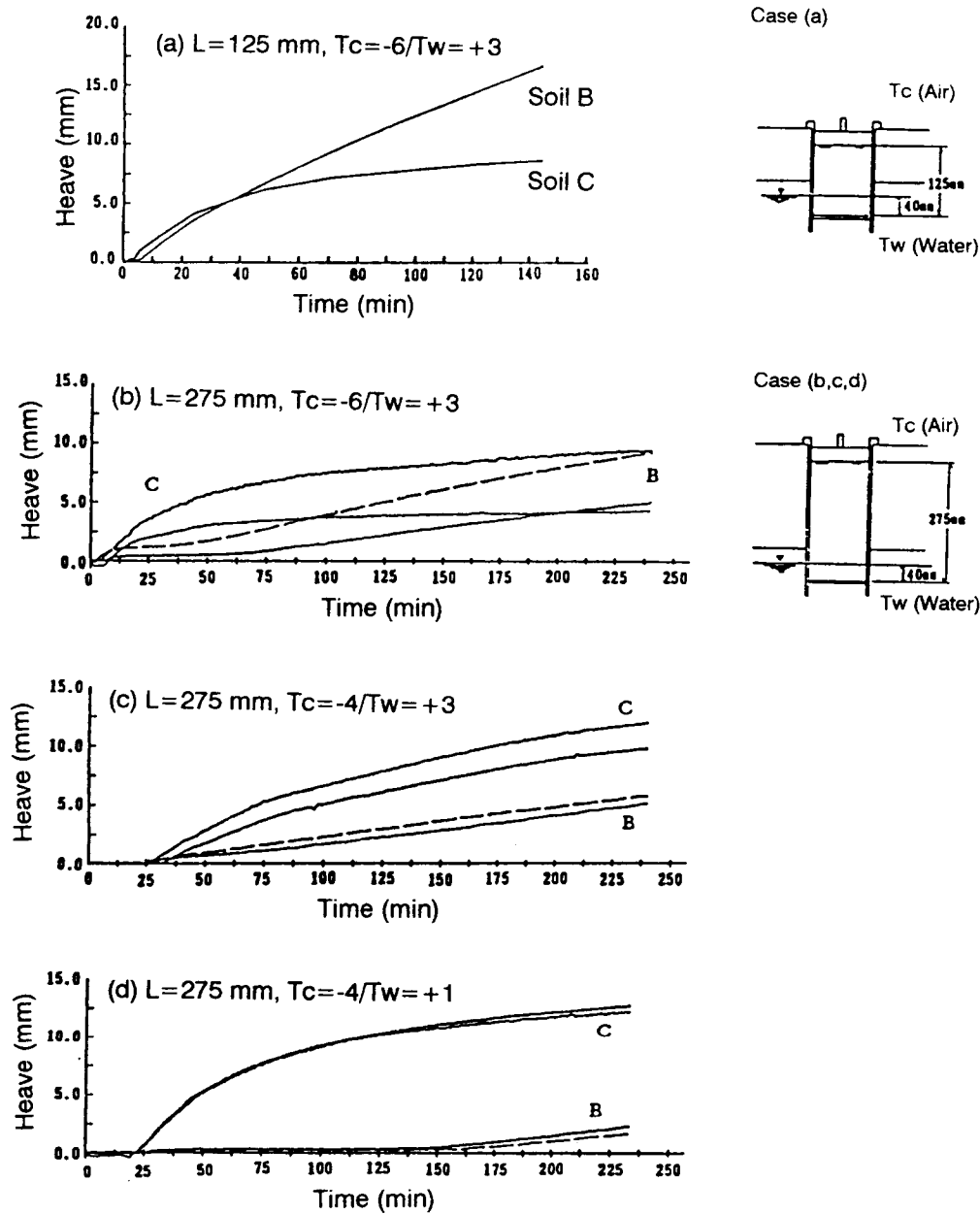


Figure 4.2 Frost Heave versus Test Boundary Condition (after Ito et al. 1989)

construction costs. Therefore, the role of the conventional frost test which is used to determine the frost susceptibility of a soil is very important.

Based on the observations of a number of researchers, it may be concluded that frost heave susceptibility test results should be presented together with their relationship to the groundwater level. To this end, frost heave must be evaluated using a set of ice segregation parameters which allow the amount of frost heave to be predicted as a function of groundwater level. The conventional frost heave susceptibility test, which is conducted with a 12.5 cm long specimen and its criteria, cannot predict frost heave with the relationship to the groundwater level. The simplest change to the conventional test is to use a longer specimen.

The SFFT facility built in JHRI may be classified as a test with an extreme length specimen. The SFFT may predict field frost heave under various boundary temperature conditions and groundwater levels. A number of soils were tested in the SFFT facility and the test results have been used to design expressway embankments. However, tests conducted in the SFFT facility require a substantial amount of time and they are expensive. The SFFT cannot substitute for the conventional laboratory frost heave susceptibility test when it is necessary to consider a numbers of soils associated with the variation of embankment material.

4.5 Laboratory Test Procedure to Predict the Influence of Groundwater Level

The proposed laboratory test procedure is based on either one of two engineering frost heave models, the segregation potential (SP), and discrete ice lens (DIL) models.

Frost heave is evaluated by a set of ice segregation parameters with both the SP and DIL models. The proposed procedure to extract ice segregation parameters from the freezing tests is based on the idealization of a freezing soil introduced by Gilpin (1980). Later Nixon (1991) simplified Gilpin's idealization to extract the DIL parameters. Ito et al. (1993) demonstrated the compatibility between the parameters, characterizing the SP and DIL models. The equation to evaluate the DIL parameters is expressed as:

$$\frac{K_f \left(\frac{G_f}{V_{ff}} - \frac{L}{K_f} \right)}{K_{ff}} = \frac{\left(\frac{\alpha + 1}{\alpha} (1.09P_o - P_u) \right)^\alpha}{k_0 \beta^{1+\alpha}} \quad (4.1)$$

where,

- K_f, K_{ff} = thermal conductivities of the frozen soil and frozen fringe,
- G_f = temperature gradients of the frozen soil behind the ice lens,
- V_{ff} = water flow velocity to the ice lens base,
- L = latent heat of fusion of water,
- β = thermal constant,
- α, k_0 = DIL ice segregation parameters, and
- P_o, P_u = overburden pressure and suction.

In Eq. 4.1 two pressures are combined into one pressure term $(1.09P_o - P_u)$, while in the SP theory they are treated separately (Nixon 1991). Based on Eq. 4.1 the effects of overburden pressure and suction (distance to the groundwater table) on frost heave are equivalent. Therefore, the influence of the groundwater level on frost heave can be evaluated with a series of freezing tests at various overburden pressures. Indeed, it is

much easier to control overburden pressure in a freezing test than suction at the frost front.

The DIL parameters can be also estimated with the equation used to define SP:

$$\frac{V_{ff}}{G_{ff}} = (SP) = \frac{k_0 \beta^{1+\alpha}}{\left(\frac{\alpha+1}{\alpha} (1.09 P_o - P_u)\right)^\alpha} \quad (4.2)$$

Eq. 4.2 shows the compatibility of the SP and DIL parameters. In Eq. 4.1 the overall temperature gradient of the frozen fringe (G_f) can substitute for G_{ff} . Evaluation of G_f or G_f' is much easier than that of the temperature gradient of the frozen fringe G_{ff} . The evaluation of K_f/K_{ff} may be uncertain. In Eq. 4.2, on the other hand, there is no need to evaluate K_f/K_{ff} if G_{ff} can be accurately measured.

To interpret the series of laboratory tests conducted at various overburden pressures, the terms in the left side of Eqs. 4.1 and 4.2 are plotted on a log-log graph with $(1.09P_o - P_u)$ as the abscissa. The DIL parameters can be extracted from the plot with α as the slope and the intersection (b) is used to calculate k_0 as

$$k_0 = \frac{\left(\frac{\alpha+1}{\alpha}\right)^\alpha}{10^b \beta^{\alpha+1}} \quad (4.3)$$

Knowing α and k_0 , SP can be calculated from Eq. 4.2, which shows the relationship between SP and the combined effect of the overburden pressure plus groundwater level.

4.6 Research Program

To validate the proposed method, the ice segregation parameters predicted by the proposed method were compared with the parameters obtained from the conventional frost heave susceptibility tests, SFFTs and field observations. The material used for this research is Asahikawa soil which was used for expressway construction at Asahikawa, Japan. The physical properties of Asahikawa soil are given in Table 4.1 and Figure 4.3.

4.7 Description of the Test Facilities and Procedures

Tests by the Proposed Laboratory Procedure

The laboratory test program was conducted at Oregon State University (OSU). The material used was air dried Asahikawa soil passing a 425 micron sieve. The specimens were prepared by consolidating a slurry to 300 kPa pressure. The specimens were placed into the freezing cell. Following the application of overburden pressure, hydraulic conductivity tests were conducted on each specimen prior to freezing. A detailed description of the test equipment and procedure are given by Ito et al. (1993). The test equipment and boundary conditions were shown in Figure 4.4 and Table 4.2. A total of eight tests were conducted using a step freezing method with different boundary conditions.

During a test, the frost heave, water intake, and temperatures at both ends and along the cell wall, were monitored. The data obtained from the test were analyzed to calculate the temperature gradients (G_f' and G_{ff}), the water intake velocity (v), and flow

Table 4.1 Physical Properties of Asahikawa Soil

Specific Gravity	2.68
Grain Size, %	
Gravel (5.0mm <)	1.5
Sand (0.075-5.0mm)	52.5
Silt (0.002-0.075mm)	27.0
Clay (<0.002mm)	19.0
Consistency, %	
Liquid Limit	52.3
Plastic Limit	24.6

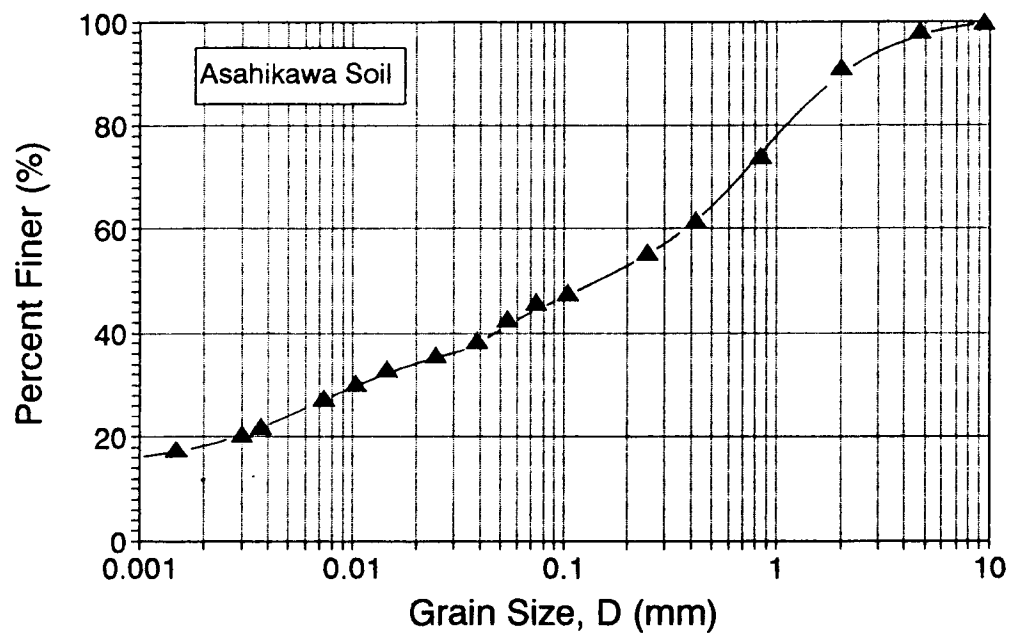


Figure 4.3 Grain Size Distribution of Asahikawa Soil

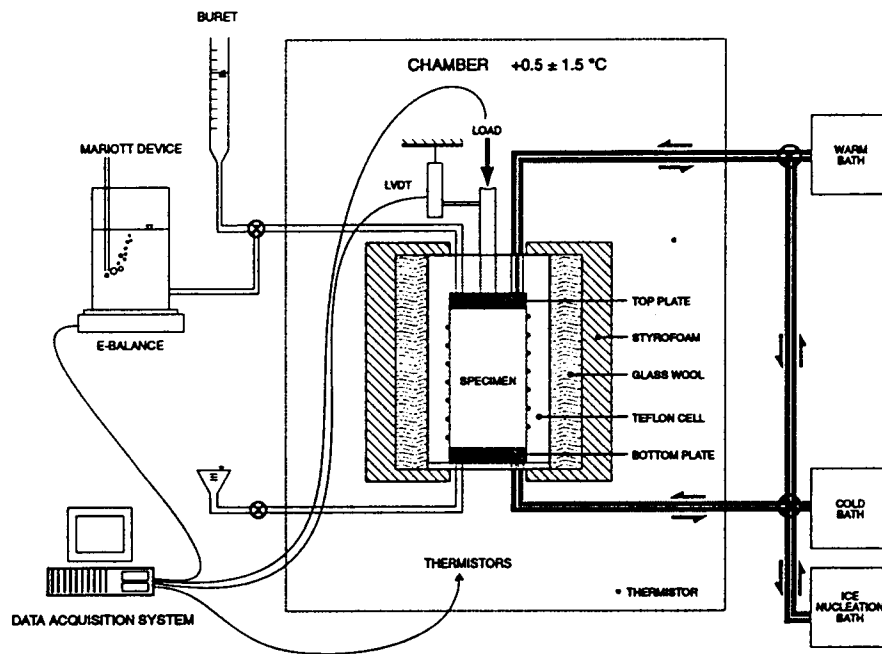


Figure 4.4 Step Freezing Test System

Table 4.2 Test Boundary Conditions Using the Proposed Test Method

Test No.	Tw (°C)	Tc (°C)	Overburden Pressure (kPa)	Specimen Height (mm)
1	+0.5	-2.1	50	95
2	+0.5	-2.1	100	95
3	+0.5	-2.1	200	95
4	+0.5	-2.1	25	95
5	+0.4	-1.2	70	140
6	+0.4	-1.3	15	115
7/1	+0.7	-1.3	15	125
7/2	+0.7	-4.7	15	125
8	+1.6	-4.6	45	101

velocity to the base of an ice lens (V_{fp}) (or heave velocity divided by 1.09). The suction was estimated knowing the hydraulic conductivity (3×10^{-8} cm/s) which was measured prior to the test and thickness of the unfrozen part of the specimen (which was taken as the distance from the interpolated 0°C isotherm to the base of the specimen). The test result was evaluated at the end of transient freezing or at the formation of the final ice lens. The terms in the left side of Eqs. 4.1 and 4.2 were plotted on a log-log graph with $(1.09P_o - P_u)$ as the abscissa. In all, two points were plotted from one test to obtain a set of reliable ice segregation parameters.

Test Procedure and Criteria for JH's Conventional Frost Susceptibility Test

To evaluate the frost susceptibility of subgrade soils and soils in the upper part of an embankment, JH uses a laboratory frost heave test. The test system is illustrated in Figure 4.5. A maximum of nine specimens can be tested at one time. A specimen 15 cm in diameter and 12.5 cm in height is made by compacting material passing a 37.5 mm sieve. The compacted soil specimen is allowed to soak in a vacuum container to obtain 100 % saturation before placement in the test chamber. Following placement, the specimen temperature is allowed to equilibrate at approximately $+3.0^\circ\text{C}$. The test begins by lowering the upper chamber temperature to -6°C . The freezing system controls air chamber temperature to freeze nine specimens; the warm side temperature is maintained constant. The conventional frost susceptibility criteria does not require any temperature based information. Frost heave is recorded by a displacement transducer.

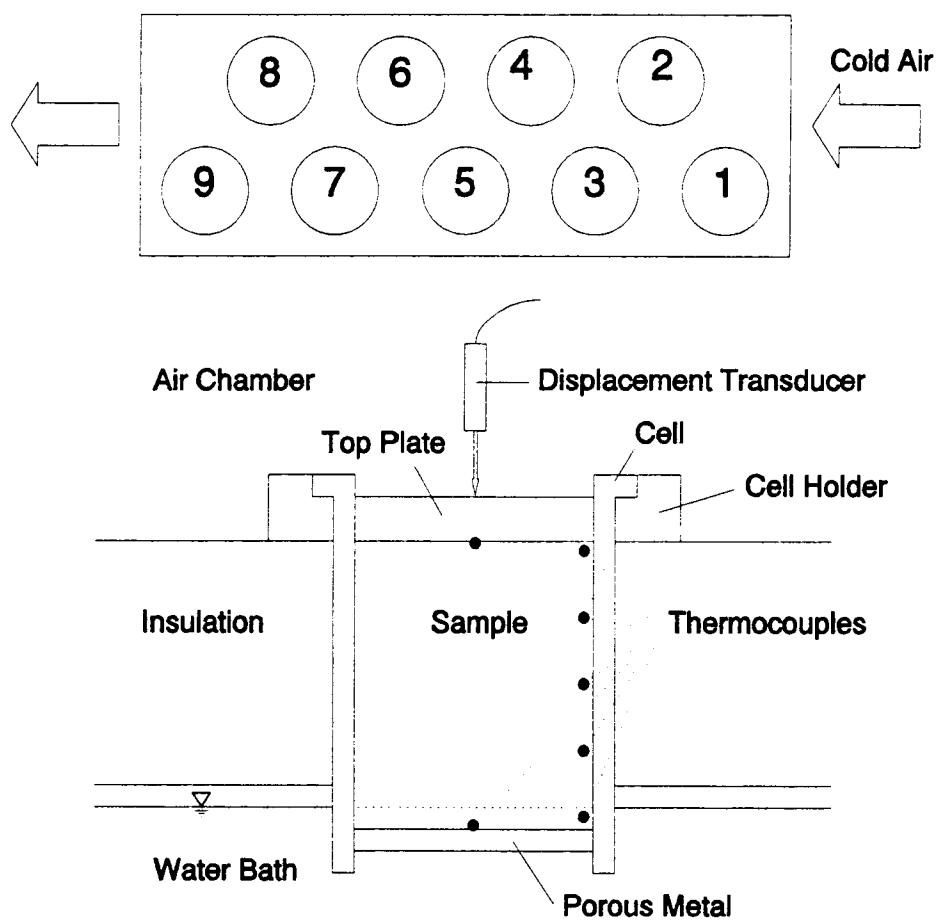


Figure 4.5 Frost Susceptibility Test System

After six days of freezing, the frost susceptibility is evaluated by averaging the results of a minimum of three specimens. Table 4.3 is used to evaluate the frost susceptibility. As can be seen, the criterion is based on the heave ratio which is computed from the total frost heave and visual classification of the frozen specimen.

The advantage of the conventional method is that nine specimens can be tested at one time. There are several problems with this method. First, the test result is influenced by the location of each sample since only the air temperature at the center of the chamber is controlled. Second, it is impossible to use the test result for field prediction since the boundary temperature data are lacking. Third, the criterion based on a "visual observation" is very subjective. Fourth, although this method has been successful for rejecting frost susceptible materials, it has also been noted that the method rejects many soils which may be non-frost susceptible.

In the current research program, the freezing tests conducted under the conditions in Table 4.4 were first interpreted with conventional criteria (Table 4.3). Next the results were analyzed with the procedure described in the preceding section. The conventional test system was used with different temperature and overburden pressure conditions. Teflon was installed between the specimen and cell wall to reduce friction. In addition, thermocouples were specially installed for this research at the both ends and along each specimen to monitor the temperature distribution around the specimen. The suction was estimated given the hydraulic conductivity (3×10^{-8} cm/s), which was previously obtained, the length of unfrozen part of the specimen, and the frost heave velocity.

Table 4.3 Conventional Frost Susceptibility Criteria

Class No.	Description	Heave Ratio	Judgement
1	Concrete state	< 5 %	Accept
		> 5 %	Caution
2	Concrete w/ Hairlike Ice	< 5 %	Caution
		> 5 %	Reject
3	Thin to thick ice lens	NA	Reject
4			
5			

$$\text{Heave Ratio} = (\text{Frost Heave} / \text{Initial Specimen Height}) \times 100 \%$$

Visual Classification



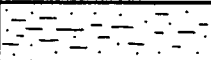
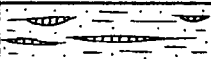

Class No.	Description	Sketch	Observation
1	Concrete		No Segregated Ice
2	Concrete/Hair		A Few Segregated Ice
3	Thin Frost		Discontinuous Ice
4	Frost		Ice Lens t=1-2mm
5	Frost Column		Ice Lens Column

Table 4.4 Test Boundary Conditions Using the Conventional Frost Susceptibility Test System

Test No.	No. of Specimen	Water (°C)	Tc (°C)	Top Plate Weight (kg)
BD2	4	+3.5	-6	1.5×4
BE2	7	+6.4	-6.8	1.5×2,5×3,10×2
BE4	7	+3.3	-4.7	1.5×2,5×3,10×2
BE6	7	+4.9	-5.8	1.5×2,5×3,10×2

SFFT Facility

Since its construction at JHRI in 1986, the SFFT facility has been used to evaluate the influence of groundwater level on frost heave for various soils used in northern expressway construction. Figure 4.6 illustrates the SFFT facility. The facility consists of two cubic soil containers ($4 \times 4 \times 4$ m freezing cells) and the freezing house unit, which is movable between the two containers so that one container is freezing, while one container is under specimen preparation. The temperature inside the house can be controlled. The temperature at the base of each container can be controlled independently. The sides and bottom of each container are heavily insulated. The inner wall surface was covered with a metal skin. A thin plastic plate was installed on the surface of the skin to reduce the friction between it and soil. Water is supplied from the base through a 30 cm thick sand layer.

The facility can simulate the field condition by controlling the chamber and base temperatures with a programmable temperature controller. The frost heave at the surface and inside the specimen, temperatures in the chamber and specimen, and water supply are recorded during a test. It is also possible to manually observe the frozen depth, surface heave and water content change (with a nuclear device) during a test.

The soil which is planned to be used for embankment construction is transported from the construction site and stored. The specimen is compacted in the container at the natural water content, which is similar to the actual construction practice at the site.

Table 4.5 presents the test boundary condition used for this research. All the tests presented in this paper were conducted with a constant air chamber temperature of -6 °C.

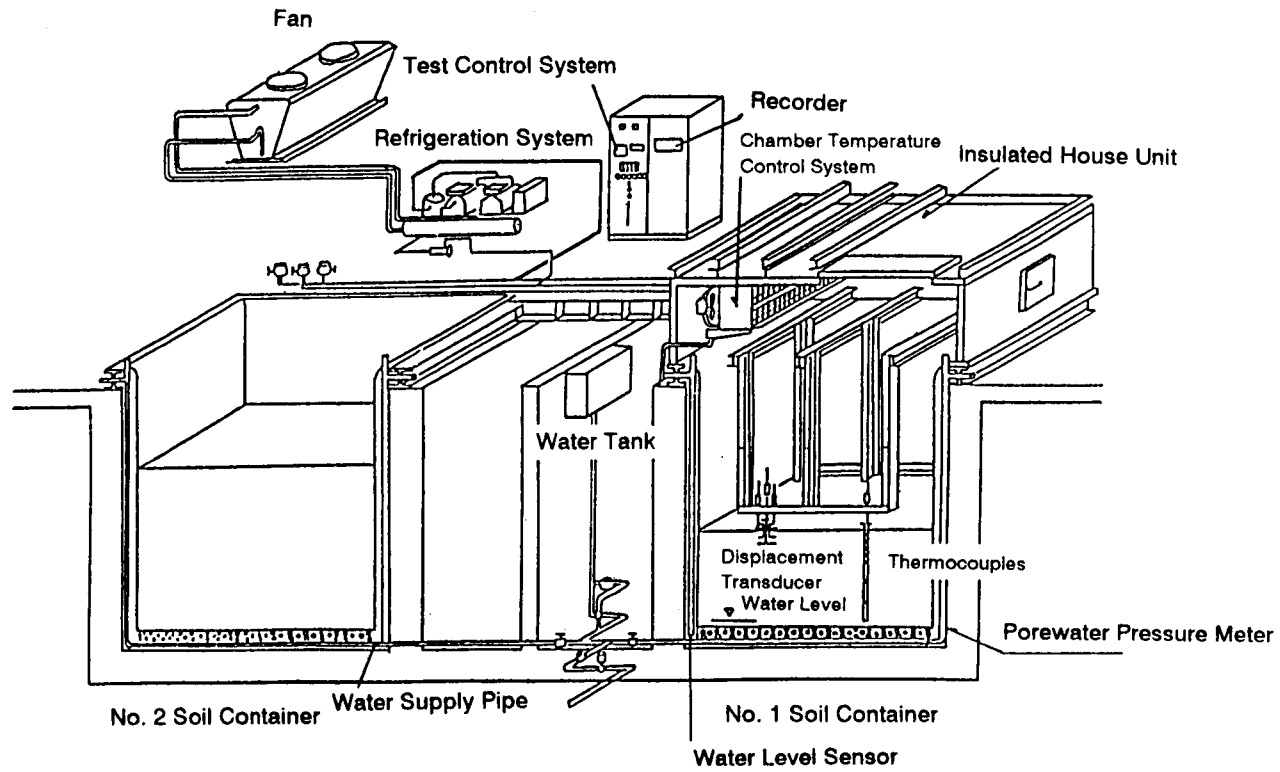


Figure 4.6 Semi-Full Scale Freezing Test System

Table 4.5 Test Boundary Conditions Using the SFFT

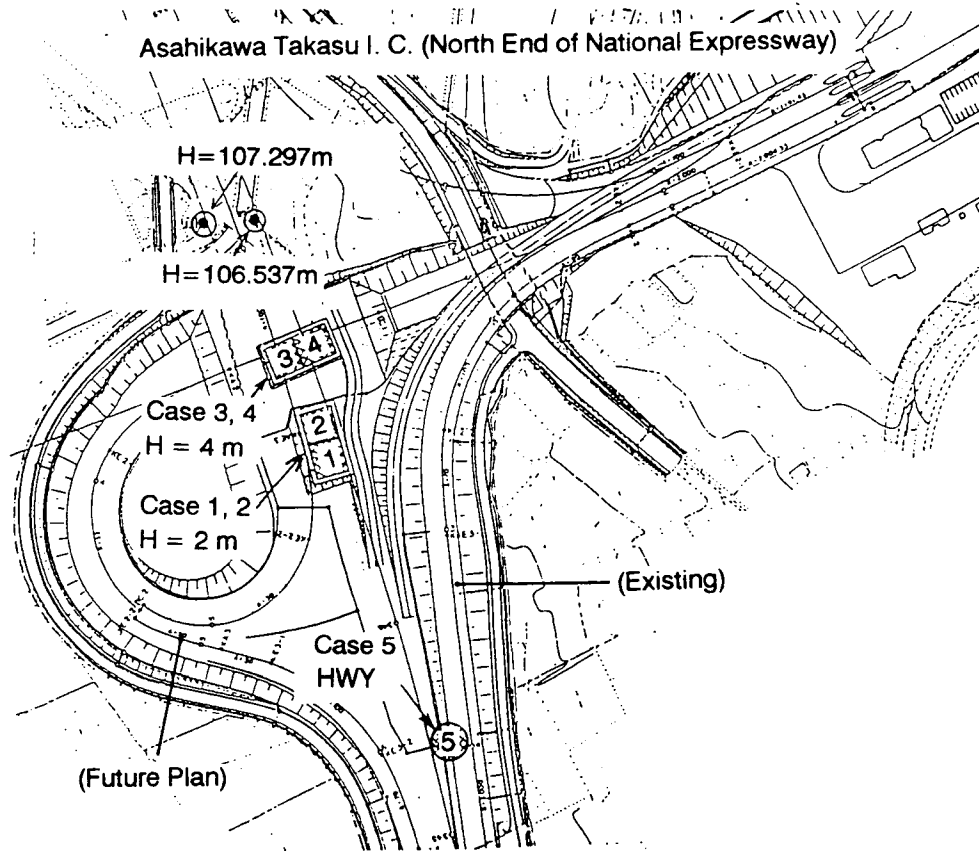
Test No.	Thickness (m)	GWT GL-(m)	Chamber (°C)	Bottom (°C)	γ_d (g/cm ³)	w (%)
1-1	2.8	-1.0	-6.0	+4.8	1.56	19.9
1-2					1.51	19.0
2-1	3.0	-2.0	-6.0	+7.8	1.56	19.1
2-2					1.57	18.9
3	3.0	-0.5	-6.0	+4.9	1.58	18.6
4	3.0	-2.5	-6.0	+9.1	1.53	18.4
5	3.0	-3.0	-6.0	+10.4	1.51	17.9

Field Frost Heave Test Yard

The Asahikawa test yard was constructed at the north end of Japan's national expressway network in 1989 to investigate freezing problems of embankments. Figure 4.7a presents the general plan view of the test yard. Within the yard, four embankments were constructed with Asahikawa soil to observe frost heave. Two embankments were two meters in height and two were four meters in height. For each height, one embankment was constructed using the standard practice (i.e. a replacement of the upper layer of frost susceptible soil with crushed stone). The other embankment was constructed entirely with the frost susceptible material (Asahikawa soil). In the present study, only the observations from the two embankments constructed without replacement of soils were considered. Then the surfaces were paved with asphalt concrete.

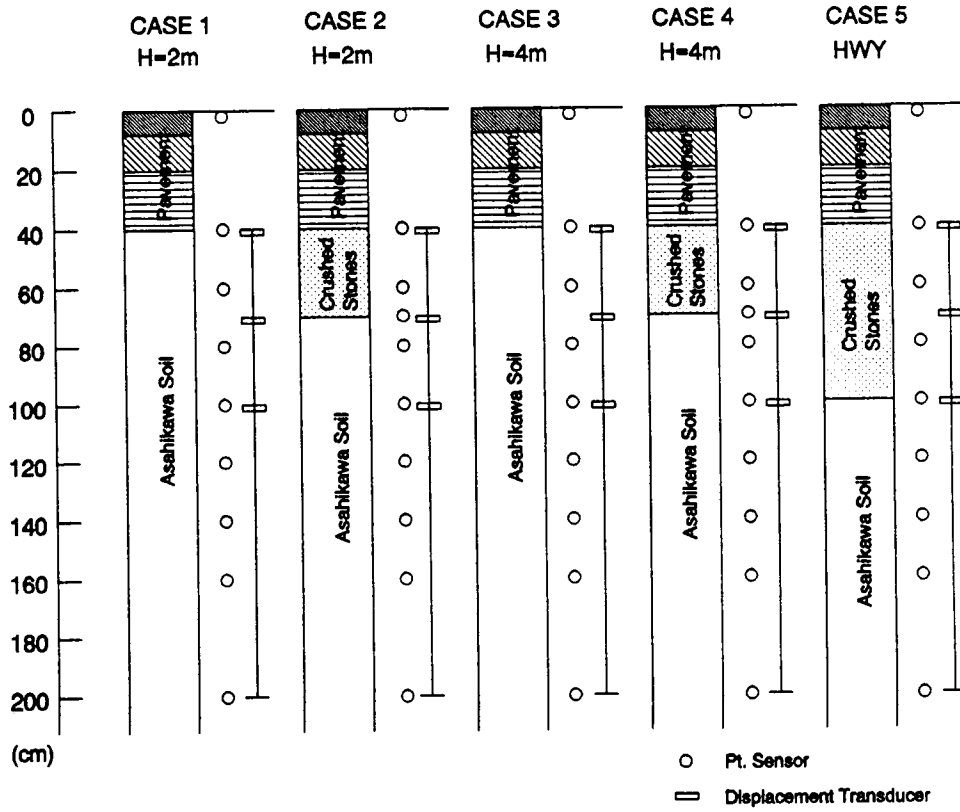
The temperatures and displacements (frost heave) in the ground were measured. Figure 4.7b illustrates the locations of temperature sensors and displacement transducers. The displacement transducers were anchored at a 200 cm depth which was 50 cm deeper than the expected maximum freezing depth at the site. They were designed to measure frost heave when the frost front reached the 40, 70 and 100 cm depth from the roadway surface. The temperature distribution in the ground was monitored with nine to ten platinum temperature sensors placed in each embankment.

The data were recorded at one hour intervals with an automatic data acquisition system. Observations of the four embankments have been made since 1990. The data



(a) Site Location

Figure 4.7 Asahikawa Frost Heave Observation Site



(b) Observation Sensors

Figure 4.7, Continued Asahikawa Frost Heave Observation Site

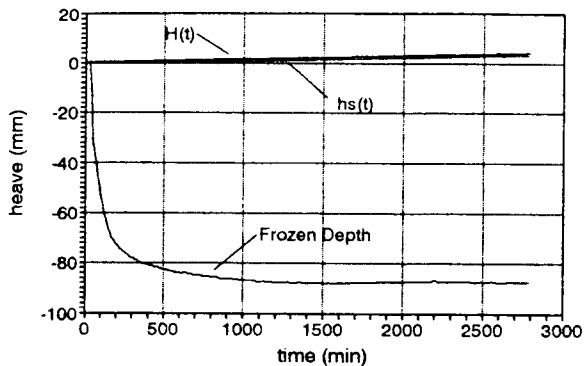
presented in this paper were collected during winter 1990-1991 and 1991-1992 for the Case 1 and 3.

4.8 Test Results

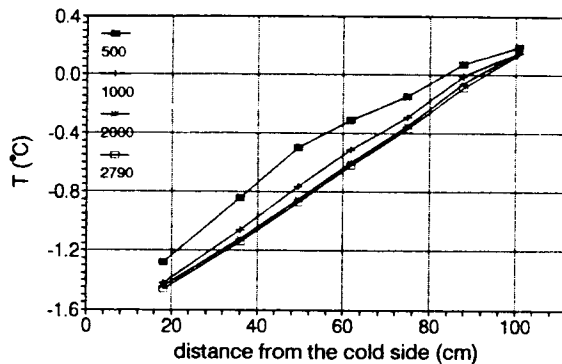
The test results from the proposed laboratory method were analyzed to extract the DIL ice segregation parameters. The relationship between frost heave and groundwater level was expressed in terms of SP. The extracted parameters from the conventional system, SFFT, and field observation were compared with the values predicted from the proposed method.

Prediction of Ice Segregation Parameters from the Proposed Method

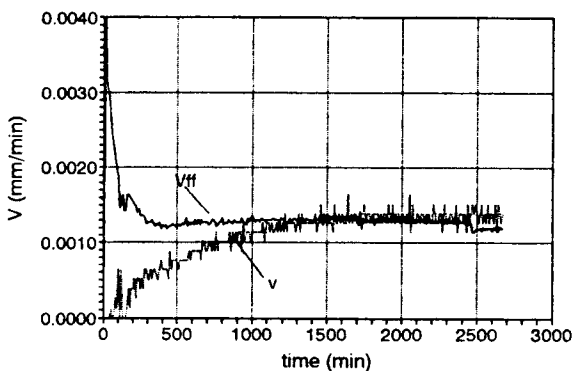
The results from test A-3 are presented in Figure 4.8 to illustrate the extraction procedure of ice segregation parameters from a freezing test. In Figure 4.8a, the total frost heave (H) is directly measured by LVDT and the segregational heave (h_s) is computed from the water intake data. Knowing H and h_s , the two flow velocities V_{ff} and v are computed in Figure 4.8c. The frozen depth is the distance from the top of the specimen (initial height) to the 0 °C isotherm. Figure 4.8b presents an example of the change in the temperature distribution in the sample. Knowing Figure 4.8b, the frozen depth (Figure 4.8a) is interpolated and the temperature gradients of the fringe (G_{ff}) and the frozen part of the soil (G_f') are computed in Figure 4.8d. The ice segregation parameters can be defined at the end of transient freezing in the freezing test. This time



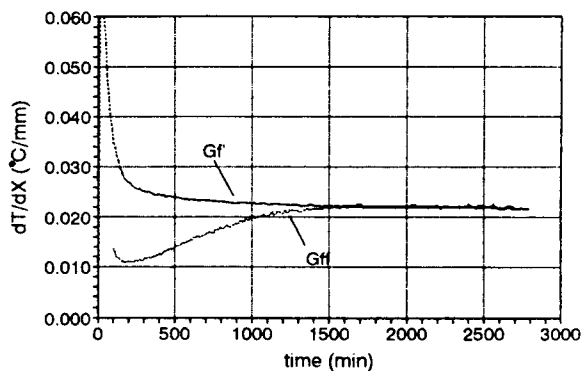
(a) Heave and Frozen Depth



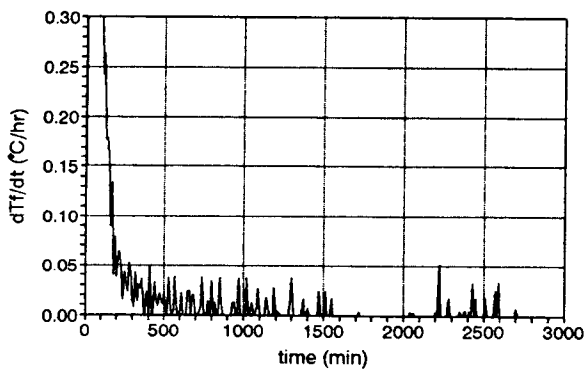
(b) Temperature Distribution



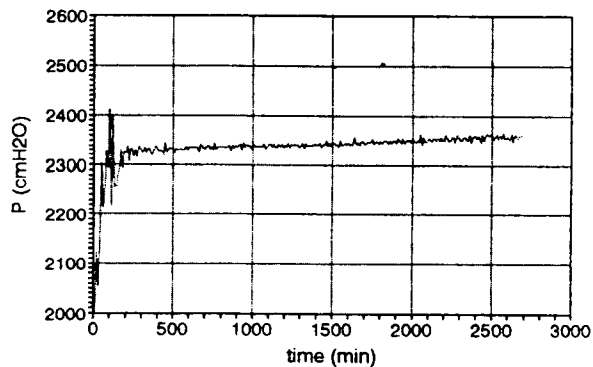
(c) Vff and v



(d) Temperature Gradients

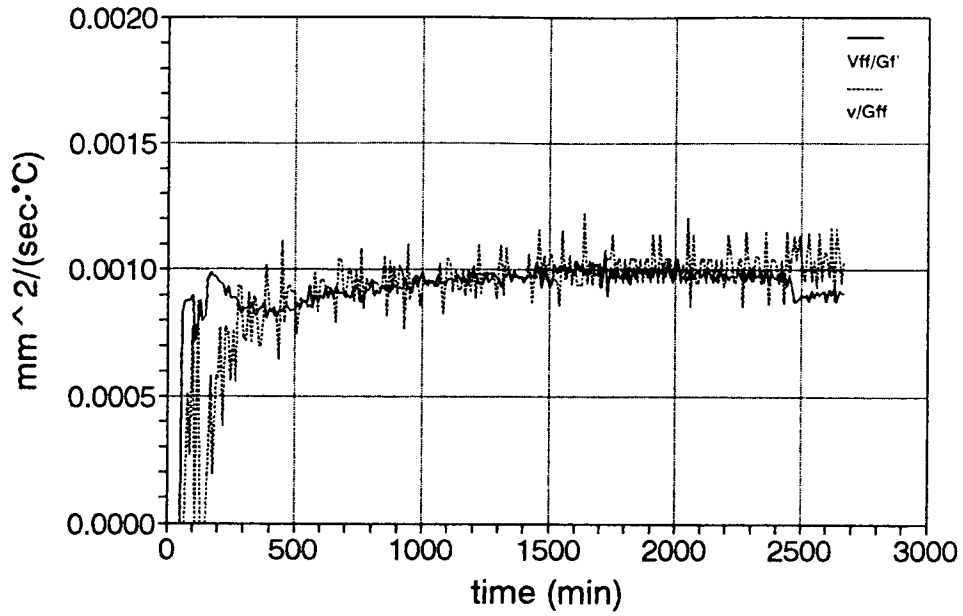


(e) Rate of Cooling



(f) 1.09Po-Pu

Figure 4.8 Results from Test A-3



(g) V_{ff}/G_f' and v/G_{ff}

Figure 4.8, Continued Results from Test A-3

can be defined either by the rate of cooling of a frozen fringe (Figure 4.8e) (which is computed from G_{ff} and the velocity of the frost front advancement) or by the relationship between V_{ff} and v (Figure 4.8c). For test A-3, the end of transient freezing was determined from Figure 4.8c. The end of transient freezing is read as approximately 1250 min. The suction (P_u) is computed by knowing the length of the unfrozen part of the soil and the hydraulic conductivity. Then the combined pressure term ($1.09P_o - P_u$) is computed in Figure 4.8f. Finally, the ratios v/G_{ff} and V_{ff}/G_f' at 1250 min are evaluated from Figure 4.8g.

The results of eight tests were analyzed using Eqs. 4.1 and 4.2. The results were summarized as follows: the log-SP(Eq. 4.2) vs pressure, and the log(1/SP) (Eq. 4.1) vs pressure. Johansen's method (Frivik 1980; ISGF 1991) was used to estimate K_f in Eq. 4.1 (re. Table 4.6). Given the unfrozen water content (Figure 4.9), initial water content, and assuming the soil particle conductivity $k_s = 2.5$ W/mK, K_f was computed independently with Johansen's method. K_f/K_{ff} was assumed to be 1.1 for all tests. The evaluated ice segregation parameters were observed to be distributed over a wide range (re. Figures 4.10a and 4.10b). However, the good agreement observed in the parameters obtained by Eqs. 4.1 and 4.2 indicated that the test procedure was reliable. The evaluated parameters for the lower pressure tests are scattered at the lower position in Figure 4.10a and at the higher position in Figure 4.10b. The results presented in Figures 4.10a and 4.10b exhibited greater scatter than expected. Figure 4.9 provides an explanation for the scatter. In Figure 4.10a, tests A-4, A-6, A-7a, A-7b, and A-8 resulted in greater SP than tests A-1, A-2, A-3, and A-5. This may be supported by the lower unfrozen water

Table 4.6 Thermal Conductivity of a Freezing Soil (after ISGF 1991)

$$k_u = k^\circ + (k_u^1 - k^\circ) \cdot K_e,$$

$$\text{or } k_f = k^\circ + (k_f^1 - k^\circ) \cdot K_e$$

where,

k°	$= 0.034 \cdot n^{-2.1}$	dry conductivity
k_u^1	$= 0.57^n \cdot k_s^{(1-n)}$	unfrozen saturated
k_f^1	$= 2.3^n \cdot k_s^{(1-n)}$	frozen conductivity
K_e	$= S_r$	frozen
	$= 0.68 \cdot \log S_r + 1$	clay content < 2%, unfrozen
	$= 0.94 \cdot \log S_r + 1$	clay content > 2%, unfrozen
K	$= k_f + (k_u - k_f) \cdot w_u / w_{\text{tot}}$	consideration of the unfrozen water content
q		quartz content
S_r		degree of saturation
w_{tot}		total water content (% by dry weight)
w_u		unfrozen water content (% by dry weight)
n		porosity
K_e		Kersten number
k_s		particle conductivity
K, k		thermal conductivity (W/mK)

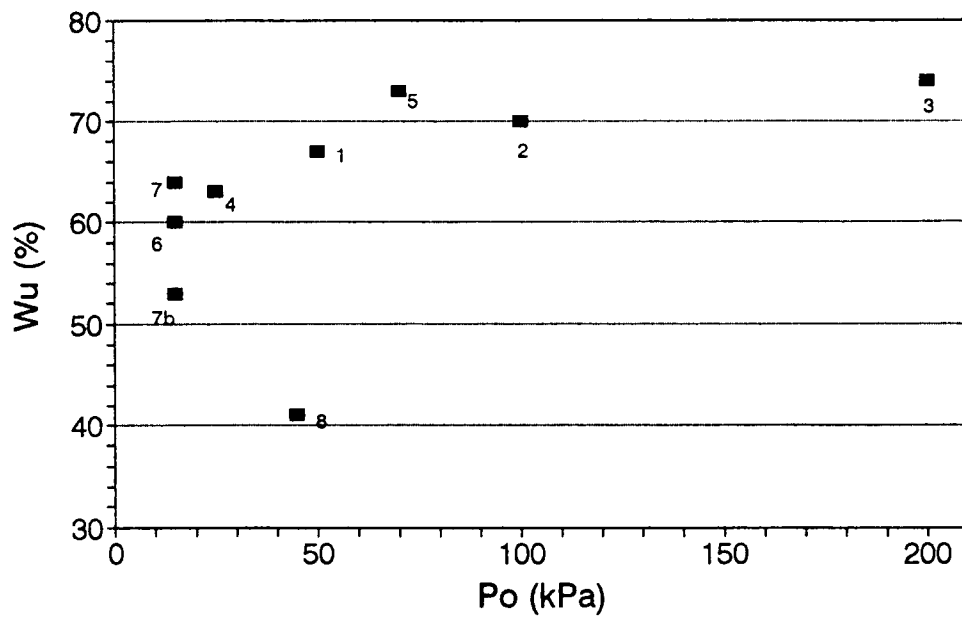
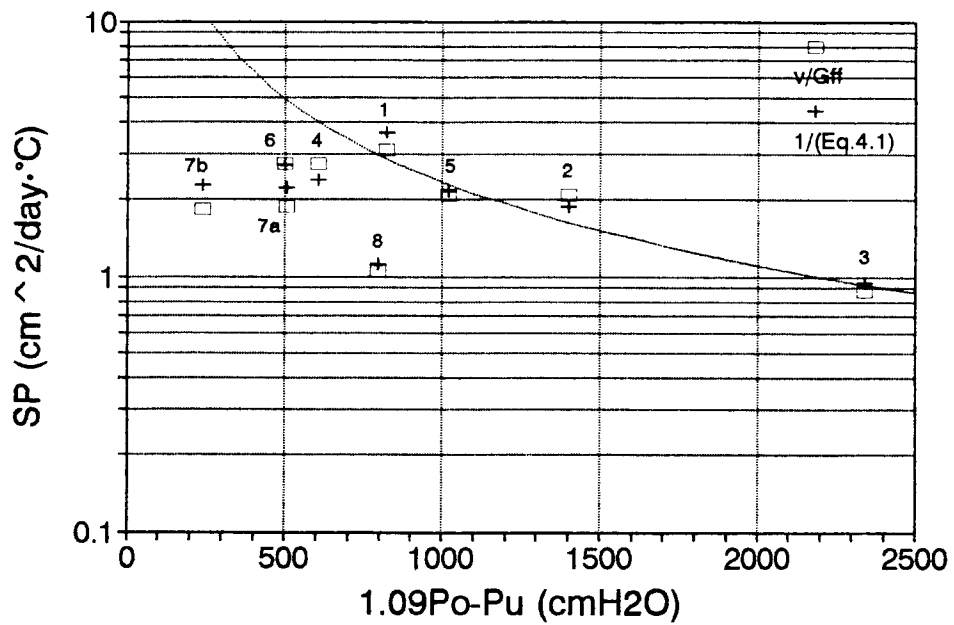
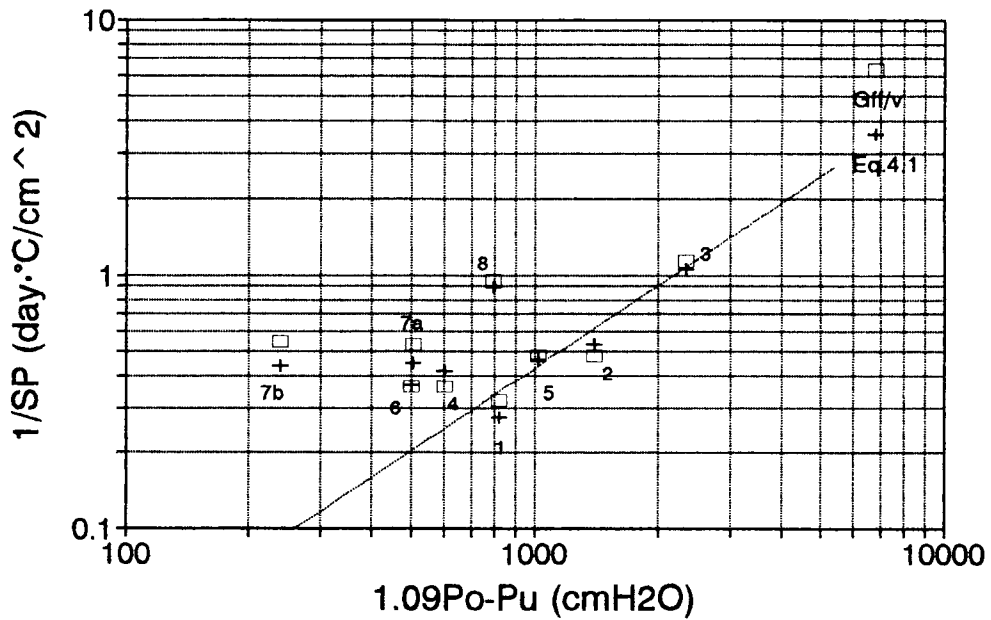


Figure 4.9 Unfrozen Water Content versus Overburden Pressure



(a) v/G_{ff} , $1/(Eq.4.1)$



(b) G_{ff}/v , Eq.4.1

Figure 4.10 Evaluation Ice Segregation Parameters

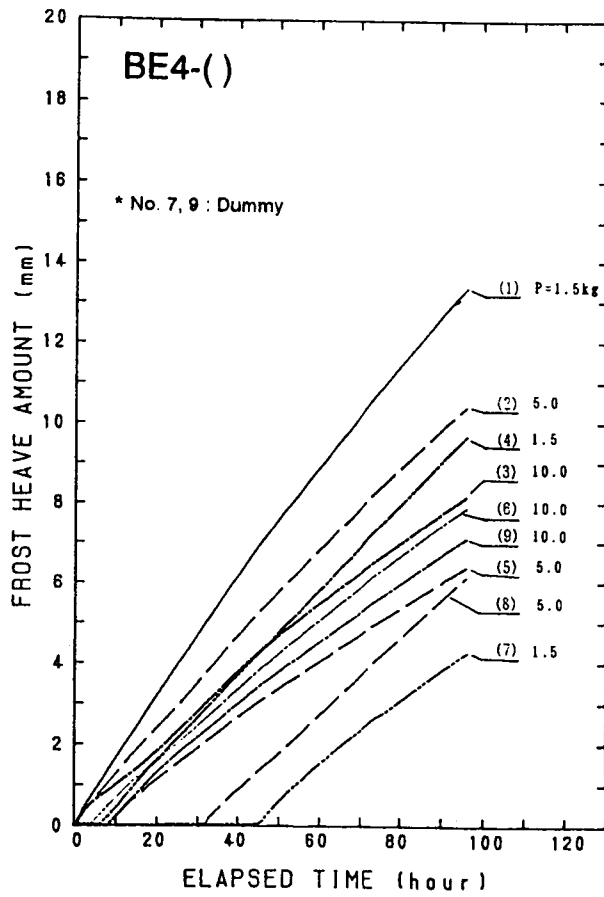
content in A-4, A-6, A-7a, A-7b, and A-8 in Figure 4.10. The less unfrozen water content and lower SP are related to the lower pressure (Figure 4.10a). It was also noted that extremely small heaves occurred if the samples were frozen with extremely steep temperature gradient conditions (e.g. A-7b and A-8). The same tendency was observed previously in the tests with Calgary silt (Ito et al. 1993). To predict field frost heave in which the temperature gradient is very shallow and the frost front progresses very slowly, it is recommended that the ice segregation parameters with the greater unfrozen water contents be used. Therefore, the DIL parameters were extracted by linear regression of the points A-1, A-2, A-3, and A-5 in Figure 4.10b as $\alpha = 1.08$ and $k_0 = 2.49 \times 10^{-5}$ cm/day. Using these values from α and k_0 , SP can be reconstructed as a line on Figure 4.10a.

In a cut section where hydraulic conductivity is higher, in general, than the compacted embankment from the same soil and when the frost heave is not so severe, the suction is approximately equal to the distance from the groundwater table to the frost front. Therefore, the pressure term can directly relate to the sum of overburden pressure (or the weight of soil) and the distance from the frost front to the groundwater table. For compacted embankments, where hydraulic conductivity may be smaller, this approximation may be conservative, but can be used for design purpose. Therefore, the line drawn on Figure 4.10a represents a conservative estimate of SP or ice segregation parameter for design purposes.

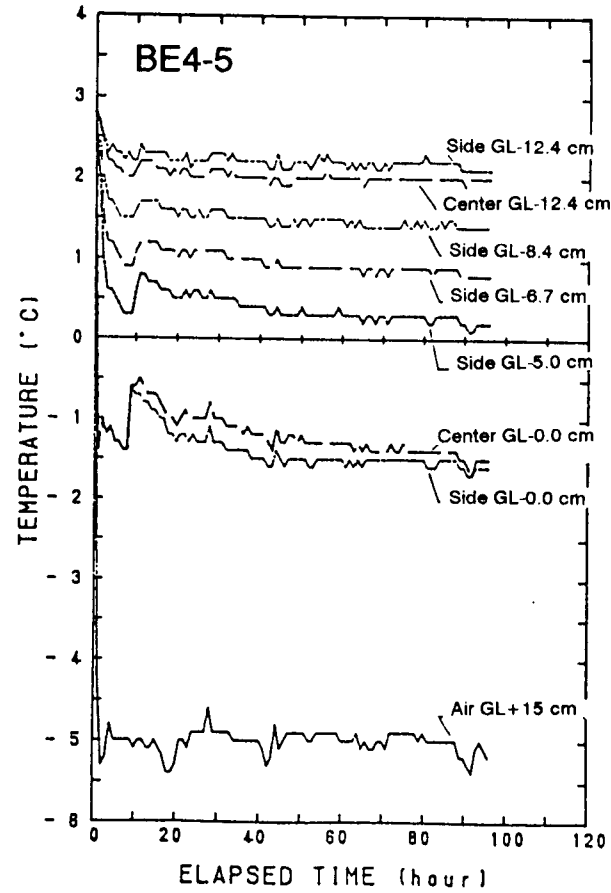
Analysis of the Frost Susceptibility Test by the Conventional Method

Figure 4.11 presents an example from the JH's conventional frost heave test with Asahikawa soil. The results were evaluated according to the conventional criteria. As a result, it was reported that the heave ratio was approximately 10 to 30 % and the frozen class No. was three to five according to the criteria in Table 4.3. After a four day test, several ice lenses were usually observed in the frozen specimen. According to the criteria, the visibility of ice lenses is the typical feature of the frost susceptible soil. The temperature gradients in the tests were approximately the same as the ones used in the standard frost heave test procedure and the test period was four days, which was two days shorter. Thus, the soil would show greater frost susceptibility if the tests were conducted with the standard procedure. Therefore, it was concluded that this soil be evaluated as "highly frost susceptible soil". For highway construction, all materials up to 100 cm depth from the pavement surface (approximately 60 cm from the base of pavement) should be replaced with crushed aggregate.

The amount of frost heave observed depends on the location of the specimens in the test chamber, indicating the non-uniformity of freezing condition in the chamber. This is a major shortcoming in this type of freezing test system, which uses cold side air temperature controlling method. In addition, the temperature information to describe the test boundary condition is lacking in the system and the evaluation criteria.



(a) Frost Heave vs Time



(b) Temperatures vs Time

Figure 4.11 Frost Heave Test Result by the Conventional Frost Susceptibility Test System

Analysis of the Frost Susceptibility Test For Modified Conventional Method

The conventional method was modified by installing thermocouples. This improvement was to provide additional temperature information to the conventional method. As a result, ice segregation parameters became to be evaluated. The overall temperature gradient in the frozen soil G_f' was computed by dividing the specimen top temperature by the thickness of the frozen part of the specimen. Assuming $K_f/K_{ff} = 1.0$, $G_f = G_f'$, and $L/K_f = 0.2$, the relation between the left hand side of Eq. 4.1 and $(1.09P_o - P_u)$ was plotted. The suction P_u was computed given the hydraulic conductivity 3×10^{-8} cm/sec in the unfrozen soil, which was directly measured in the specimen.

Figure 4.12 presents the test result using the modified conventional method. As can be seen, the data is scattered. This is due to the poor accuracy of the thermocouple temperature readings. However, the results clearly indicated the general tendency that the greater the pressure term the smaller the SP. Therefore, it is likely that the conventional frost susceptibility test system can be used to evaluate ice segregation parameters with minor modification. Although the accuracy of the individual points in Figure 4.12 may not be completely reliable, the large number of data points appear to compensate for the scatter. The DIL parameters can be evaluated as $\alpha = 0.91$ and $k_o = 4.80 \times 10^{-6}$ cm/day.

Result and Analysis of SFFT

Figure 4.13 illustrates an example of a typical test result from the SFFT. Figure 4.14 presents the relationship between the total frost heave at 45 days and the distance

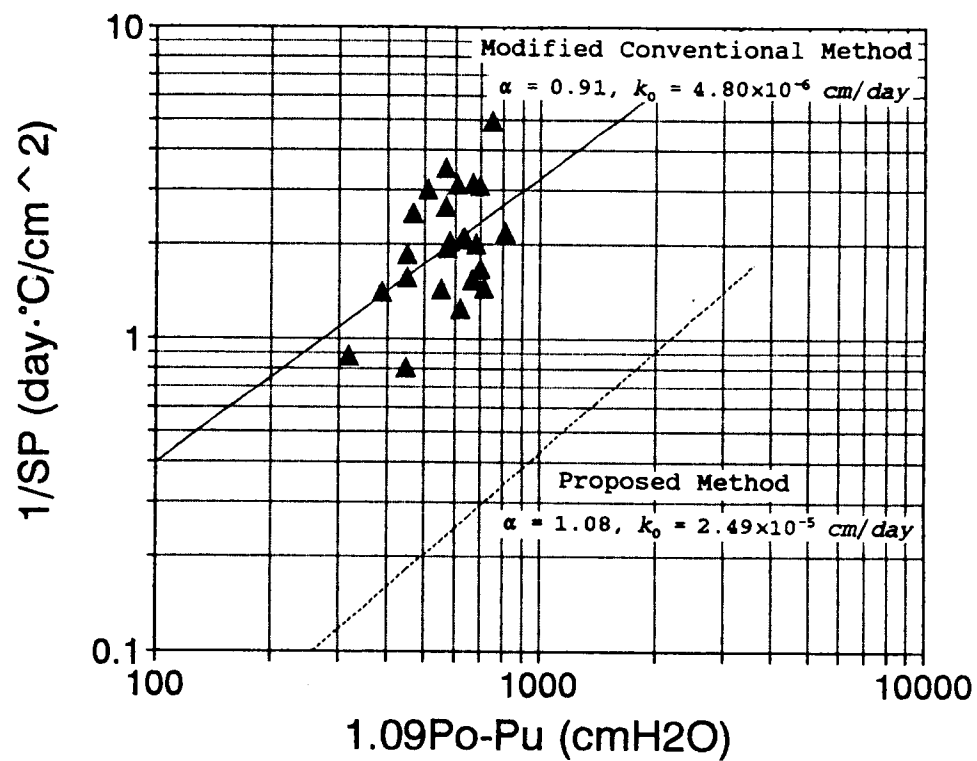
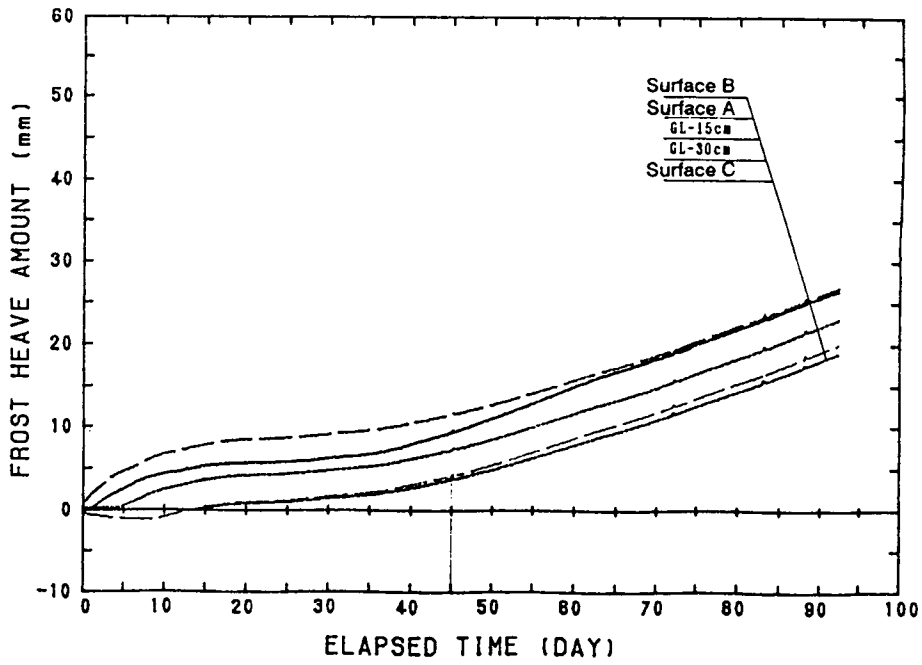
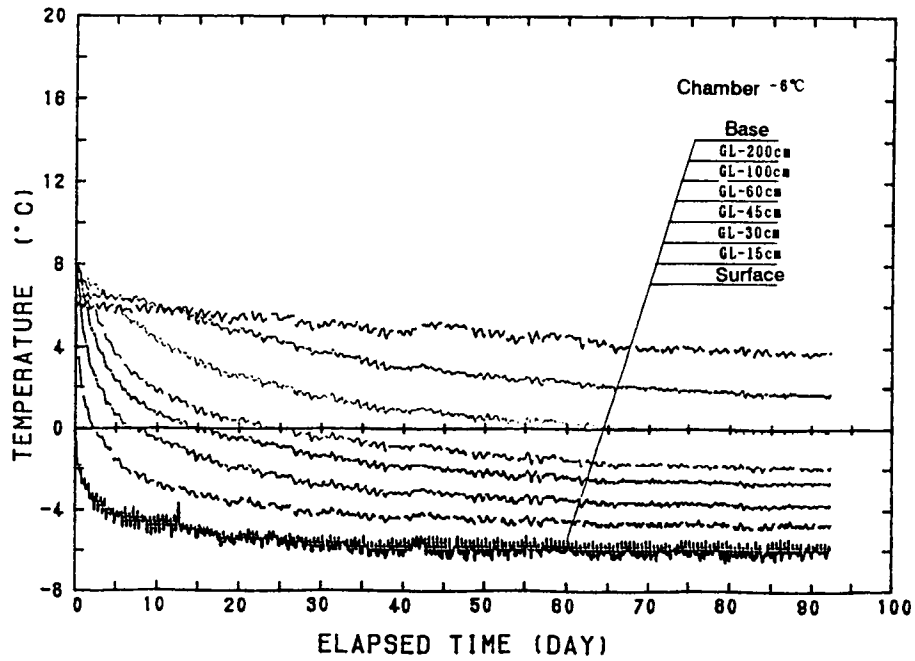


Figure 4.12 Extraction of DIL Parameters from the Modified Conventional Frost Susceptibility Test Result



(1) Frost Heave vs time



(2) Temperature Change vs time

Figure 4.13 Frost Heave Test Result by the SFFT

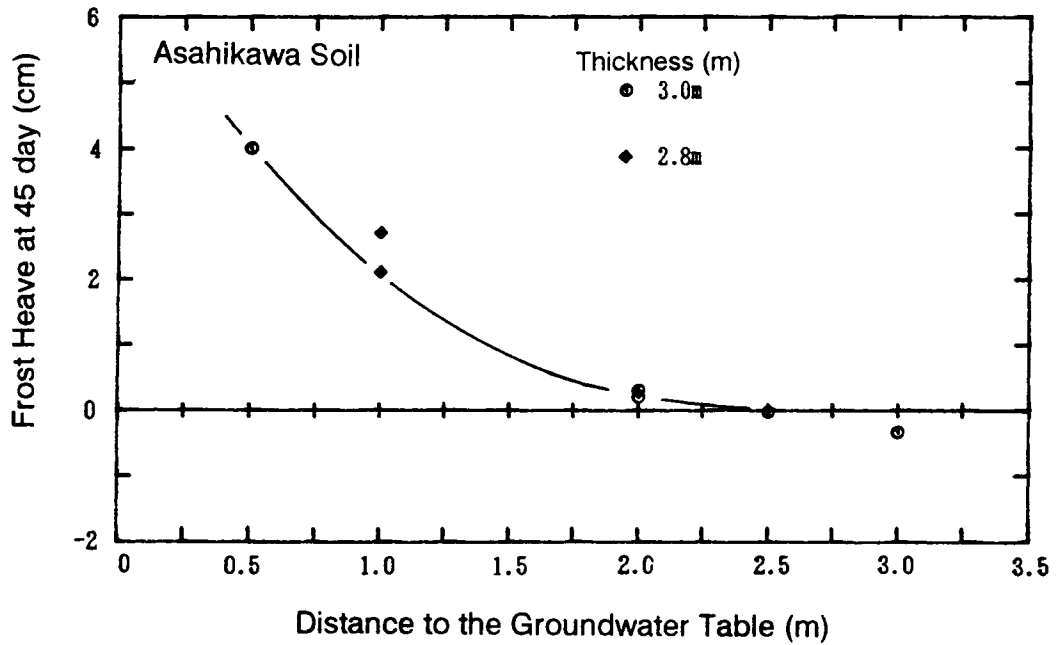


Figure 4.14 Frost Heave at 45 Days versus Groundwater Level

to the groundwater table from the surface. It was observed that the lower the groundwater level the smaller the amount of heave and heave velocity. However, Figure 4.14 does not provide any information that would allow one to predict the field frost heave because of the lack of boundary information. In order to predict the frost heave under field conditions, ice segregation parameters, which are independent of the test boundary condition, should be evaluated.

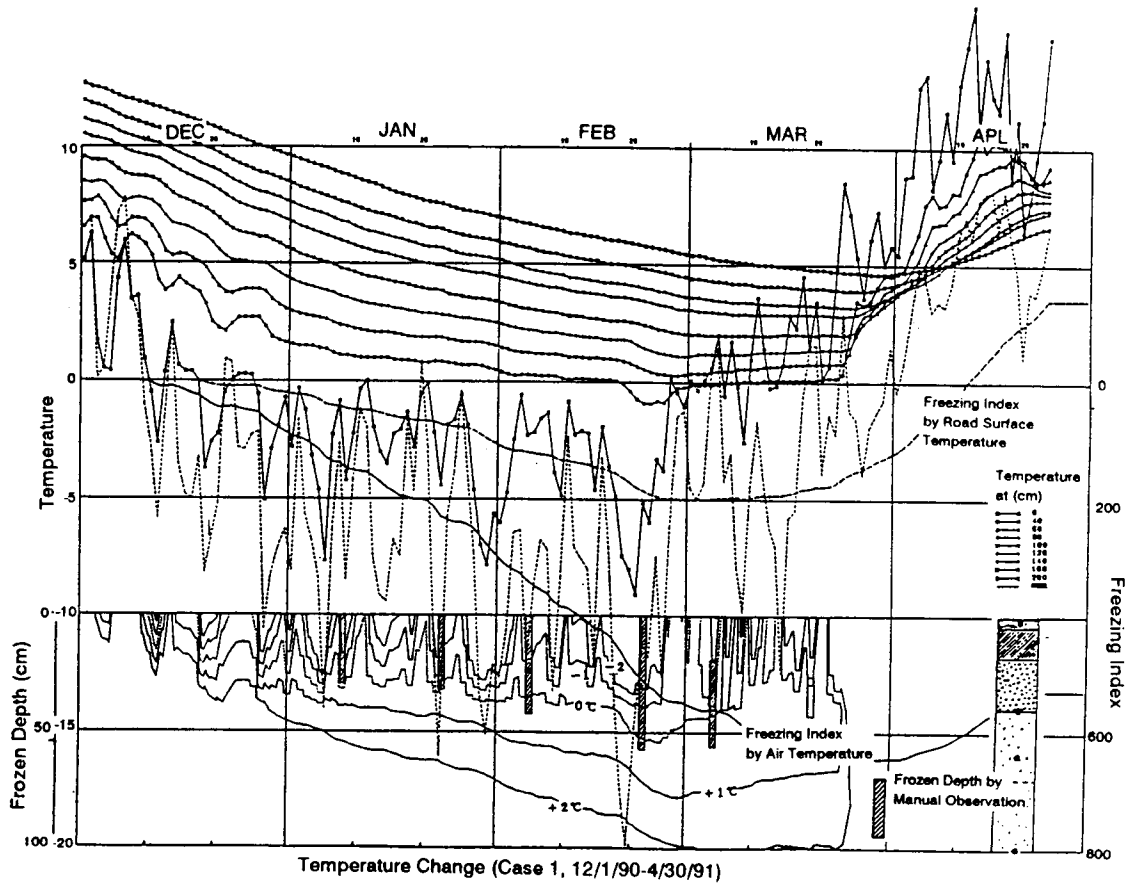
To estimate ice segregation parameters from the SFFT results, the overall temperature gradient of frozen part of soil (G_f'), was estimated with two adjacent thermocouple readings in the frozen soil close to the 0 °C isotherm location. Using the same assumptions used in the previous section ($K_f/K_{ff} = 1.1$, $L/K_f = 0.2$, and $G_f = G_f'$), the relation between the term in the left side of Eq. 4.1 and $1.09P_o - P_u$ can be obtained in a log-log graph. The hydraulic conductivity was assumed as 3×10^{-8} cm/sec. The overburden pressure is computed by multiplying the frozen depth times the unit weight of the soil. The results are tabulated in Table 4.7.

Result and Analysis of the Field Test

Figure 4.15a illustrates an example of the field frost heave observation (e.g. Toya et al. 1992). The maximum frozen depth barely exceeded into Asahikawa soil in Cases 1 and 3 during the winters of 1990-91 and 1991-92. Therefore, no data are available from the displacement transducers at 70 and 100 cm, and Cases 2 and 4. The frost heave versus time relationship in the coldest period of the 1991-92 winter is illustrated in Figure 4.15b.

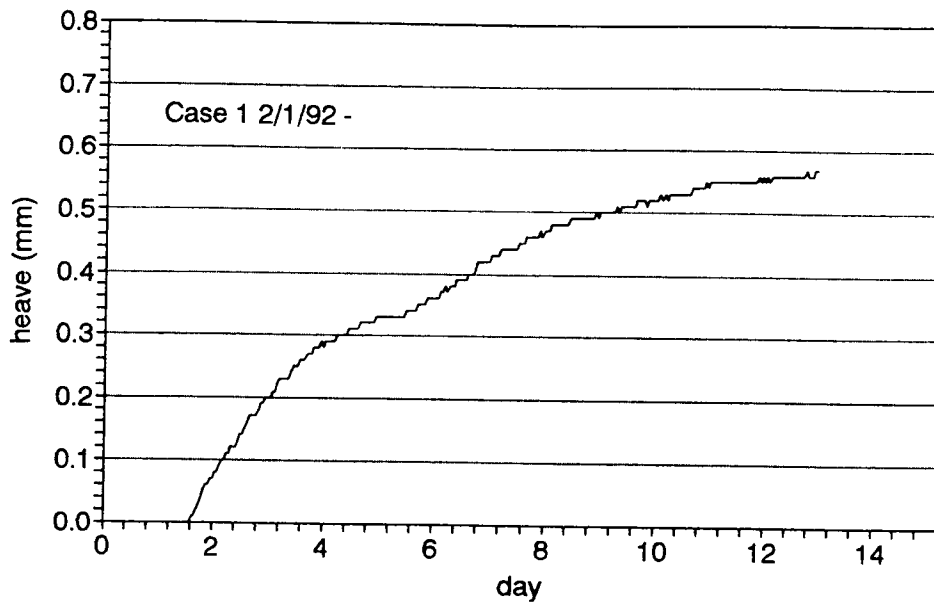
Table 4.7 Ice Segregation Parameters from SFFT

Test No.	time day	f-depth cm	Vh mm/day	Gf' C/mm	SP cm ² /day C	1.09Po-Pu cmH ₂ O
1-1	80	74	0.350	0.0045	0.757	3629
1-2	80	75	0.280	0.0045	0.586	2821
2-1	37.5	45	0.104	0.0093	0.095	6291
2-2	37.5	49	0.034	0.0093	0.031	2059
3	32.5	42	0.895	0.0093	0.975	1794
4	40	45	0.116	0.0080	0.124	9246
5	-	-	0	-	-	-



(a) Temperature

Figure 4.15 Field Frost Heave Observation (after Toya et al. 1992)



(b) Frost Heave

**Figure 4.15, Continued Field Frost Heave Observation
(after Toya et al. 1992)**

In order to evaluate the ice segregation parameters, G_f' and the heave velocity were measured and the assumption, $K_f/K_{ff} = 1.1$, $L/K_f = 0.2$, and $G_f = G_f'$, were used. The ice segregation parameters were tabulated in Table 4.8.

4.9 Discussion

Figure 4.16 shows the plots of ice segregation parameters from SFFT and field observations with the predicted lines from the proposed method and modified conventional test system. Good agreement was observed between the design SP by the proposed method and the results from the SFFT. This is significant because it means that the simple laboratory test can easily predict the performance of the SFFT. The scatter in the SFFT results are considered to be related to local difference of frost heaves; some sections of the specimen may be confined when other sections were heaving.

The field test results plot well below the design SP by the proposed method. But a relatively good agreement was observed in the relationship between the field test results and the modified conventional method. This is believed to be related to the smaller hydraulic conductivity in the compacted embankment. In general, the hydraulic conductivity of the compacted soil is smaller than that of the original ground. Further, the embankment is considered to be under unsaturated conditions which might result in the smaller hydraulic conductivity. On the other hand, in the proposed method the specimen was prepared by consolidating the slurry allowing water flow through the base of a specimen. The design SP obtained from the proposed method gives a conservative estimate of frost heave in the embankment.

Table 4.8 Ice Segregation Parameters from the Field Observation

CASE	time date	f-depth cm	Vh mm/day	Gf' °C/mm	SP cm ² /day·°C	1.09Po-P cmH ₂ O
C1 90-91	2/21/91	50	0.1120	0.0080	1.997	437
C1 91-92	2/2/92	50	0.1270	0.0085	2.196	437
C3 90-91	2/21/91	60	0.0150	0.0080	0.194	612
C3 91-92	2/2/92	55	0.0053	0.0090	0.059	612

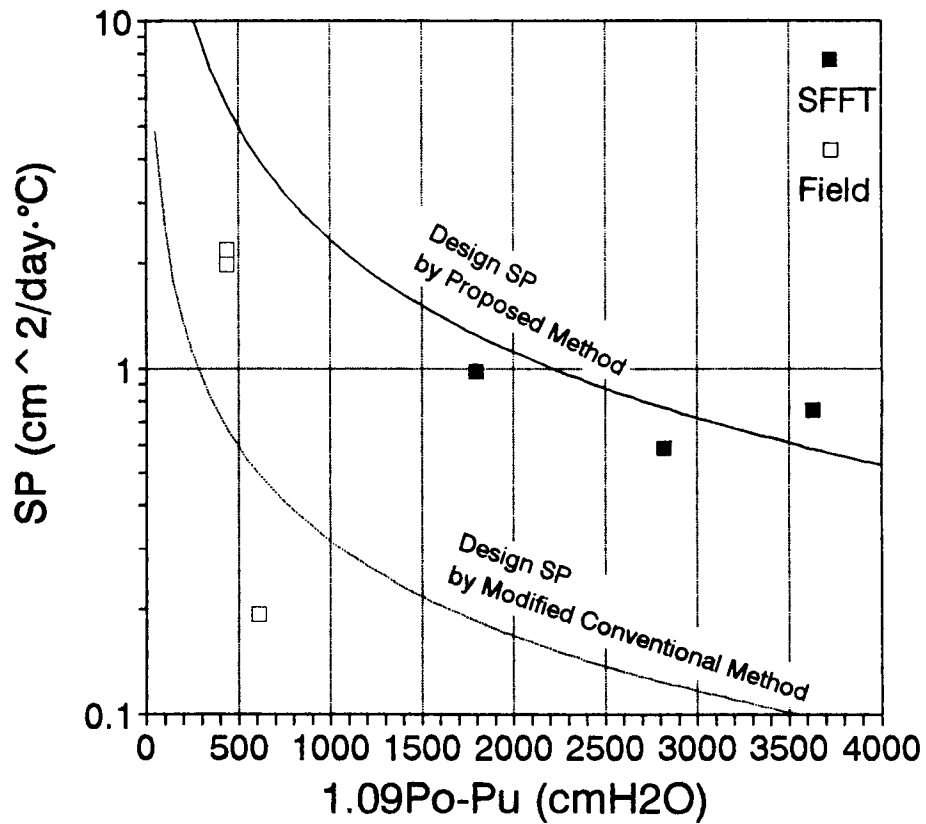


Figure 4.16 Ice Segregation Parameters: Predicted versus Observed

4.10 Summary and Conclusion

A procedure to estimate the ice segregation parameters in association with the groundwater level was demonstrated. The proposed test procedure is conducted with a step freezing test system with different overburden pressures instead of the different groundwater levels. The result from a modified conventional frost susceptibility test system was also interpreted by the proposed procedure to evaluate the ice segregation parameters. The ice segregation parameters evaluated from the proposed laboratory method and conventional test system were compared with the parameters calculated from the SFFT and field observations.

The proposed test method provides a practical estimate of ice segregation parameters for field problems. It was concluded that the proposed procedure will give the upper bound of ice segregation parameters in field prediction, and can be used for a conservative estimate, which may be satisfactory for design purposes. The simple laboratory procedure proposed may replace the SFFT, which is time consuming and expensive.

4.11 References

1. Bell, J. R., Allen, T., and Vinson, T. S., "Properties of Geotextiles in Cold Regions Applications," In *Proc., Fourth International Conference on Permafrost*, 1983, pp. 51-56.
2. Frivik, P. E., "State of the Art Report. Ground Freezing: Thermal Properties, Modeling of Processes and Thermal Design," In *Proc., Second International Symposium on Ground Freezing*, 1980, pp. 115-133.
3. Gilpin, R. R., "A Model for the Prediction of Ice Lensing and Frost Heave in Soils," *Water Resources Research*, Vol. 16, No. 5, 1980, pp. 918-930.
4. Henry, K. S., "Laboratory Investigation of the Use of Geotextiles to Mitigate Frost Heave," *CRREL Report*, 90-6, 1990.
5. ISGF Working Group 2, "Guidelines for Mechanical and Technical Design of Frozen Soil Structure," In Reports from *Sixth International Symposium on Ground Freezing*, China, 1991, pp. 1-21.
6. Ito, Y., Wakatsuki, Y., Kawaragawa, Z., and Ryokai, K., "Study on Frost Heave Problem of Highway (Part. 1), Problems of the Frost Susceptibility Test," In *Proc., 24th Annual Conference of Japan Society of Soil Mechanics and Foundation Engineering*, 1989, pp. 1051-1052.
7. Ito, Y., Vinson, T. S., and Nixon, J. F., "Examination of the Approximation Used to Interpret Freezing Tests and Verification of the Compatibility of the Segregation Potential and Discrete Ice Lens Frost Heave Models," manuscript, 1993.
8. Ito, Y., Vinson, T. S., Nixon, J. F., and Stewart, D., "An Improved Step Freezing Test to Determine Segregation Potential," manuscript, 1993.
9. Japan Highway Public Corporation Design Specification No. 1, 1983, pp. 78-85.
10. Japan Highway Public Corporation Sapporo Construction Bureau, "Doh-oh Expressway Frost Heave Field Observation Report", 1990.
11. Kawaragawa, Z., Wakatsuki, Y., and Ito, Y., "Study on Frost Heave Problem of Highway Part. 2, Influence of Groundwater Table," In *Proc., 24th Conference of Japan Society of Soil Mechanics and Foundation Engineering*, 1989, pp. 1053-1054.

12. Konrad, J. M., and Morgenstern, N. R., "The Segregation Potential of a Freezing Soil," *Canadian Geotechnical Journal*, Vol. 18, 1981, pp. 482-491.
13. McGaw, R., "Frost Heaving versus Depth to Water Table," *Highway Research Record No. 393*, 1972, pp. 45-55.
14. Nixon, J. F., "Discrete Ice Lens Theory for Frost Heave in Soils," *Canadian Geotechnical Journal*, Vol. 28, 1991, pp. 843-859.
15. Sezai, T., Mishima, N., and Kikuchi, S., "Frost Heave Prevention in Cold Regions - Problems Related to the Conventional Practice and Frost Susceptibility Test-," *Japan Highway Public Corporation Laboratory Report S.59*, 1985, pp. 13-33.
16. Taber, S., "Frost Heaving," *Journal of Geology*, Vol. 37, 1929, pp. 428-461.
17. Taber, S., "The Mechanics of Frost Heaving," *Journal of Geology*, Vol. 38, 1930, pp. 303-317.
18. Tsuchiya, F., Tsuji, S., Mishima, N., and Yokota, S., "Frost Heave Reduction Using Capillary Break Effect of Geotextiles," *Journal of Japan Society of Agricultural Engineering*, Vol. 60, No. 12, 1992, pp. 1123-1126.
19. Weiyue, G., and Xiaozu, Xu., "Field Observations of Water Migration in Unsaturated Freezing Soils with Different Ground Water Tables," In *Proc., Fifth International Symposium on Ground Freezing*, Rotterdam, 1988, pp. 59-64.

4.12 Notation

The following symbols are used in this paper:

G_f	=	temperature gradient of the frozen soil behind the ice lens;
G_f'	=	overall temperature gradient of the frozen soil;
G_{ff}	=	temperature gradient of the frozen fringe;
K_f	=	thermal conductivity of the frozen soil,
K_{ff}	=	thermal conductivity of the frozen fringe;
k_0	=	hydraulic conductivity of the frozen soil at -1 °C;
L	=	latent heat of fusion of water;
P_o	=	overburden pressure;
P_u	=	suction at the frozen fringe - unfrozen soil interface or at the frost front;
V_{ff}	=	water flow velocity in the frozen fringe;
α	=	slope of the relationship between hydraulic conductivity and temperature; and
β	=	thermal constant.

5.0 A Probabilistic Approach for Frost Heave Prediction -Discrete Ice Lens Model with Point Estimate Method for Parameter Evaluation-

by

Yuzuru Ito, Ted S. Vinson, and Solomon C. S. Yim

Abstract

A probabilistic analysis of frost heave prediction was formerly presented by Guymon et al. They demonstrated the usefulness of the probabilistic approach, using Rosenblueth's Point Estimate Method (PEM), which requires only parameter means and their standard deviation. Unfortunately, the ice segregation parameters input by Guymon et al. were estimated from several trial computations since they were difficult to evaluate from a laboratory test.

Later two frost heave models; the segregation potential (SP) and discrete ice lens (DIL) models were developed. These models are based on ice segregation parameters measured in simple one dimensional freezing tests. This is a great advantage of the two models. It appeared that a probabilistic approach would work well with either of the two frost heave models.

A probabilistic frost heave model based on the DIL model was developed. Comparisons were made between the computed and actual frost heave observed in laboratory tests and under field conditions. In the computations for laboratory test, a numerical method was used; in the computations for the field observations, an approximate equation was used.

Predicted frost heave was similar to frost heave observed in the laboratory and field. The shape parameters of the probability distribution (beta distribution) in the computed frost heave were very similar to the ones observed in the field. It was concluded that the DIL model used with the parameters evaluated by the PEM approach may also be used for frost heave prediction.

5.1 Introduction

A probabilistic approach of frost heave prediction was first presented by Guymon et al. (1981). The probabilistic approach developed was based on their deterministic model and Rosenblueth's Point Estimate Method (PEM) (Rosenblueth 1975, 1981) which requires knowledge of only parameter means and their standard deviation. The computer simulation results were compared with the field observations. Good agreement was observed for the amount of frost heave and the shape parameter of the beta distribution for the probability density function (pdf). The ice segregation parameters used in their work were evaluated by trial and error, not from measurements in laboratory tests. This was related to the fact that the ice segregation parameters governing their model were very difficult to obtain from laboratory tests.

In the past two engineering frost heave models have been developed by Konrad (1981) and Nixon (1987). The main difference between these models and the model by Guymon et al. (1981) is that the two models are based on the ice segregation parameters which are easily extracted directly from laboratory freezing tests. In the Segregation Potential (SP) model, the parameter SP can be defined by the ratio of water intake

velocity (v) and temperature gradient at the frozen fringe (G_{ff}) at the formation of the final ice lens or at the end of transient freezing. SP is related to the hydraulic conductivity of the frozen fringe and the suction at its base. In the Discrete Ice Lens (DIL) model, the ice segregation parameters α and k_o , which are extracted from the results of the freezing tests, directly express the hydraulic conductivity in the frozen fringe.

The ice segregation parameters governing these models can be estimated with satisfactory accuracy if proper freezing tests and analysis are conducted (Ito et al. 1993). This is a great advantage of the two models since the parameters governing the hydraulic conductivity of a freezing soil, which used to require a complicated test to measure, can be estimated from a series of simple freezing tests. Therefore, it is expected that a PEM probabilistic approach may be more appropriate for the SP or DIL model in which the parameter means and their standard deviation can be easily established from laboratory freezing tests.

5.2 Statement of Purpose

The purpose of the research work presented herein was to demonstrate a probabilistic approach to predict frost heave based on the DIL model and the PEM method. The scope of the work includes a description of the DIL model and PEM method, computation of the laboratory freezing test and field frost heave using the ice segregation parameters evaluated by PEM, and probabilistic interpretation of the computed frost heave.

5.3 Discrete Ice Lens Model

The complete description of the DIL model was presented by Nixon (1987). The ice segregation parameters in the DIL model directly express the hydraulic conductivity of the frozen fringe, and they can be evaluated from simple freezing tests. Although there are several models whose ice segregation parameters also describe hydraulic conductivity of the frozen soil, only the DIL parameters can be extracted from a series of simple freezing tests. This is one of the greatest advantages of the DIL model.

The details of the model were described by Nixon (1991). Briefly in the DIL model, linear temperature distribution was assumed throughout the freezing soil (re. Figure 5.1). This assumption is valid when a slowly advancing frost front is similar to the field situation. The following heat balances hold at the frozen soil - frozen fringe interface:

$$K_f G_f - K_{ff} G_{ff} = LV_{ff} \quad (5.1)$$

and at the frost front:

$$K_{ff} G_{ff} - K_u G_u = L \frac{dH_f}{dt} \quad (5.2)$$

where, $K_f, K_{ff}, K_u =$ thermal conductivities of frozen part, frozen fringe and unfrozen part of the soil,

$G_f, G_{ff}, G_u =$ temperature gradients of frozen part, frozen fringe and unfrozen part of the soil,

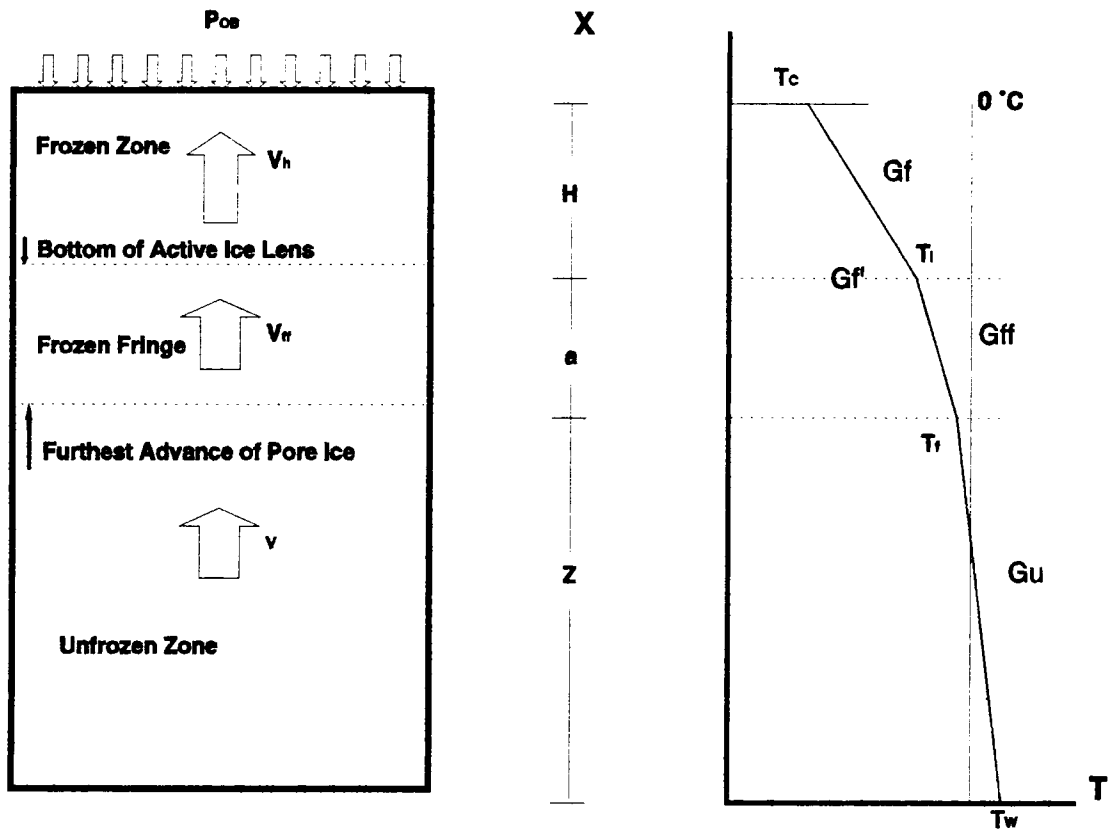


Figure 5.1 Frost Heave Model (modified from Gilpin 1980)

- L = latent heat of fusion of water,
 V_{ff} = water flow velocity to the ice lens base, and
 H_f = amount of water frozen in a frozen fringe.

The amount of water frozen for a fringe of thickness a and an ice lens temperature T_l is evaluated assuming the unfrozen water content (W_u) with the relationship; $W_u = A(-T)^B/w_{tot}$ (Anderson et al. 1972). Integration through the frozen fringe produced

$$H_f = na \left(1 + \frac{A((-T_f)^{1+B} - (-T_l)^{1+B})}{w_{tot}(1+B)(T_f - T_l)} \right) \quad (5.3)$$

- where, n = porosity,
 A, B = constants expressing W_u ,
 w_{tot} = total water content,
 T_f = temperature at the frost front, and
 T_l = temperature at the ice lens base.

The amount of water frozen in the fringe is a function of two variables, a and T_l , both of which vary with time. The rate of advance of the frost front (da/dt) can be computed from

$$L \frac{dH_f}{dt} = L \left(\frac{dH_f}{da} \cdot \frac{da}{dt} + \frac{dH_f}{dT_l} \cdot \frac{dT_l}{dt} \right) = (Q_{ff} - Q_u) \quad (5.4)$$

- where, $Q_{ff} = K_{ff}G_{ff}$ and $Q_u = K_uG_u$.

The mass - flow equation in the frozen fringe was developed assuming a 9 % phase expansion for each unit volume of water frozen,

$$\frac{d}{dx} \left(k \frac{dP_w}{dx} \right) = 0.09 n \frac{dW}{dt} \quad (5.5)$$

where, k = hydraulic conductivity in the frozen fringe, and

P_w = water pressure in the frozen fringe.

The hydraulic conductivity at temperature T (below 0 °C) is expressed as

$$k = \frac{k_0}{\left(\frac{T}{-1^\circ \text{C}} \right)^\alpha} \quad (5.6)$$

where, k_0 = hydraulic conductivity at -1 °C, and

α = constant.

In order to solve Eq. 5.5, a finite difference numerical solution (e. g. Press et al. 1986) was used in each step with the boundary conditions at the base of the ice lens:

$$P_w = 1.09 P_o + \beta T_l \quad \text{at } x = 0 \quad (5.7)$$

where, P_o = overburden pressure,

β = thermal constant, and

x = distance from the ice lens base.

and at the frost front:

$$P_w = P_u \quad \text{at } x = a \quad (5.8)$$

Knowing the pressure distribution, the water flow velocity to the ice lens base V_{ff} is computed and substituted in Eq. 5.1. Several iterations are carried out to find the ice lens temperature T_l that satisfies Eq. 5.1. When T_l becomes known, Eq. 5.4 is used to obtain the rate of advance for the frost front da/dt .

To predict the location of a new ice lens, the ice pressure (P_i) is computed as

$$P_i = \frac{P_w - \beta T}{1.09} \quad (5.9)$$

A new ice lens starts to form in the frozen fringe where

$$P_i > P_o + P_{sep} \quad (5.10)$$

where P_{sep} is separation pressure.

5.4 Extraction of the DIL Parameters

The DIL parameters can be determined from a series of step freezing tests with different overburden pressures. The temperature gradients of the frozen part or frozen fringe and the heave or water intake velocities are evaluated at the end of transient freezing or at near steady state conditions. The following relation is used to extract the DIL parameters:

$$\frac{K_f \left(\frac{G_f}{V_{ff}} - \frac{L}{K_f} \right)}{K_{ff} \left(\frac{G_f}{V_{ff}} - \frac{L}{K_f} \right)} = \frac{\left(\frac{\alpha + 1}{\alpha} (1.09 P_o - P_u) \right)^\alpha}{k_0 \beta^{1+\alpha}} \quad (5.11)$$

Replacing the expression on the left side with Y and $(1.09P_o - P_u)$ as X in Eq. 5.11,

$$Y = \alpha X + \log \frac{\left(\frac{\alpha + 1}{\alpha} \right)^\alpha}{k_0 \beta^{\alpha+1}} \quad (5.12)$$

The plots of X and Y produce the slope α and the intersection b . The k_0 is computed from:

$$k_0 = \frac{\left(\frac{\alpha + 1}{\alpha} \right)^\alpha}{10^b \beta^{\alpha+1}} \quad (5.13)$$

5.5 Limitation of the DIL model

The numerical method to solve Eq. 5.5 has not been developed yet because of the difficulty in evaluating the condition when frost front advancing rapidly. However, an approximation of the right hand side as zero does not greatly influence the total heave (Nixon 1993). For the work presented herein, the right hand side of Eq. 5.5 is approximated as zero. Actually, under the field conditions in which the frost front is progressing very slowly, the right hand side of Eq. 5.5 can be approximated as zero.

5.6 Simplified Equations for Field Frost Heave Prediction

For field predictions, Eq. 5.11 can be used directly to compute heave velocity knowing the temperature gradient:

$$V_h = 1.09 V_{ff} = \frac{G_f}{\frac{K_{ff}}{K_f} \frac{1}{SP} + \frac{L}{K_f}} \quad (5.14)$$

where,

$$SP = \frac{k_0 \beta^{1+\alpha}}{\left(\frac{\alpha+1}{\alpha} (1.09 P_o - P_u) \right)^\alpha} \quad (5.15)$$

This is equal to the form proposed by Nixon (1987) if K_f/K_{ff} is assumed as 1. Nixon also stated that the heave velocity can be computed knowing the temperature gradient in the frozen soil above the frost front when the frost front is advancing very slowly.

For the design of civil engineering structures in a seasonal frost area, several methods are proposed to predict the maximum frost heave. For example, Saarelainen (1992) proposed the following approximate equations based on field observations:

$$\frac{h}{z_f} = \frac{2SP}{m^2} + 0.09n \quad (5.16)$$

where, h = frost heave,
 z_f = frozen depth,
 SP = segregation potential, and
 m = constant.

Eq. 5.16 is very convenient to use when only the maximum frost heave is of concern, such as, for highway design in seasonal frost heave areas. Given maximum allowable frost heave, the predicted mean frost heave and its standard deviation will give the probability of occurrence in which the frost heave exceeds the maximum allowable value for a pre-determined probability distribution function.

5.7 Probabilistic Frost Heave Prediction

The Point Estimate Method (PEM) was introduced by Rosenblueth (1975). This method has been applied to a wide range of engineering problems. A solution can be obtained knowing only the parameter means and their standard deviations. In addition, the function to obtain a solution may either be given in the form of algebraic function, tables, graphs, or numerical method. Guymon et al. (1981) first applied PEM for frost heave analysis. The details of the PEM method was described by them and Harr (1987). The formulation required for this research is explained following Harr (1987).

PEM method

For a function of three random variables $y = y(x_1, x_2, x_3)$, the eight point estimates are:

$$y_{\pm\pm\pm} = y(\bar{x}_1 \pm \sigma[x_1], \bar{x}_2 \pm \sigma[x_2], \bar{x}_3 \pm \sigma[x_3]) \quad (5.17)$$

and the eight weighing functions are expressed as

$$\begin{aligned} p_{+++} &= p_{---} = \frac{1}{2^3} (1 + \rho_{12} + \rho_{23} + \rho_{31}) \\ p_{++-} &= p_{--+} = \frac{1}{2^3} (1 + \rho_{12} - \rho_{23} - \rho_{31}) \\ p_{+-+} &= p_{-+-} = \frac{1}{2^3} (1 - \rho_{12} - \rho_{23} + \rho_{31}) \\ p_{+--} &= p_{-++} = \frac{1}{2^3} (1 - \rho_{12} + \rho_{23} - \rho_{31}) \end{aligned} \quad (5.18)$$

where ρ_{ij} is correlation coefficient of the random variables x_i and x_j .

The sign of ρ_{ij} is determined by the sign of the multiplication of ij , that is, $i = (-), j = (+)$ yields $ij = (-)(+) = (-)$.

The M th expectation is obtained from

$$E[y^M] = p_{+++}y_{+++}^M + p_{++-}y_{++-}^M + \dots + p_{---}y_{---}^M \quad (5.19)$$

The expected value is equivalent to the first moment $E[y] = y$. Given the first and second moments, the variance can be computed:

$$V[y] = E[y^2] - (E[y])^2 \quad (5.20)$$

The advantages of the application of PEM for the DIL model is that the ice segregation parameters governing frost heave can be obtained from a set of simple freezing tests, while in the models such as Guymon et al. (1981) the ice segregation parameters can not be determined from such tests. Therefore, they used the best estimated parameters after several trial computation. Considering the DIL parameters are measured whereas their parameters are estimated, the PEM based DIL model is expected to be more reliable (assuming both models represent frost heave equally). Further it was suggested that the evaluated DIL parameters may have smaller variations if an appropriate laboratory tests are conducted (Ito et al. 1993).

Probabilistic Frost Heave Prediction

The probabilistic approach establishes the range of frequency of occurrence of frost heave. Based on a comprehensive field study of a roadway in Hanover, NH, Chamberlain et al. (1981) noted that the beta distribution best represented the frequency of occurrence of frost heave. He reported the lower bound $Lb = y - 2\sigma_y$ and the upper bound $Ub = y + 3\sigma_y$ of the beta distribution for the field study. Once a beta distribution is determined, confidence limits and other information of the probability distribution function $f(y)$ can be established (Harr 1987).

The beta distribution is shown in Figure 5.2. The respective percentage points p represent the area under the probability distribution curve for a beta variate x in the

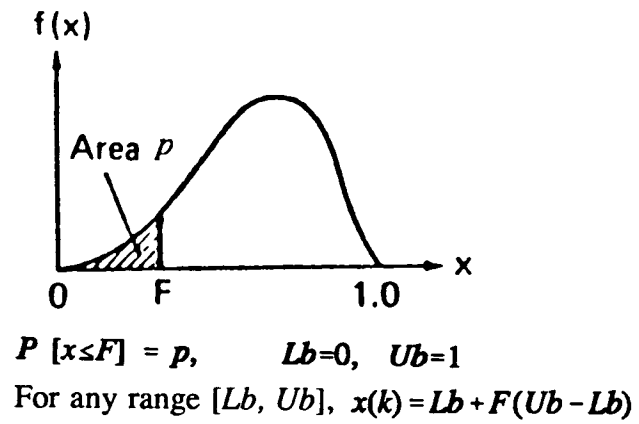


Figure 5.2 Beta Distribution (after Harr 1987)

interval 0 to 1 or $Lb = 0$ and $Ub = 1$, p is the probability that the beta variate x will be equal to or less than F , or

$$P [x \leq F] = p \quad (5.21)$$

For any range $[Lb, Ub]$,

$$x(p) = Lb + F(Ub - Lb) \quad (5.22)$$

The probability that the beta variate x will be equal to or less than $x(p)$ is expressed as

$$P[x \leq x(p)] = \frac{\int_0^F z^\gamma (1-z)^\delta dz}{\int_0^1 z^\gamma (1-z)^\delta dz} \quad (5.23)$$

where the shape γ and δ are obtained from the expected value $E[x] = x$ and the standard deviation σ of the variate from

$$\begin{aligned} \gamma &= \frac{X^2}{Y^2} (1 - X) - (1 + X) \\ \delta &= \frac{\gamma + 1}{X} - (\gamma + 2) \end{aligned} \quad (5.24)$$

where, $X = (x - Lb)/(Ub - Lb)$ and $Y = \sigma/(Ub - Lb)$.

The information required for the probability is the mean, coefficient of variation, minimum (Lb), and maximum (Ub).

5.8 Simulation of a Laboratory Test Result

A laboratory frost heave test with Calgary silt was simulated to demonstrate the applicability of the probabilistic approach to the DIL frost heave model. The properties of the Calgary silt are as follows: liquid limit = 23.7 %; plastic limit = 15.4 %; passing no. 200 = 84 %; % clay size = 26 %. The ice segregation parameters were extracted from a set of laboratory frost heave tests for Calgary silt. According to Ito et al. (1993), the best estimate of the DIL parameters were obtained from the lower line of Figure 5.3 and were $E[\alpha] = 1.15$, $\sigma[\alpha] = 0.042$, $E[k_0] = 2.51 \times 10^{-5}$ cm/sec, and $\sigma[k_0] = 8.56 \times 10^{-6}$ cm/sec. In estimation of the parameter k_0 , the PEM method was used because the relationship between k_0 and α was given in the form Eq. 5.13. The coefficient of correlation between α and k_0 was assumed as $\rho = -.75$.

Effect of the Change of Parameters on Simulation Result

Figure 5.4 presents the simulation result using the mean parameters given in Table 5.1 and the test result of C-13. As can be seen, good agreement was obtained in the observed frost heave and predicted heave, implying the validity of the DIL model. The significance of the example is that no trial and error approach was conducted to adjust the input parameters to obtain the good agreement.

Next a sensitivity analysis was performed with each input parameter. Each input parameter was changed, while maintaining the other parameters constant. Figure 5.5 presents the difference of the heave velocities when each input parameter changed. As

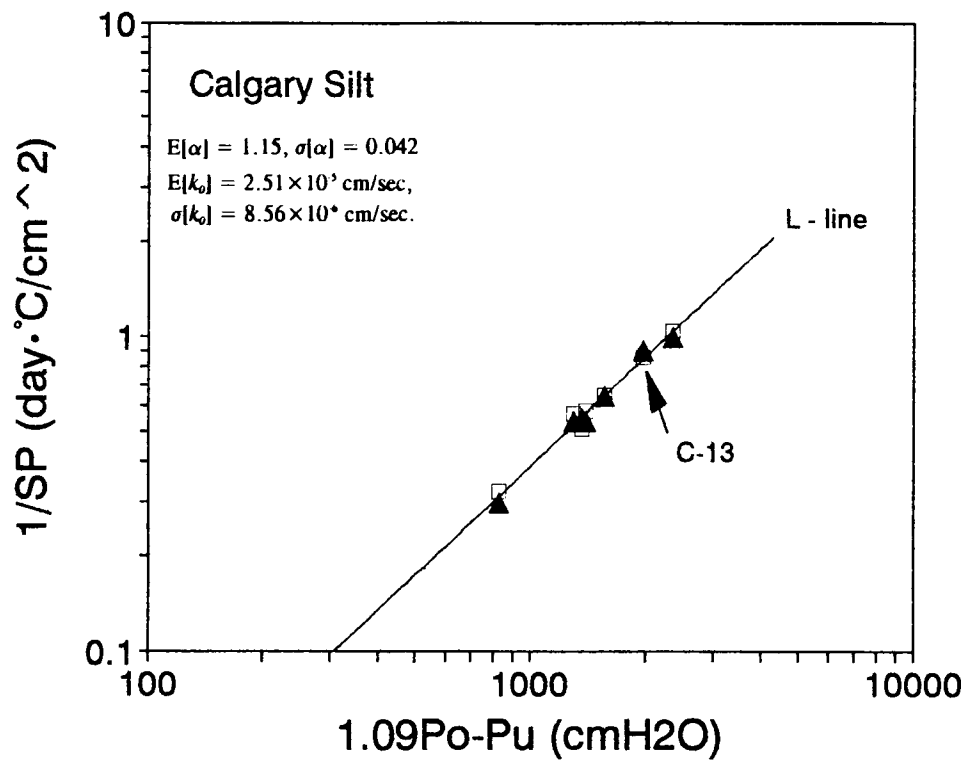


Figure 5.3 Extraction of the DIL Parameters (modified from Ito et al. 1993)

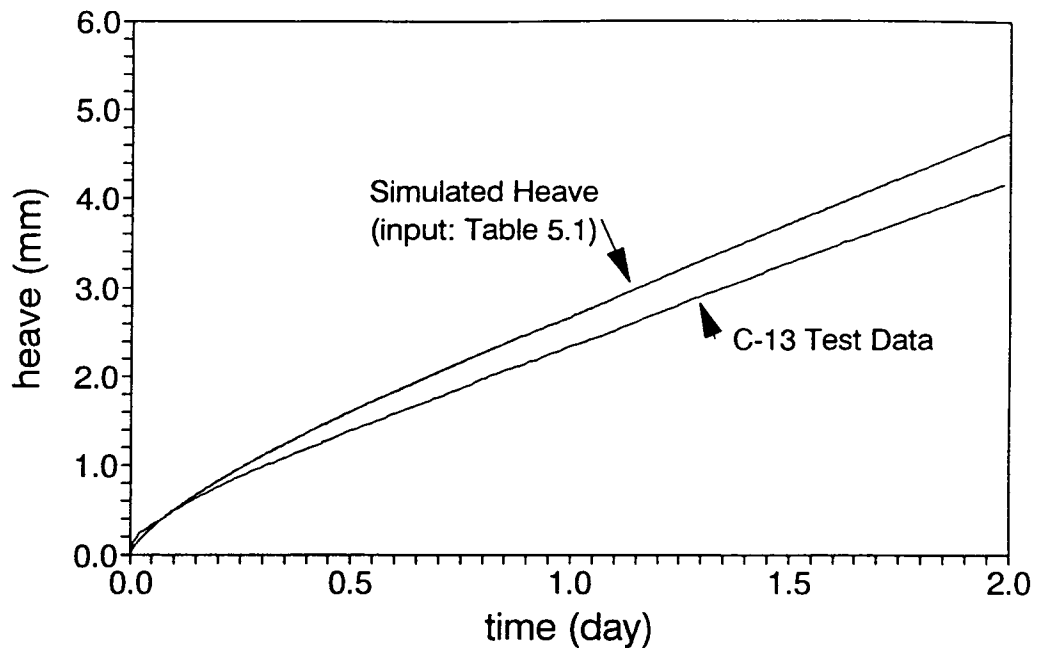


Figure 5.4 Simulation of the Laboratory Test Result Using the Mean Parameters

Table 5.1 Mean Input Parameters

Parameters	Values
T_w	0.45 °C
T_c	-1.55 °C
l_0	11.2cm
n	0.19
P_o	160kPa
P_{sep}	25kPa
K_f	450cal/(day·cm·°C)
K_u	360cal/(day·cm·°C)
α	1.148
k_o	2.36x10 ⁻⁵ cm/day
k_u	2.59x10 ⁻³ cm/day
A	0.11
B	-0.15
a	0.1cm
X_o	0.1cm
t	0.001day

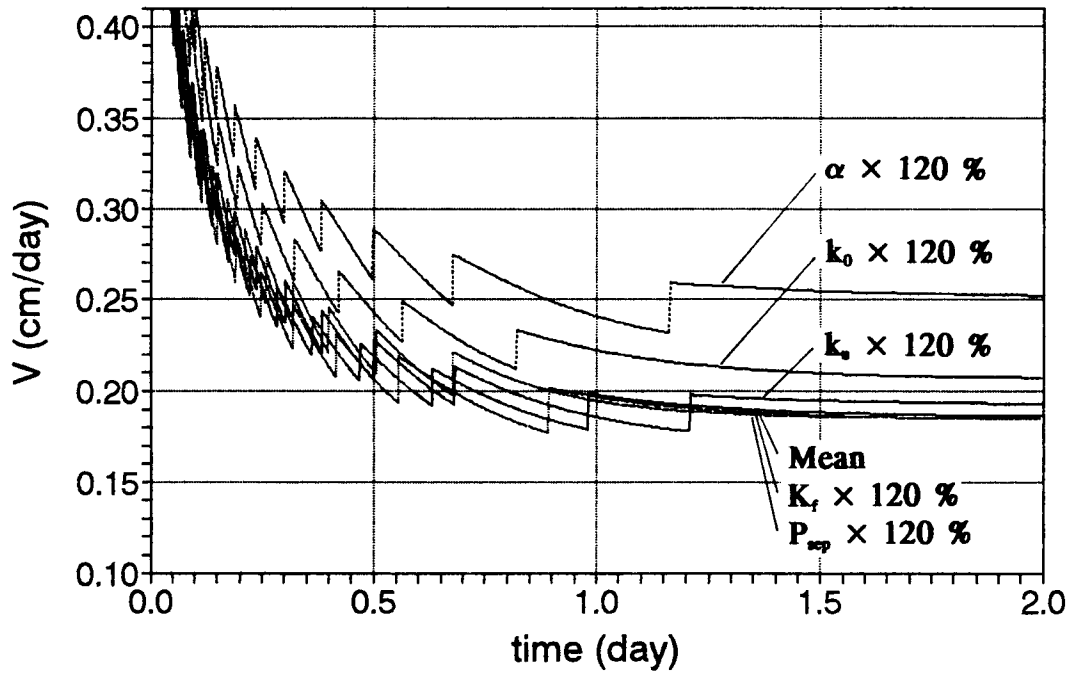


Figure 5.5 Sensitivity Analysis Comparing Heave Velocity for Mean and Mean plus Twenty Percent DIL Parameters

expected and demonstrated by Nixon (1991), the influence was the greatest when the parameters related to hydraulic conductivity of the frozen soil changed.

Based on the result in Figure 5.5, it was concluded that the parameters which must be considered in their order of priority were α , k_o , and k_u for this soil. Therefore, the PEM approach of the parameter estimation was determined to be conducted with these three parameters.

PEM Simulation

It appeared that the three parameters used for the PEM approach are correlated with each other: (1) the greater α the smaller k_o ; (2) the greater k_o (or the greater portion of clay particles) the smaller k_u ; (3) the greater k_u (or the greater portion of large particles) the greater α . Several soil types must be tested to correctly evaluate the coefficients of correlation between the three parameters. Though the evaluated coefficients of correlation between the parameters are not available, it is suggested by Harr (1987) that 0.75/-0.75 are reasonable estimates if some correlation was expected from an engineering point of view.

The α and b can be obtained directly from the regression of X and Y in Eq. 5.12. The k_o is computed with Eq. 5.13 knowing α and b . The correlation between α and b can be conservatively estimated as - 0.75. Since the form of the function to obtain k_o is known in addition to the parameter means and standard deviations, the PEM method can be used to estimate k_o .

Two simulations were conducted assuming: (1) there is no correlation between the parameters; (2) the correlations are assumed as stated above. The Lb and Ub of the beta distribution are decided following Guymon et al. (1981). The result is summarized in Tables 5.2 and 5.3. The ratios of the maximum and minimum of the frost heave and heave velocity in Table 5.2 are approximately 2 indicating the difficulty in predicting frost heave from the deterministic model. As can be seen in Table 5.3, the coefficients of variation (CV) decreased when the correlations among the parameters were assumed as above. The shape parameters γ of about 3.9 and δ of about 5.7 for heave amount and 3.7 and 5.3 for heave velocity were obtained. These values are close enough to Guymon et al. (1981)'s result of γ of about 3.5 and δ of about 5.0, and much closer to Chamberlain et al (1981)'s field observation ($\gamma = 3.6$, $\delta = 5.2$) and Albany County Airport data ($\gamma = 3.8$, $\delta = 5.4$). Therefore, it is concluded that the DIL model can reasonably predict frost heave. An advantage of the DIL model is that the ice segregation parameters can be evaluated directly from the frost heave test. The probability that the heave and heave velocity does not exceed the mean value plus two standard deviation are presented at the last column of Table 5.3. For example, the probability for the range of frost heave is read 97 to 98 %. It is also possible to compute for the specific frost heave value.

5.9 Simulation of Field Frost Heave Observation at Asahikawa, Japan

The DIL ice segregation parameters extracted from laboratory tests were used to predict frost heave under field conditions. For the field condition, where the temperature

Table 5.2 PEM Computation Example

α	k_o	k_u	H at 2 day	V_s at 1 day
+	+	+	0.6286	0.2571
+	+	-	0.5759	0.2159
+	-	+	0.3471	0.1341
+	-	-	0.3373	0.1226
-	+	+	0.5921	0.2120
-	+	-	0.5145	0.2138
-	-	+	0.3246	0.1293
-	-	-	0.3079	0.1318
0	0	0	0.4424	0.1830
			cm	cm/day

Table 5.3 Probabilistic Analysis of the Laboratory Test

Frost Heave								
ρ	Mean H	σ_y	CV	Lb	Ub	γ	δ	$p[y < y + 2\sigma_y]$
0	0.45	0.13	28	0.06	0.97	3.94	5.49	97
0.75	0.44	0.10	22	0.14	0.84	3.92	5.70	98
	cm	cm	%	cm	cm			%
Heave Velocity								
ρ	Mean V_h	σ_y	CV	Lb	Ub	γ	δ	$p[y < y + 2\sigma_y]$
0	0.177	0.050	28	0.028	0.375	3.72	5.28	97
0.75	0.175	0.042	24	0.047	0.345	3.74	5.32	97
	cm/day	cm/day	%	cm/day	cm/day			%

gradient is very shallow and the frost front is slowly advancing, Nixon (1987) has suggested that the DIL model can be solved without coupling the heat balance equation to the mass flow equation. This means that if one has a reliable method to predict the temperature gradients or the temperature gradient is known in the field situation, the heave velocity can be computed simply by Eq. 5.14.

The field temperature data from Asahikawa test yard, Japan, (Toya et al. 1992) was used for the field prediction. The physical properties of Asahikawa soil is as follows: liquid limit = 52.3 %; plastic limit = 24.6 %; passing no. 200 = 46 %; % clay size = 19 %. The ice segregation parameters were estimated by Ito et al. (1993) as $\alpha = 0.914$ (CV = 10 %) and $k_o = 4.82 \times 10^{-6}$ cm/day (CV = 30 %). Assuming the pressure term is 500 cmH₂O, SP is estimated as 0.565 cm²/day°C (CV = 13 %). The K_{ff}/K_f was assumed to be 0.9 (CV = 5 %), and the mean value of G_f as the measured value in the field (CV = 10 %). The computed vs the actual heave are plotted in Figure 5.6.

As the temperature gradient used is not the exact temperature gradient of the frozen soil, it is not appropriate to directly compare the two heave values. However, it is implied in Figure 5.6 that the proposed procedure may be feasible if we have a reliable model to predict the geothermal condition. The shape parameters γ of 3.8 and δ of Figure 5.6 were obtained in Table 5.4. These are very close to the values previously obtained by Guymon et al. (1981) and Chamberlain et al. (1981).

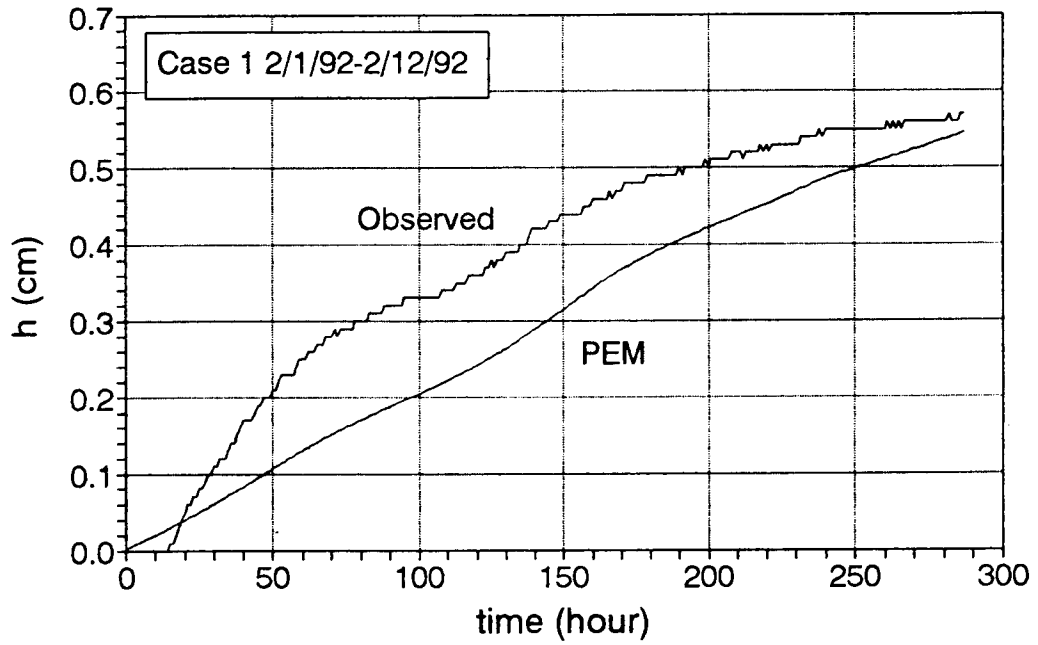


Figure 5.6 Simulation of the Field Test at Asahikawa

Table 5.4 Probabilistic Analysis of the Field Test

Mean H	σ_y	CV	Lb	Ub	γ	δ	$p[y < y + 2\sigma_y]$
0.545	0.138	25	0.131	1.097	3.84	5.46	98
cm	cm	%	cm	cm			%

5.10 Summary and Conclusion

The probabilistic approach was applied to the DIL model. In comparison with Guymon et al.'s (1981) work, it was demonstrated that the probabilistic approach to the DIL frost heave model worked well to assess frost. The advantage of the DIL model is that the ice segregation parameters can be determined from the laboratory freezing test, not from the results of trial and error. The simulation result using the parameters obtained from the laboratory freezing test showed remarkable agreement with the actual test result. This result suggested that the DIL model can be used for frost heave prediction. Also the estimated correlation between the parameters was observed to reduce the probability range. In addition, the shape parameters of the probability distribution by the PEM method were very similar to those previously obtained by Guymon et al. (1981) and closer to the parameters observed in the field by Chamberlain et al. (1981). These results also confirm the applicability of the DIL model.

5.11 References

1. Anderson, D. M., and Tice, A. R., "Predicting Unfrozen Water Contents in Frozen Soils From Surface Area Measurements," *Highway Research Record No. 393*, 1972, pp. 12-18.
2. Chamberlain, E. J., Guymon, G. L., and Berg, R. L., "Probabilistic Approach to Determine Frost Heave," Seminar on the Prediction of Frost Heave, University of Nottingham, England, 1981.
3. Guymon, G. L., Harr, M. E., Berg, R. L., and Hromadka, T. V., "A Probabilistic-Deterministic Analysis of One-Dimensional Ice Segregation in a Freezing Soil Column," *Cold Region Science and Technology*, 5, 1981, pp. 127-140.
4. Harr, M. E., "Reliability Based Design in Civil Engineering," McGraw-Hill, New York, 1987.
5. Ito, Y., Vinson, T. S., and Nixon, J. F., "Examination of the Approximation Used to Interpret Freezing Tests and Verification of the Compatibility of the Segregation Potential and Discrete Ice Lens Frost Heave Models," manuscript, 1993.
6. Ito, Y., and Vinson, T. S., "Method to Predict the Influence of Ground Water Level on Frost Heave," manuscript, 1993.
7. Konrad, J. M., and Morgenstern, N. R., "The Segregation Potential of a Freezing Soil," *Canadian Geotechnical Journal*, Vol. 18, 1981, pp. 428-491.
8. Nixon, J. F., "Ground Freezing And Frost Heave - A Review," *Northern Engineer*, Vol. 19, 1987, pp. 8-19.
9. Nixon, J. F., "Discrete Ice Lens Theory for Frost Heave in Soils," *Canadian Geotechnical Journal*, Vol. 28, 1991, pp. 843-859.
10. Nixon, J. F., (Personal Communication), 1993.
11. Press, W. H., Flannery, B. P., Teukolsky, S. A., and Vetterling, W. T., "Numerical Recipes," Cambridge University Press, Cambridge, 1986.
12. Rosenblueth, E., "Point Estimates for Probability Moments," *Proc., Nat. Acad. Sci. USA*, Vol. 72, No. 10.

13. Rosenblueth, E., "Two-Point Estimates in Probabilities," *Applied Mathematical Modelling*, Vol. 5, 1981, pp. 329-335.
14. Sarelainen, S., "Modelling Frost Heaving and Frost Penetration in Soils at Some Observation Sites in Finland," *Technical Research Center of Finland (VTT) Publications 95*, 1992.
15. Toya, k., Katsura, T., Mori, H., and Saito, M., "Field Frost Heave Observation on Highway Embankment," In *Proc., Japan Highway Public Corporation Annual Conference*, H. 4, Osaka, 1992. (in Japanese)

5.12 Notation

The following symbols are used in this chapter:

A, B	=	constants;
a	=	thickness of the frozen fringe;
CV	=	coefficient of variation;
$E[]$	=	expectation;
G_f	=	temperature gradient of frozen part of the soil;
G_f'	=	overall temperature gradient of the frozen soil;
G_{ff}	=	temperature gradient of the frozen fringe;
G_u	=	temperature gradient of the unfrozen soil;
H_f	=	amount of water frozen in the frozen fringe;
K_f	=	thermal conductivity of frozen soil;
K_{ff}	=	thermal conductivity of the frozen fringe;
K_u	=	thermal conductivity of the unfrozen soil;
k	=	hydraulic conductivity in the frozen fringe;
k_0	=	hydraulic conductivity of the frozen soil at $-1\text{ }^\circ\text{C}$;
L	=	latent heat of fusion of water;
Lb	=	lower bound;
m	=	constant;
n	=	porosity;
P_i	=	ice pressure;
P_o	=	overburden pressure;
P_{sep}	=	separation pressure;
P_u	=	suction at the frost front;
P_w	=	water pressure in the frozen fringe;
p	=	probability;
p_{+++}	=	weighing function;
SP	=	segregation potential;
T	=	temperature;
T_f	=	temperature at the frost front;
T_l	=	temperature at the ice lens base;
Ub	=	upper bound;
w_{tot}	=	total water content;
V_{ff}	=	water flow velocity to the base of the ice lens;
V_h	=	heave velocity;
x	=	distance from the ice lens base;
z_f	=	frozen depth;
α	=	constant;
β	=	thermal constant;
γ, δ	=	shape parameters;
ρ	=	coefficient of correlation; and
σ	=	standard deviation.

6.0 Conclusion

6.1 Summary

An improved frost heave test method was proposed and simplifying approximations to obtain ice segregation parameters were examined. The improvements to the test method included an accurate water intake measurement with an electric balance and the use of shallower test temperature boundary conditions. The approximations examined were various combinations of the temperature gradient and flow velocities in the freezing soils. The scatter observed in the evaluated ice segregation parameters were interpreted in relation to the unfrozen water. The compatibility of the segregation potential (SP) (Konrad and Morgenstern 1981) and discrete ice lens (DIL) (Nixon 1991) parameters was discussed based on the idealized frozen soil model by Gilpin (1980).

A method to evaluate the influence of ground water level on frost heave was proposed. This method uses the combined pressure term, which is the sum of the overburden pressure and suction. Finally, a probabilistic approach was presented to widen the application of the ice segregation parameters obtained under the improved method.

6.2 Conclusion

The conclusions based on the research presented in this thesis are as follows:

- (1) The accuracy of the water intake measurement was greatly improved by the use of an electric balance.
- (2) The water intake measurement with an electric balance not only provides

an accurate water intake velocity, but also enables one to precisely identify the end of transient freezing (when the ice segregation parameters are most often evaluated).

- (3) It was suggested that the shallower temperature boundary condition in the step freezing test may decrease the change of ice segregation parameters and ease their evaluation.
- (4) For the soil used in this research, the possible combinations of the flow velocity and temperature gradient, which meaningfully define SP from an engineering point of view, are the ratios of: (i) the water intake velocity (v) and temperature gradient in the frozen fringe (G_{ff}); and (ii) the heave velocity divided by 1.09 (V_{ff}) and temperature gradient in the frozen soil of a soil over an ice lens (G_f) or overall temperature gradient in the frozen soil (G_f').
- (5) The scatter observed in the evaluation of the ice segregation parameters was related to the variation of unfrozen water content associated with pressure change.
- (6) The compatibility between the SP and DIL parameters was demonstrated; if freezing test results are interpreted using both models, a greater reliability in the evaluated ice segregation parameters can be expected.
- (7) It was demonstrated that the laboratory freezing test with different overburden pressures can be substituted for the time consuming and expensive test to predict the influence of groundwater level on frost heave.

- (8) The DIL model was combined with the point estimate method (PEM). It was observed that there was good agreement in the shape parameters of the probability distribution function of the computation result and field observation.

6.3 Future Study

Although valuable results were obtained in this research program and directly applicable to solve field frost heave problems, there are several topics which should be examined in future studies. They are:

- (1) A number of different types of soil must be tested by the improved test procedure and evaluation method to verify the conclusions obtained in this research.
- (2) The unfrozen water content should be measured by the direct method, such as the nuclear magnetic resonance (NMR) method to check the observation in this research.
- (3) The sample preparation method, which may produce the condition of the field compacted soil, must be studied to improve the accuracy of the ice segregation parameter prediction.
- (4) More data may be necessary to identify the probability distribution function governing field frost heave.

6.4 References

1. Gilpin, R. R., "A Model for the Prediction of Ice Lensing and Frost Heave in Soils," *Water Resources Research*, Vol. 16, No. 5, 1980, pp. 918-930.
2. Konrad, J. M., and Morgenstern, N. R., "The Segregation Potential of a Freezing Soil," *Canadian Geotechnical Journal*, Vol. 18, 1981, pp. 428-491.
3. Nixon, J. F., "Discrete Ice Lens Theory for Frost Heave in Soils," *Canadian Geotechnical Journal*, Vol. 28, 1991, pp. 843-859.

Bibliography

1. Akagawa, S., "X-Ray Photography Method for Experimental Studies of the Frozen Fringe Characteristics of Freezing Soil," *CRREL Report*, 90-5, 1990.
2. Anderson, D. M., and Tice, A. R., "Predicting Unfrozen Water Contents in Frozen Soils From Surface Area Measurements," *Highway Research Record No. 393*, 1972, pp. 12-18.
3. Bell, J. R., Allen, T., and Vinson, T. S., "Properties of Geotextiles in Cold Regions Applications," In *Proc., Fourth International Conference on Permafrost*, 1983, pp. 51-56.
4. Chamberlain, E. J., Guymon, G. L., and Berg, R. L., "Probabilistic Approach to Determine Frost Heave," Seminar on the Prediction of Frost Heave, University of Nottingham, England, 1981.
5. Guymon, G. L., Harr, M. E., Berg, R. L., and Hromadka, T. V., "A Probabilistic-Deterministic Analysis of One-Dimensional Ice Segregation in a Freezing Soil Column," *Cold Region Science and Technology*, 5, 1981, pp. 127-140.
6. Harr, M. E., "Reliability Based Design in Civil Engineering," McGraw-Hill, New York, 1987.
7. Frivik, P. E., "State of the Art Report. Ground Freezing: Thermal Properties, Modeling of Processes and Thermal Design," In *Proc., Second International Symposium on Ground Freezing*, 1980, pp. 115-133.
8. Fukuda, M., Ogawa, S., and Kamei, T., "Prediction of Field Frost Heave Using the Segregation Potential Theory," *Japan Society of Civil Engineers Reports*, No.400, 1988, pp. 253-259.
9. Gassen, Wim van., and Sego, D. C., "Problems with the Segregation Potential Theory," *Cold Region Science and Technology*, 17, 1989, pp. 95-97.
10. Gilpin, R. R., "A Model for the Prediction of Ice Lensing and Frost Heave in Soils," *Water Resources Research*, Vol. 16, No. 5, 1980, pp. 918-930.
11. Gilpin, R. R., "A Frost Heave Interface Condition for Use in Numerical Modelling," In *Proc., Fourth Canadian Permafrost Conference*, Calgary, Alberta, 1982, pp. 459-465.

12. Henry, K. S., "Laboratory Investigation of the Use of Geotextiles to Mitigate Frost Heave," *CRREL Report*, 90-6, 1990.
13. Ito, Y., Wakatsuki, Y., Kawaragawa, Z., and Ryokai, K., "Study on Frost Heave Problem of Highway (Part. 1), Problems of the Frost Susceptibility Test," In *Proc., 24th Annual Conference of Japan Society of Soil Mechanics and Foundation Engineering*, 1989, pp. 1051-1052. (in Japanese)
14. Ito, Y., Kawaragawa, Z., and Ryokai, K., "Study on Frost Heave of Highway (Part. 3) - Interpretation of Frost Heave Test," In *Proc., 25th Annual Conference of Japan Society of Soil Mechanics and Foundation Engineering*, 1990. (in Japanese)
15. Ito, Y., Vinson, T. S., Nixon, J. F., and Stewart, D., "An Improved Step Freezing Test to Determine Segregation Potential," manuscript, 1993.
16. Ito, Y., Vinson, T. S., and Nixon, J. F., "Examination of the Approximation Used to Interpret Freezing Tests and Verification of the Compatibility of the Segregation Potential and Discrete Ice Lens Frost Heave Models," manuscript, 1993b.
17. Ito, Y., and Vinson, T. S., "Method to Predict the Influence of Ground Water Level on Frost Heave," manuscript, 1993c.
18. Japan Highway Public Corporation Design Specification No. 1, 1983, pp. 78-85. (in Japanese)
19. Japan Highway Public Corporation Sapporo Construction Bureau, "Doh-oh Expressway Frost Heave Field Observation Report", 1990. (in Japanese)
20. Kawaragawa, Z., Wakatsuki, Y., and Ito, Y., "Study on Frost Heave Problem of Highway Part. 2, Influence of Groundwater Table," In *Proc., 24th Conference of Japan Society of Soil Mechanics and Foundation Engineering*, 1989, pp. 1053-1054. (in Japanese)
21. Konrad, J. M., "Frost Heave Mechanics," Ph. D. thesis, Department of Civil Engineering, University of Alberta, Edmonton, Alberta, 1980.
22. Konrad, J. M., and Morgenstern, N. R., "A Mechanistic Theory of Ice Lens Formation in Fine-Grained Soils," *Canadian Geotechnical Journal*, Vol.17, 1980, pp. 473-486.
23. Konrad, J. M., and Morgenstern, N. R., "The Segregation Potential of a Freezing Soil," *Canadian Geotechnical Journal*, Vol.18, 1981, pp. 482-491.

24. Konrad, J. M., and Morgenstern, N. R., "Prediction of Frost Heave in the Laboratory During Transient Freezing," *Canadian Geotechnical Journal*, Vol.19, 1982, pp. 250-259.
25. Konrad, J. M., and Morgenstern, N. R., "Effects of Applied Pressure on Freezing Soils," *Canadian Geotechnical Journal*, Vol.19, 1982b, pp. 494-505.
26. Konrad, J. M., "Procedure for Determining the Segregation Potential of Freezing Soils," *Geotechnical Testing Journal*, Vol.10, No.2, 1987.
27. Konrad, J. M., "Influence of Freezing Mode on Frost Heave Characteristics," *Cold Region Science and Technology*, 15, 1988, pp. 161-175.
28. Kujara, K., "Factors Affecting Frost Susceptibility and Heaving Pressure in Soils," Ph. D. thesis, Department of Civil Engineering, University of Oulu, Oulu, Finland, 1991.
29. McCabe, E. Y., and Kettle, R. J., "Thermal Aspects of Frost Action," In *Proc., Fourth International Symposium on Ground Freezing*, Sapporo, pp. 47-54.
30. McGaw, R., "Frost Heaving versus Depth to Water Table," *Highway Research Record No. 393*, 1972, pp. 45-55.
31. Miller, R. D., "Freezing and Heaving of Saturated and Unsaturated Soils," *Highway Research Record 393*, TRB, National Research Council, Washington, D. C., 1972, pp. 1-11.
32. Loch, J. P., and Kay, B. D., "Water Redistribution in Partially Frozen Saturated Silt Under Several Temperature Gradients and Overburden Loads," *Journal of the Soil Science Society of America*, Vol.42, No.3, 1978.
33. Loch, J. P., "Influence of the Heat Extraction Rate on the Ice Segregation Rate of Soils." *Frost i Jord*, No.20, 1979.
34. Nixon, J. F., "Field Frost Heave Prediction Using the Segregation Potential Concept," *Canadian Geotechnical Journal*, Vol.19, 1982, pp. 526-529.
35. Nixon, J. F., "Ground Freezing And Frost Heave - A Review," *Northern Engineer*, Vol. 19, 1987, pp. 8-19.
36. Nixon, J. F., "Discrete Ice Lens Theory for Frost Heave in Soils," *Canadian Geotechnical Journal*, Vol. 28, 1991, pp. 843-859.
37. Nixon, J. F., Personal Communication, 1993.

38. Press, W. H., Flannery, B. P., Teukolsky, S. A., and Vetterling, W. T., "Numerical Recipes," Cambridge University Press, Cambridge, 1986.
39. Rosenblueth, E., "Point Estimates for Probability Moments," *Proc., Nat. Acad. Sci. USA*, Vol. 72, No. 10.
40. Rosenblueth, E., "Two-Point Estimates in Probabilities," *Applied Mathematical Modelling*, Vol. 5, 1981, pp. 329-335.
41. Svec, O. J., "A New Concept of Frost-Heave Characteristics of Soils," *Cold Region Science and Technology*, 16, 1989, pp. 271-279.
42. Penner, E., "Aspects of Ice Lens Growth in Soils," *Cold Region Science and Technology*, 13, 1986, pp. 91-100.
43. Reike, R. D., "The Role of the Specific Surface Area and Related Index Properties in the Frost Heave Susceptibility of Soils," M.S.thesis, Oregon State University, Corvallis, 1982.
44. Reike, R. D., Vinson, T. S., and Mageau, D. W., "The Role of the Specific Surface Area and Related Index Properties in the Frost Heave Susceptibility of Soils," In *Proc., Fourth International Conference on Permafrost*, National Research Council, Washington, D. C., 1983.
45. Saarelainen, S., "Modelling Frost Heaving and Frost Penetration in Soils at Some Observation Sites in Finland," *Technical Research Center of Finland (VTT) Publications 95*, 1992.
46. Sezai, T., Mishima, N., and Kikuchi, S., "Frost Heave Prevention in Cold Regions - Problems Related to the Conventional Practice and Frost Susceptibility Test-," *Japan Highway Public Corporation Laboratory Report S.59*, 1985, pp. 13-33.
47. Taber, S., "Frost Heaving," *Journal of Geology*, Vol. 37, 1929, pp. 428-461.
48. Taber, S., "The Mechanics of Frost Heaving," *Journal of Geology*, Vol. 38, 1930, pp. 303-317.
49. Toya, k., Katsura, T., Mori, H., and Saito, M., "Field Frost Heave Observation on Highway Embankment," In *Proc., Japan Highway Public Corporation Annual Meeting*, H. 4, Osaka, 1992. (in Japanese)

50. Tsuchiya, F., Tsuji, S., Mishima, N., and Yokota, S., "Frost Heave Reduction Using Capillary Break Effect of Geotextiles," *Journal of Japan Society of Agricultural Engineering*, Vol. 60, No. 12, 1992, pp. 1123-1126. (in Japanese)
51. Weiyue, G., and Xiaozu, Xu., "Field Observations of Water Migration in Unsaturated Freezing Soils with Different Ground Water Tables," In *Proc., Fifth International Symposium on Ground Freezing*, Rotterdam, 1988, pp. 59-64.
52. Vinson, T. S., Ahmad, F., and Rieke, R. D., "Factors Important to the Development of Frost Heave Susceptibility Criteria for Coarse-Grained Soils," *Transportation Research Record 1089*, 1984, pp. 124-131.